NASA CONTRACTOR REPORT

NASA CR-154

NASA CR-154

MEASUREMENT OF THE LOWEST PRESSURES IN SPACE AND THE LABORATORY

by Wallace Kreisman

Prepared under Contract No. NASw-705 *by*
GEOPHYSICS CORPORATION OF AMERICA
Bedford, Mass.
for

NATIONAL AERONAUTICS AND SPACE ADMINISTRATION • WASHINGTON, D. C. • FEBRUARY 1965

NASA CR-154

MEASUREMENT OF THE LOWEST PRESSURES IN SPACE AND THE LABORATORY

By Wallace Kreisman

Prepared under Contract No. NASw-705 by
GEOPHYSICS CORPORATION OF AMERICA
Bedford, Massachusetts

for

NATIONAL AERONAUTICS AND SPACE ADMINISTRATION

For sale by the Office of Technical Services, Department of Commerce,
Washington, D.C. 20230 -- Price $5.00

ABSTRACT

18203

A description is given of the design, construction and operational characteristics of two demountable, metal ultra high vacuum systems, a mercury diffusion pump system and a combination liquid helium cryopump-ion pump system. The diffusion pump system attained pressures as low as 10^{-13} torr and was used for low pressure vacuum gauge calibration. The liquid helium cryopump system reached pressures in the low 10^{-11} torr region with only limited bake outs and exhibited a "clean" residual gas mass spectrum. The two systems were studied to determine their low pressure limitations and sources of residual gas.

author

TABLE OF CONTENTS

LIST OF ILLUSTRATIONS

LIST OF ILLUSTRATIONS (Continued)

LIST OF ILLUSTRATIONS (Continued)

1. INTRODUCTION

In recent years, the possibility of directly measuring the density and composition of the outer reaches of the Earth's atmosphere, the Moon's atmosphere, and the atmospheres of the planets has become a reality. With the advent of the satellite and the deep space probe, both of which operate in an extremely low pressure environment, it has already been demonstrated that gas density and composition measurements can be made directly.[1,2,3] At 500 Km altitude in the Earth's atmosphere, the pressure is of the order of 1×10^{-8} torr; at 700 Km, the pressure has decreased to 1×10^{-9} torr.[4] In the interplanetary space of the solar system, estimates of particle density run from 10,000 to 100 or so particles/cm^3[5], corresponding to equivalent pressures of 2.8×10^{-13} to 2.8×10^{-15} torr under standard conditions. The particle density in interstellar space has been estimated at 1 particle/cm^3.[6] It is clear that in the outer regions of any planetary atmosphere, particle measuring instruments must be capable of responding to a few hundred or a few thousand particles/cm^3.

In addition to the necessity of measuring the total gas pressure and the composition of unknown atmospheres, the space age has brought with it a requirement for operating complex mechanical, electrical, and optical systems in the low pressure environment of space. Space vehicle components and entire space vehicles must be designed to withstand the effects of extremely low pressures. Space simulation chambers

are needed to duplicate the conditions of space for the purpose of developing and testing components and systems.

To aid in the development of low pressure measurement instruments and at the same time provide an extremely low pressure environment that could be used for space simulation, a research program was undertaken to design and develop two different all metal vacuum systems capable of reaching pressures as low as 10^{-13} torr. The two systems were designed to be large enough for laboratory experimentation and yet serve as small scale prototypes of much larger, all metal systems suitable for testing critical space vehicle components. One of the systems constructed has found an immediate application in the testing and calibration of ultra high vacuum gauges and mass spectrometers. Both systems have been utilized to study the residual gases that remain in low pressure chambers and to study the factors that limit the attainment of low pressures.

Both vacuum systems were constructed in a modular fashion. Each component was flanged so that it could readily be removed for cleaning, repair or replacement. Most of the vacuum components were unique in that they represented new designs. The two vacuum systems constructed were: 1. A mercury diffusion pump system; and 2. A combination ion pump, liquid helium cryopump system.

The metal mercury diffusion pump unit was designed on the basis of several years of experience with glass mercury diffusion pump

systems of the Venema type.[7,8] The new metal design was planned to provide a number of advantages not shared by the glass ensemble. Breakage of the glass systems had been a serious problem and, of course, this was eliminated in the new system.

The permeation of helium gas from the ambient atmosphere through the pyrex walls of the glass system had set a limit to the lowest pressures which could be created, and the technology and materials of the glassblower had limited the size of the critical vacuum components. These limitations were clearly no longer present in a metal system. In addition, the possibility of baking the metal system at higher temperatures and of using flanged connections to attain demountability made the metal construction very attractive.

As it turned out, the metal mercury diffusion pump system was highly successful in all respects. The objectives and advantages sought were obtained. The system consistently attained ultimate pressures in the 10^{-12} and 10^{-13} torr region after overnight bakeout at 450°C. The residual gas in the test chamber appeared to originate mainly in the mass spectrometer that was used to make the analysis. A number of interesting and important conclusions were reached regarding systems of this type. These will be presented in the following sections.

The ion pump, liquid helium cryopump system utilized a pumping technique that was quite different from that of diffusion pumping.

The atoms and molecules pumped by a diffusion pump are removed from the system and eventually exhausted to the atmosphere. Ion pumps and cryopumps operate by storing atoms and molecules in and on surfaces within the pump. It is natural to expect that the two types of pump would have different operating characteristics and that one would be more suitable than the other for certain applications.

The next few sections of this report contain detailed descriptions of the design, construction, and operating characteristics of the new vacuum systems. Following this material, there is a presentation of the results of residual gas analysis and experiments that were performed to study the factors that could limit the attainment of very low pressures. The last section summarizes the information obtained during the course of the program.

2. EXPERIMENTAL OBJECTIVES

The first objective of the research program to be described herein was to design, build, test, and place in operational use two unique and different ultra high vacuum systems capable of attaining pressures of 10^{-13} torr. These two systems were:

(1) A metal cryopump-ion pump system utilizing either one of the following ion pump designs:

(a) A modified, scaled-up version of a magnetron type cold cathode ionization gauge.

(b) A multiple cell pump consisting of six or more anode-cathode pairs of the same general dimensions as those used in magnetron type cold cathode ionization gauges.

(2) A metal, modified, Venema type mercury diffusion pump system equipped to be used for vacuum gauge calibration.

The second objective of the research program was to study and use the two low pressure systems as follows:

(1) Study the residual gas composition in the two low pressure systems. An ultra sensitive mass spectrometer would be used for this purpose.

(2) Use the ultra sensitive mass spectrometer and a calibrated Bayard Alpert gauge to calibrate a magnetron type cold cathode ionization gauge at the lowest pressures attainable.

The third objective of the program was to examine experimentally those factors which could limit the attainment of very low pressures and to make use of all the information gained to provide design data for building larger high vacuum chambers for space simulation.

It is well known that very low pressures in the 10^{-12} and 10^{-13} torr range (and below) can be obtained with the use of liquid helium. Redhead and Hobson[9] used the technique of immersing a cold finger of their all glass system into liquid helium to lower the system pressure. Recently, cryopump panels have become available for cooling with helium vapor, and some double wall vacuum systems using cryopump panels have reached low pressures. Most of the current commercial systems use oil diffusion pumps in combination with the cryopanels.

One objective of the design of a cryopump-ion pump system was to determine the manner in which an ion pump and a cryopump would work together to produce low pressures. It was anticipated that the system pressure would be reduced to the 10^{-9} or 10^{-10} torr region by the ion pump and then taken lower by the cryopump. Since a liquid helium cryopump should not pump helium (except, possibly, by cryotrapping of helium atoms by other condensing atoms and molecules), it was expected that the ion pump would keep the helium partial pressure at a low level.

The cryopump to be described in this report was designed to be appended to any kind of vacuum system. In particular, the cryopump would be mounted on top of the system in much the same way that a diffusion

pump would be mounted below a system. There were no cryopanels or filling lines to be installed within a chamber or through chamber walls. In this way, a better comparison could be made between a low pressure diffusion pump system and a low pressure cryopump system.

It was hoped that the use of a liquid helium cryopump would produce a "clean background" free of all gases other than helium, so that experiments involving the ion pumping and re-emission of helium could be carried out eventually. It would also be of interest to use a liquid helium cryopump system to experiment with hydrogen gas at pressures below 10^{-7} torr.

The two ion pumps to be developed for this research program were intended to be true ion pumps, rather than getter-ion pumps. By excluding titanium and other such active materials from the pump construction, it was hoped that all, or at least most, of the pumping action would take place by ion burial in the cathode walls.

The major residual gas in a getter-ion pumped system is known to be hydrogen gas. It was speculated that the hydrogen gas originated in either the titanium or in components of the pump that were not properly vacuum fired. It was planned to construct two ion pumps in which all of the components were vacuum fired.

Because a magnetron type geometry appeared to be favorable for cold cathode gauges that operate at low pressures, it was logical to use the same geometry for the ion pumps. One of the pumps, in fact, was just a larger,scaled-up version of a cold cathode ionization gauge. The second

pump was unique in that it was made demountable, and its multiple magnetron type pumping cells could be modified as desired.

Experiments were planned to measure the pumping speed of the ion pumps, the ultimate pressures attained after various bakeouts, and the composition of the residual gas. The operational characteristics of the pumps such as starting at low pressures, variation of pump current with pressure and anode voltage, and variation of pumping speed with anode voltage were considered to be of interest.

Very low pressures of the order of 10^{-13} torr have been obtained in recent years with all glass mercury diffusion pump systems of the "Venema" type.[10] It has been shown that a pumping fluid such as mercury can be completely prevented from backstreaming into the vacuum chamber by the proper choice and use of cold traps. Oil pumping fluids, on the other hand, can be dissociated by the pump into low molecular weight fractions, including molecular hydrogen. These light fractions can diffuse through most cold traps and limit the ultimate pressure in the system. Inherently, then, a mercury diffusion pump system can be a "cleaner" system (in terms of residual background gas) and a lower pressure system than an equivalent oil diffusion pump system. In fact, it was speculated that a well-designed mercury diffusion pump system would be a "cleaner" system than even an ion pumped system because of the possibility of re-emission of gases from the ion pump.

Since pressures of 10^{-13} torr had been obtained in glass mercury diffusion pump systems in which the pumping speed was limited by the glass fabrication technology, it was reasoned that larger, higher speed metal, mercury diffusion pump systems should be capable of reaching even lower pressures. The use of metal instead of glass would provide a great deal more flexibility in the fabrication of the system. In short, the use of metal would convert the small, glass, laboratory Venema type systems into large-scale, industrial type systems.

In addition to removing restrictions on system size and design configuration, the use of metal would remove the helium-through-Pyrex permeation problem and permit higher temperature bakeout of the system. Current vacuum technology provided excellent glass-to-metal sealing capability so that glass apparatus, viewing windows, etc., could be easily attached to a metal system as required. Electrical connections could be made through a metal vacuum wall by means of ceramic-metal connectors that were just as reliable as the metal-glass electrical feedthroughs that were used with a glass vacuum wall.

Among other objectives, it was planned to measure the overall pumping speed of the metal mercury diffusion pump system and compare this speed with the calculated value. The efficiency of the new,metal,liquid nitrogen cold traps would be investigated, and the effectiveness of a new design for making the cold traps non-level-sensitive would be studied.

Eventually, various low pressure measurement instruments would be connected to the test chamber of the diffusion pump system and compared.

With a mass spectrometer connected to the test chamber, it would be possible to investigate the residual gas in the system and determine some of the sources of the residual gas. In particular, it was of interest to determine the relationship between the UHV mercury diffusion pump fore-pressure and the ultimate pressure in the test chamber. The relationship between the temperature of the test chamber walls and the pressure within the test chamber would yield information about the outgassing rate of the stainless steel. Heating or cooling other portions of the system would indicate whether or not these portions were contributing to the residual gas. Finally, turning vacuum gauges on and off while monitoring the gas composition in the system would demonstrate the production of various gases by these gauges.

It was not known whether the presence of demountable flanges (copper shear seal type) seals would limit the ultimate pressure attainable. Seals that were leak tight to only 10^{-10} torr liter/sec, as measured with a standard helium mass spectrometer type leak detector, would not be adequate to permit pressures of 10^{-13} torr to be attained. Also, the effect of high temperature, long-term bakeout on the copper gasket sealed flanges was unknown.

Finally, it was conceivable that extremely low pressure would be attained, pressure so low that none of the available gauges would be adequate for its measurement. If such pressures were reached, then the low pressure limitations of various gauges could be studied.

3. SYSTEM DESIGN AND CONSTRUCTION

3.1 MERCURY DIFFUSION PUMP SYSTEM

3.1.1 Over-all Design. The first system constructed used a specially designed, bakeable, stainless steel mercury diffusion pump patterned somewhat after the glass pumps first constructed by Venema.[7] This ultra high vacuum (UHV) pump was backed by a conventional mercury diffusion pump and rotary mechanical forepump. A newly designed water baffle and isolation cold trap separated the two diffusion pumps. Between the UHV diffusion pump and the test chamber, a series of two non-level-sensitive cold traps were interposed to prevent migration of the mercury pumping fluid to the test chamber. A rotatable "vapor" valve could be installed just below the test chamber. The UHV diffusion pump, each of the non-level-sensitive cold traps, and the test chamber were fitted with large ConFlat flanges so that they could readily be disassembled. The system was constructed so that the major UHV components mentioned above could be baked out at high temperatures of at least 450°C. The test chamber was fitted with three smaller flanged tubulations to permit the attachment of vacuum gauges, mass spectrometers, or other experimental equipment. An unusual type of gas diffuser was installed within and near the flanged end of the test chamber to permit pure gases to be introduced. The gas diffuser was connected via calibrated capillary tubes to a small "gas inlet" chamber that was pumped by a separate mercury diffusion pump system.

This arrangement permitted pure gases to be introduced into the gas inlet chamber in a continuous flow fashion. A wide range of pressures of pure gas could thus be established in the gas inlet system. Of the two capillary tubes used to join the gas inlet chamber and the gas diffuser of the test chamber, only the larger bore tube was valved with an all metal, bakeable valve. The smaller bore tube had such a small vacuum conductance (about 6.0×10^{-6} liters/sec) that it would not limit the ultimate pressure attainable in the test chamber (with a gas inlet chamber pressure of 10^{-8} torr) until a pressure of 10^{-15} torr was reached.

Referring to the block diagram of Figure 1 and the photograph of Figure 2, it can be seen that all of the UHV components, the calibration capillaries, the gas inlet chamber, the bakeable valves, the gas inlet gauge, and the cold cathode gauges on the test chamber were located above an insulated table top so that they could be conveniently baked out in the same oven. The components located below the insulated table top were not baked, with the exception of the tubing that joined the UHV diffusion pump to its isolation cold trap and the tubing that joined the gas inlet chamber to its isolation cold trap.

A Welch model 1402B 140 liter/min two stage rotary mechanical pump was used to create a forepressure of the order of 10 to 20 microns for both the UHV pumping portion of the system and the gas introduction portion of the system. The mechanical pump was fitted with a vented exhaust to minimize the condensation of vapors and the subsequent

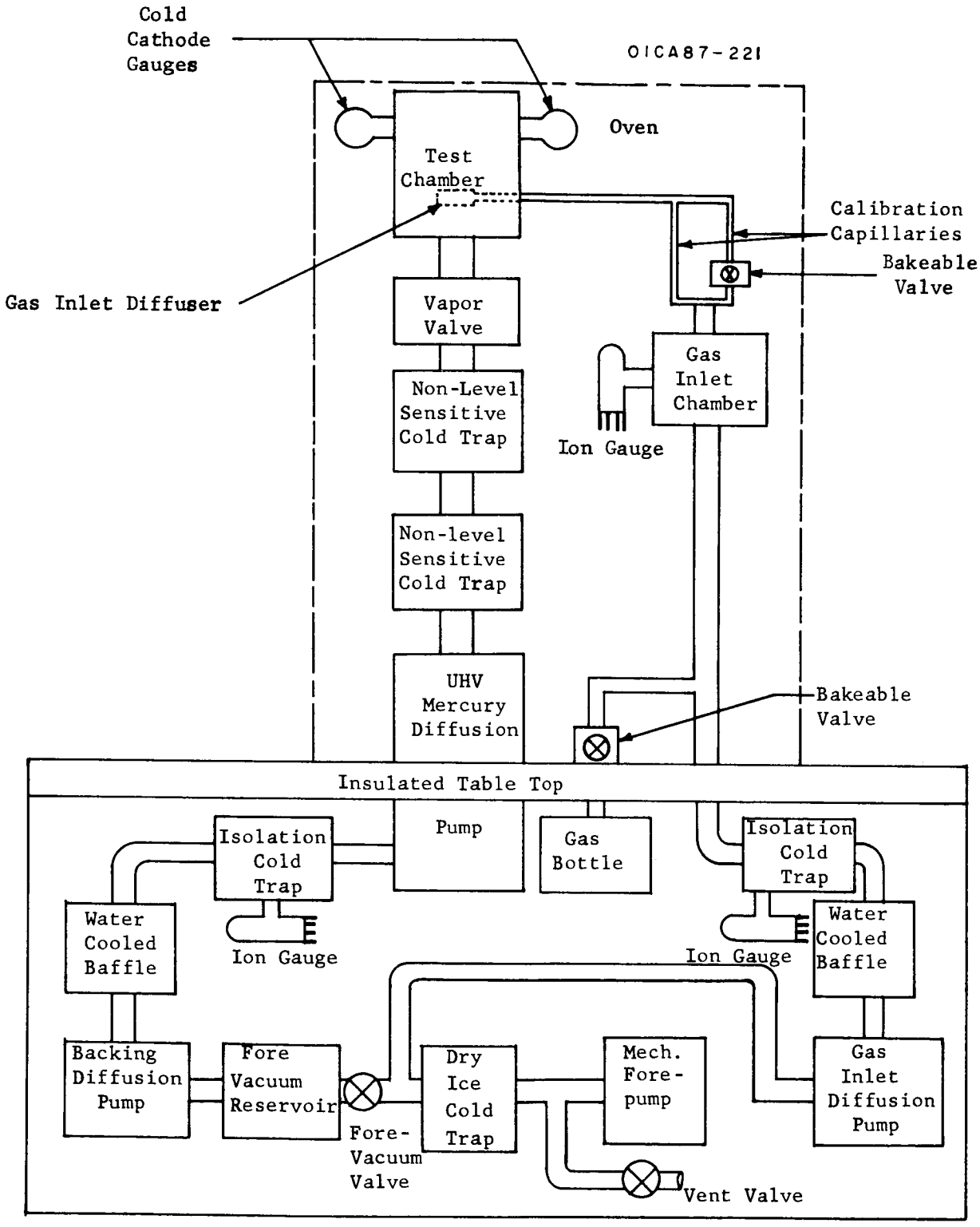

Figure 1. Block diagram of all-metal, (UHV) mercury diffusion pump system.

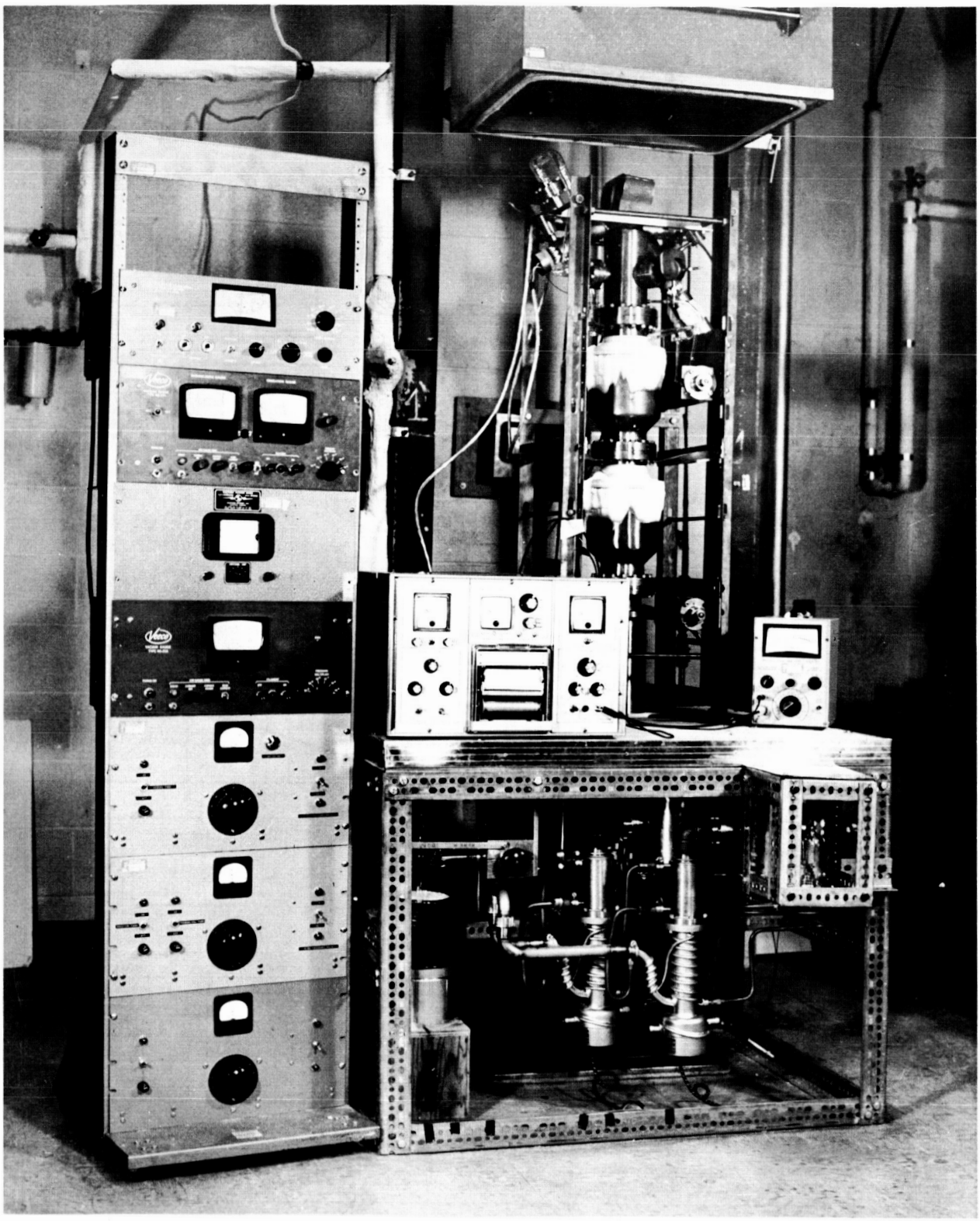

Figure 2. Photograph of mercury diffusion pump system.

contamination of the pump oil. The mechanical pump was separated from the rest of the system by a demountable glass vacuum trap that was cooled with dry ice. A stainless steel, bellows type valve using teflon gaskets and a zytel seat was connected between the mechanical pump and the dry ice cold trap to serve as a venting and leak testing valve.

A stainless steel, bellows type fore-vacuum valve was located between the dry ice cold trap and a 2 liter glass bulb that served as a fore-vacuum reservoir. The fore-vacuum valve could be closed to completely isolate the UHV pumping section from the gas introduction part of the system.

The backing diffusion pump and the gas inlet diffusion pump were Consolidated Vacuum Corporation Model MHG-40 metal mercury diffusion pumps. Specially designed water cooled baffles, to be described shortly, fitted directly over the tops of the diffusion pumps and served the purpose of reducing the loss of mercury to the isolation cold traps. The latter traps were designed for a two-fold purpose: First, they isolated the flow of mercury from one pump to another in the UHV system, and kept mercury out of the gas inlet chamber. Second, they permitted ionization gauges to be installed in these portions of the vacuum circuit. The ionization gauges were particularly valuable during the bakeout cycle since they would indicate the degree of outgassing of those parts of the system within the oven. The two isolation cold traps were mounted just below the insulated table top.

Circular cut-outs in the table top allowed these cold traps to be filled with liquid nitrogen from above the table top, and permitted the traps to be easily disassembled for cleaning.

The UHV mercury diffusion pump was designed so that the entire jet assembly could be baked out in the oven. The upper part of the pump containing the jets was located above the insulated table top, while the pump bolier was located well below the table top. This arrangement, combined with the unusual design of the pump, permitted the upper part of the pump to be baked to temperatures of 450°C and above.

The top of the UHV diffusion pump was fitted with a Varian 6" O.D. ConFlat flange so that the lower non-level-sensitive cold trap bolted directly to the pump. Both non-level-sensitive cold traps had 6" O.D. ConFlat flanges at the top and bottom. The function of the cold traps was to prevent any migration of mercury from the UHV diffusion pump into the test chamber. The upper non-level-sensitive cold trap had a specially machined 6" O.D. ConFlat flange at the top. This flange was designed to house one fixed and one moveable plate, the combination comprising a "vapor" valve. The valve had a conductance of about 10^{-2} liters/sec in the closed position and a conductance of about 350 liters/sec in the fully open position.

The test chamber consisted of a cylindrical housing closed at the top, and flanged with a 6" O.D. ConFlat flange at the bottom. A gas

inlet diffuser was mounted through the side wall of the test chamber above the flange. The function of the diffuser was to eliminate beaming of the gas flow by directing molecules radially outward toward the cylindrical side walls of the chamber. Three flanged side tubulations spaced 120^{o} apart permitted various gauges, etc.,to be connected to the test chamber.

The test chamber and the two non-level-sensitive cold traps were all bolted together,and their weight was supported by the UHV mercury diffusion pump. The diffusion pump was fastened to the insulated table top via a large stainless steel plate that rested on the table top. Hanger-type brackets bolted to the steel plate were fastened to the pump manifold. In this way, the table top and its supporting angle iron structure bore the entire weight of the system.

The two calibration capillaries that were used to limit the flow of gas from the gas inlet chamber to the test chamber were precision bore borosilicate glass capillaries. The larger capillary had a nominal bore diameter of 0.0395 inches (1 mm.),while the smaller capillary had a bore diameter of .0081 inches (0.2 mm.). The actual average diameters of these capillaries were carefully measured by weight of mercury. The capillaries were about 7 inches long. As mentioned before, a bakeable valve (Granville Phillips Type C) was used to close off the 1 mm. diameter capillary when the lowest pressures were to be attained in the test chamber. The 1 mm. diameter capillary permitted pressure reduction, flow type calibrations to be

made to pressures as high as 10^{-8} torr.

The gas inlet chamber to which the calibrated capillaries were attached was connected, via 1 inch diameter tubing, to the isolation cold trap of the gas introduction system. A 1-liter bottle of pure gas was connected through a second bakeable valve to the 1 inch diameter tubing as shown in the block diagram. Notice that the gas bottle was located just below the insulated table top so that the complete tubulation to the gas bottle was baked out (that is, before the seal-off tip on the gas bottle was broken). This arrangement guaranteed a minimum of contamination of the pure gas admitted to the system. The gas inlet chamber also contained a side tubulation to which a hot filament ionization gauge was connected. If desired, a McLeod gauge could also be connected to this side tubulation to measure the pressure in the gas inlet chamber.

The framework below the insulated table top that housed the fore-vacuum portion of the system was constructed of drilled and slotted angle iron (Acme Steel slotted angle 225). The dimensions of the framework were 42L x 36W x 33H. The table top itself had a laminated construction consisting of two sheets of 3/4-inch thick marinite 36, separated by aluminum foil, and backed by a ½-inch thick sheet of transite.

Above the insulated table top, and fastened to it with angle brackets, was a stainless steel framework that surrounded all portions

of the system that were baked. This framework was 16 inches square and 48 inches high,so that it would easily fit within the interior portion of the oven. The non-level-sensitive cold traps were braced to the stainless steel framework to rigidize the entire upper part of the system.

The oven, constructed by Gruenberg Electric Company, was of the forced draft variety and was designed to be used with the vacuum system. The internal working space within the oven measured 18 inches square by 60 inches high. Externally, the oven measured 28x24x84 inches. It was suspended by counterweighted steel cables that passed over pulleys attached to horizontal beams. The horizontal beams were supported by two 4 inch steel I-beams that rested on the concrete floor of the laboratory. Spring-loaded pulleys attached to the back of the oven at four positions engaged the edges of the I-beams and acted as vertical guides for oven movement. Provision was made to lock the oven to the I-beams. The laboratory ceiling height of 15 ft was adequate to permit the oven to be raised above the stainless steel framework.

The oven was temperature controlled by means of a Wheelco model 297 controller. The temperature range of control varied up to 540°C. Temperature was generally held constant to within a few degrees centigrade as measured with a mercury-in-glass thermometer. The power input to the oven heaters was 12 Kw at 200 volts, 3 phase.

During the system bakeout procedure, to be described later, it was customary to bake out with the oven at several fixed positions above the insulated table top. Under these conditions, it was necessary to seal off the open, bottom end of the oven. An insulating, demountable oven base was fashioned out of 1½ inch thick marinite 36 so that it would overlap the edges of the 6" O.D. ConFlat flanges of either the UHV diffusion pump or the non-level-sensitive cold traps and then extend outward to seal the oven opening. The demountable oven base consisted of four separate pieces that locked together with aluminum dowel pins. The base was supported by resting on angle iron braces connected to the stainless steel framework at the proper positions.

3.1.2. Component Design. Since most of the individual components of the UHV mercury diffusion pump system were unique in design, it will be worthwhile to describe them in greater detail. In each case, an assembly drawing of the component, with the major parts labelled, will be used to illustrate the design and construction.

UHV Mercury Diffusion Pump. The UHV pump was the central element of the entire system. It was designed to have certain features that would make it especially suitable for low pressure operation. The top jet of the pump was relatively small in diameter and was shaped to emit its vapor steam in essentially a downward direction. The spacing between the top and bottom jets was made relatively large to increase the probability of entraining gas molecules. The bottom jet,

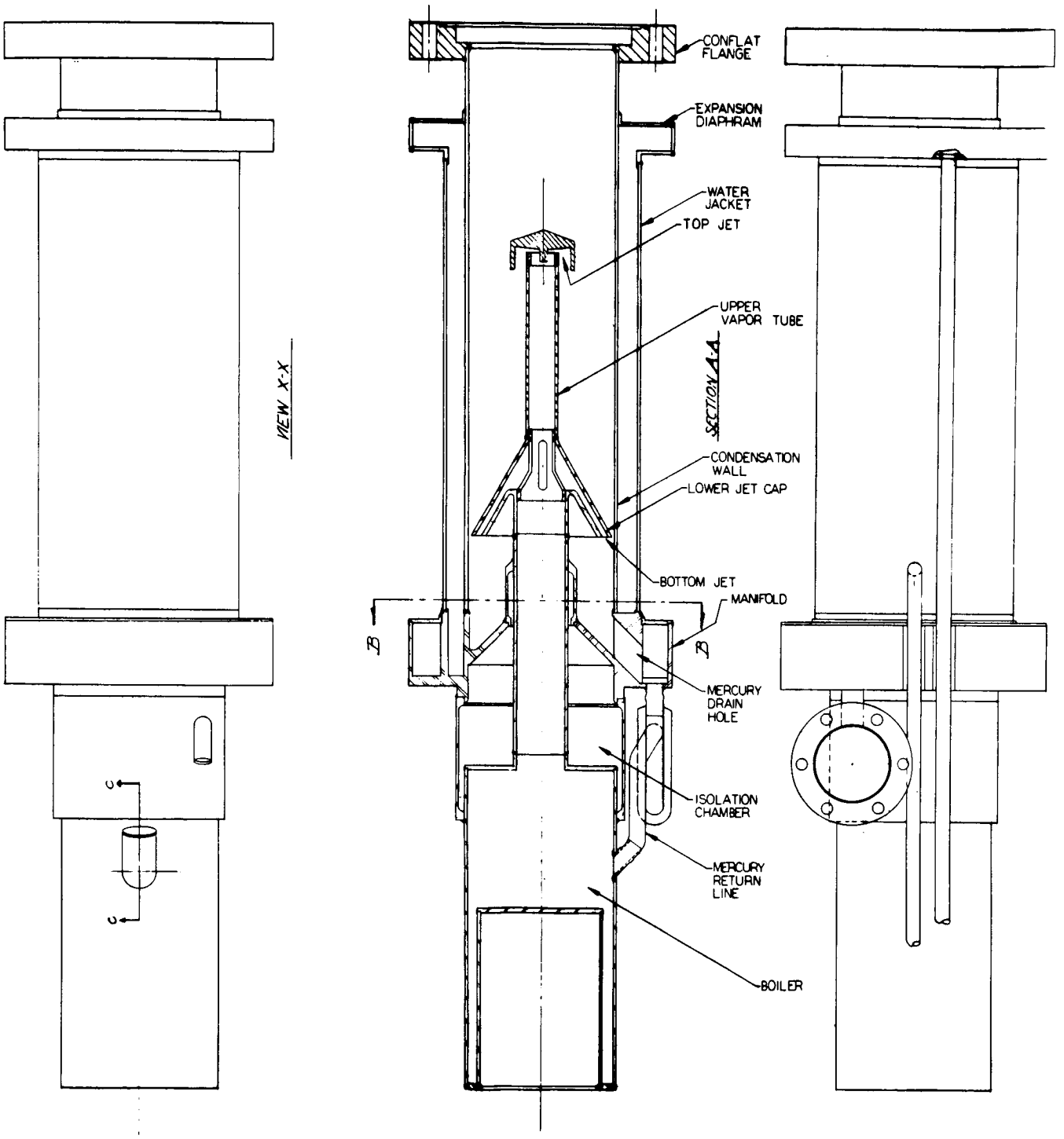

Figure 3. Mercury diffusion pump.

with its closer spacing and higher temperature vapor served to prevent back diffusion of higher pressure gas. In other words, the lower jet provided a high fore-pressure tolerance while the top jet provided a high pumping speed at low pressures.

The condensation wall (pump barrel) of this pump was kept at a uniform, low temperature by using an annular water jacket instead of the more conventional water cooled spiral coil that is soldered or brazed to the pump barrel. An expansion diaphragm near the top of the water jacket relieved any stresses that might be created by differential expansion during the bakeout period. The pump manifold located just below the water jacket was well cooled during normal pump operation. The manifold was the key element in the construction of the pump. The water jacket and jet assembly were welded to the top of the manifold while the pump boiler and isolation chamber were welded to the bottom of the manifold. An interrupted annular region near the periphery of the manifold served as a water cooled fore-vacuum line at the same time that condensing mercury was returned to the boiler via a mercury drain hole connecting the top, central portion of the manifold with the interrupted manifold volume. The mercury return line to the boiler was constructed with a glass segment so that the condensation action of the pump could be monitored. In addition, a glass viewing port was installed just above the mercury level in the re-entrant type boiler to permit viewing of the mercury surface. Unfortunately, the position of the pump boiler just below the insulated table top of the system made it almost impossible to use this viewing window.

The isolation chamber located just above the pump boiler acted as a heat insulator to separate the hot boiler from the cold manifold during normal operation. During the bakeout period, the isolation chamber served to minimize heat flow from the hot manifold to the boiler. A vacuum of 10 to 20 microns was maintained in the isolation chamber via a direct connection to the mechanical rotary pump.

The pump boiler was filled with about 6 lb of mercury. The pump heater consisted of a ceramic supported cone-shaped heating element of the type used in small parabolic reflector space heaters. A 660-watt nichrome wire heater was found to be adequate. The outside of the boiler was insulated with a stacked series of rings of marinite 36. The rings were held together with long steel rods that were threaded at the ends and capped with nuts.

The jet assembly of this pump was fabricated to permit the top jet, the upper vapor tube, and the lower jet cap to be removed for inspection and/or cleaning from the top of the pump. All other elements of the pump were permanently welded.

The pump was made almost entirely of 304 low carbon stainless steel (except for minor parts of Kovar and pyrex). All mating elements were tungsten inert gas welded (Heliarc). Wherever practicable, welds were made within an inert atmosphere welding chamber filled with Argon. It was found that these welds were almost completely free of oxidation.

The upper part of the UHV pump, including the manifold, was baked many times at various temperatures up to a maximum of 475^{o}C without

any ill effects. The pump was disassembled twice during the course of experimentation to check its condition.

Non-Level-Sensitive Cold Trap. As a result of several years of experience with glass cold traps of the Venema type,[7] it was realized that a number of modifications could be made to improve the performance and usefulness of this component. One of the principal difficulties with the original design was its sensitivity to changes in the level of the liquid nitrogen coolant. As the liquid level was lowered due to evaporation, internal surfaces of the cold trap warmed up and began to desorb large quantities of gas. This would cause the system pressure to rise. In order to keep the system pressure constant, the trap had to be filled every few minutes.

In addition to liquid level sensitivity, the old glass cold traps had low mercury vapor trapping efficiency. It was possible for mercury atoms to pass through the trap after only a single contact with a cooled inner surface. Also, because of their glass construction, the vacuum conductance of these traps was limited. Finally, the unusual glass construction of these components made them particularly susceptible to breakage.

The new stainless steel, non-level-sensitive cold trap is illustrated in Figure 4. This trap was designed so that every atom of mercury would have to make at least two collisions with a cold surface in order to pass through. On this basis, two cold traps of the new type would

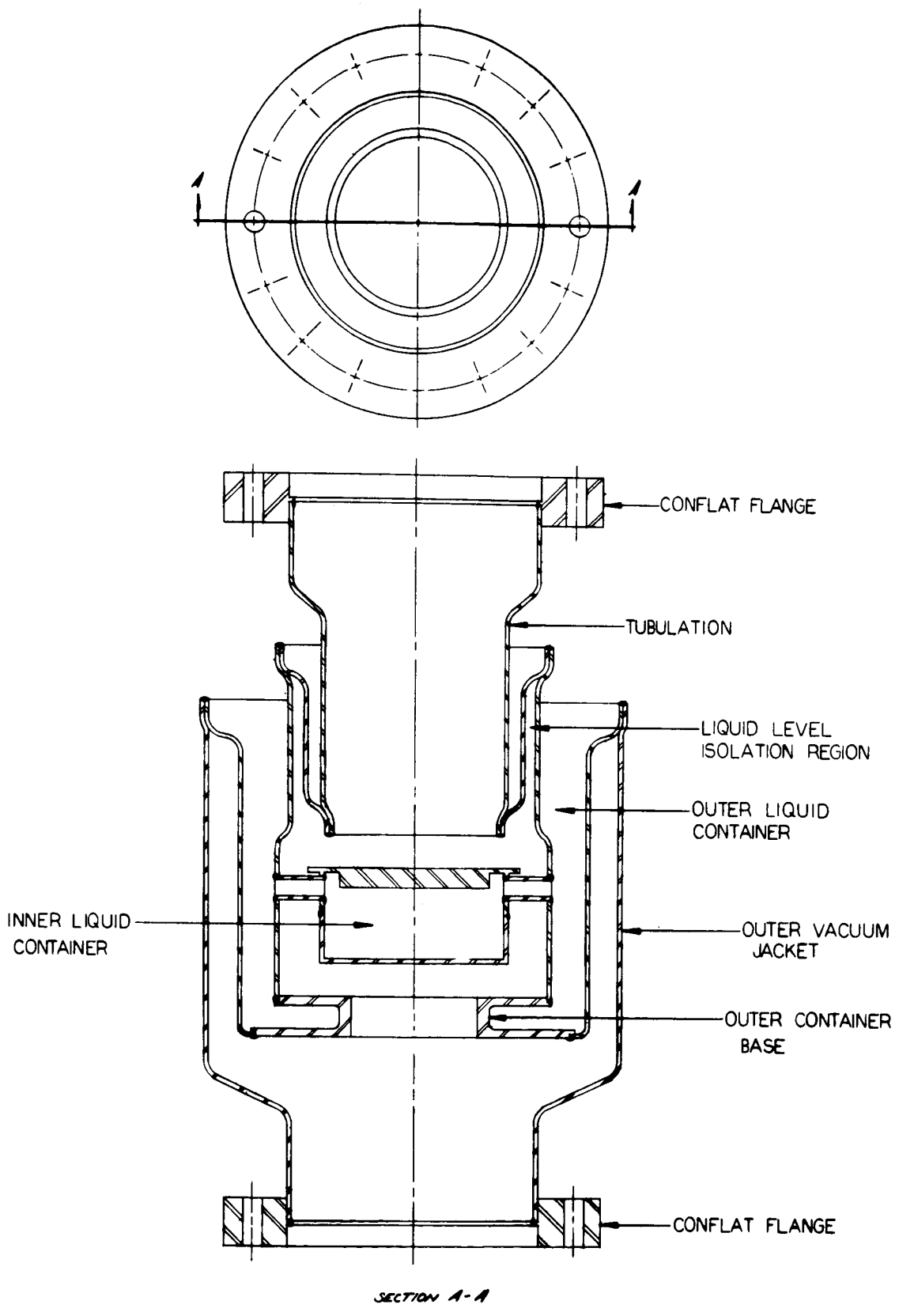

Figure 4. Non-level sensitive cold trap.

be equivalent to four cold traps of the old design. By reducing the number of cold traps required to eliminate back flow of the pumping fluid, additional benefits were gained: First, there were fewer components and vacuum connections; second, the internal surface areas were reduced so that outgassing was reduced; and third, the total vacuum conductance of the cold traps was increased.

The new cold trap was designed so that the various cylindrical elements would nest together and be self supporting under compression (under its own weight). Nesting was accomplished by a combination of machining and metal spinning operations, as can be seen in the drawing. The heliarc welds were used primarily to attain vacuum tightness rather than mechanical rigidity.

The trapping efficiency of the new design depended on the arrangement of the central, inner liquid container and the surrounding, outer liquid container. Most vapor atoms entering the bottom of the trap were condensed on the bottom cold surface of the inner container. However, some vapor atoms could move directly to the cooled inner wall of the outer container. Those atoms which did not condense on this inner wall could then move to either the cooled cylindrical side wall of the inner container or else move a greater distance upward to the liquid level isolation region. In either case, the atoms had to make at least two collisions with cold surfaces before they escaped from the trap.

The cylindrical inner container was supported at the center of the cold trap by two short horizontal tubulations. Liquid nitrogen poured into the outer liquid container would eventually reach the level of the supporting tubulations and then begin to flow into the inner liquid container. The top of the inner container was designed so that it would extend into the liquid coolant despite the presence of any trapped air bubbles.

The non-level-sensitivity of the new cold trap was insured by the buffer vacuum created in the liquid level isolation region by the vacuum system itself. Variations of the liquid level in the outer container caused no marked temperature variations of the tubulation leading to the top flange. Of course when the liquid in the outer container reached the same level as the top of the inner container, some of the gas desorbed from the walls could move directly into the tubulation. It took approximately one hour for the liquid level to fall this low.

The liquid coolant capacity of the non-level-sensitive cold trap was 950 cm^3. The flange-to-flange vacuum conductance of the cold trap was computed to be 54.2 liters/sec for nitrogen at 25°C. Two cold traps in series had a combined vacuum conductance of 27.1 liters/sec for nitrogen at 25°C.

The non-level-sensitive cold traps were second only to the UHV mercury diffusion pump in their complexity and difficulty of construction. The spinning of such elements as the outer vacuum jacket required

a great deal of experience and skill, and the entire assembly process had to be planned in advance to insure completely leak tight components.

Vapor Valve. The vapor valve was designed to play either one of two roles. It could be closed to isolate the test chamber from the rest of the pumping system, or it could be fitted with an orifice of small dimensions to limit the effective pumping speed at the test chamber. It was designed to be contained within a standard 6-inch O.D. ConFlat flange so that it would create a minimum of flow impedance and could be easily removed without affecting the remainder of the system.

The valve consisted essentially of two smooth, flat, circular plates or disks about 1/8 inch in thickness and 4-3/8 inches in diameter. The lower plate was fitted closely to a counterbore at the inside of the ConFlat flange and was pinned in position. The upper plate fitted relatively loosely in the same counterbore and rested on the fixed lower plate. The upper plate was free to rotate. A stainless steel magnet holder containing two 3/4-inch diameter holes was attached to the upper plate. Cylindrical bar magnets made of Alnico V material were placed in the 3/4-inch diameter holes and sealed vacuum tight by welding plug covers over the openings.

Both the fixed lower plate and the rotatable upper plate had D-shaped cutouts. When the two D-shaped openings were aligned, as shown in the drawing, the valve was open. When these openings were 180 degrees

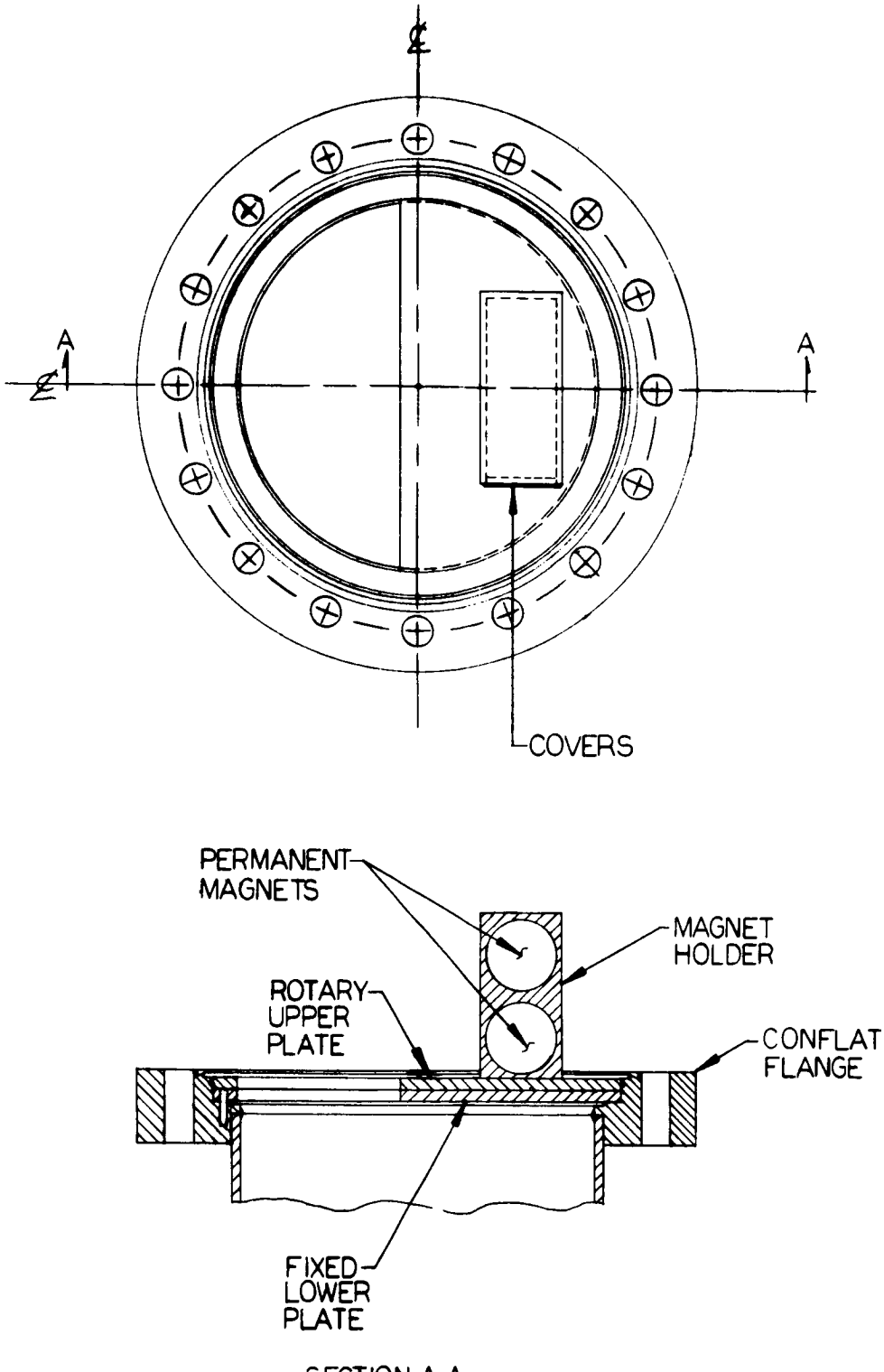

Figure 5. Vapor valve.

out of alignment, the valve was closed. The computed conductance of the valve in the closed position (based on an estimated gap of .001" between the plates) was 1.7×10^{-2} liters/sec.

The valve was operated by means of a large permanent magnet external to the system. The position of the valve could be easily determined by placing two small ball bearings made of magnetic material on the outside of the upper ConFlat flange. The ball bearings would be drawn into positions corresponding to the two edges of the magnet holder closest to the flange.

During the course of experimentation, it appeared that the plug cover sealing one of the Alnico V magnets into the magnet holder was not completely leak tight. This virtual leak prevented the lowest pressures from being attained, and so the valve plates were removed during low pressure operation.

For the limited time that the valve was operated in vacuum, a period of a week or so, there was no indication of cold welding of the plates. However, if the external magnet used to rotate the upper plate had too weak a magnetic field, there was stick-slip rotation of the upper plate.

Test Chamber. The diffusion pump system test chamber was a relatively simple component. It consisted of a cylindrical chamber 4" in diameter and 8" long. The bottom of the chamber was flanged with a 6" O.D. ConFlat flange. About midway between the top and

bottom of the chamber there were three short 1½" O.D. side tubulations. The three tubulations were spaced 120 degrees apart and were flanged with 2-3/4" O.D. ConFlat flanges.

Ordinarily, vacuum gauges or mass spectrometers were connected to the test chamber side tubulations. The tubulations were deliberately spaced 120 degrees apart so that one gauge would not "look" directly into the tubulation of another gauge. Since the tubulations were all in the same plane normal to the axis of the pumping system (and the gas inlet diffuser) and pointed toward a common point (the vertical axis of the test chamber), it was presumed that each tubulation would "see" the same pressure.

As constructed, the test chamber was permanently closed at the top. However, it would be a simple matter to remove the chamber top and weld another ConFlat flange at this location. If this were done, it would then be possible to connect additional apparatus to the chamber in a demountable fashion. For example, electrical connections could be introduced, or another pump (such as the liquid helium cryopump to be described shortly) could be attached. Such a modification would make the chamber more flexible and useful.

Not shown in the drawing of Figure 6 is the gas inlet diffuser which enters the side wall of the chamber at a point about 1 inch above the large ConFlat flange. If the gauges and/or mass spectrometers attached to the side tubulations have a negligible pumping action,

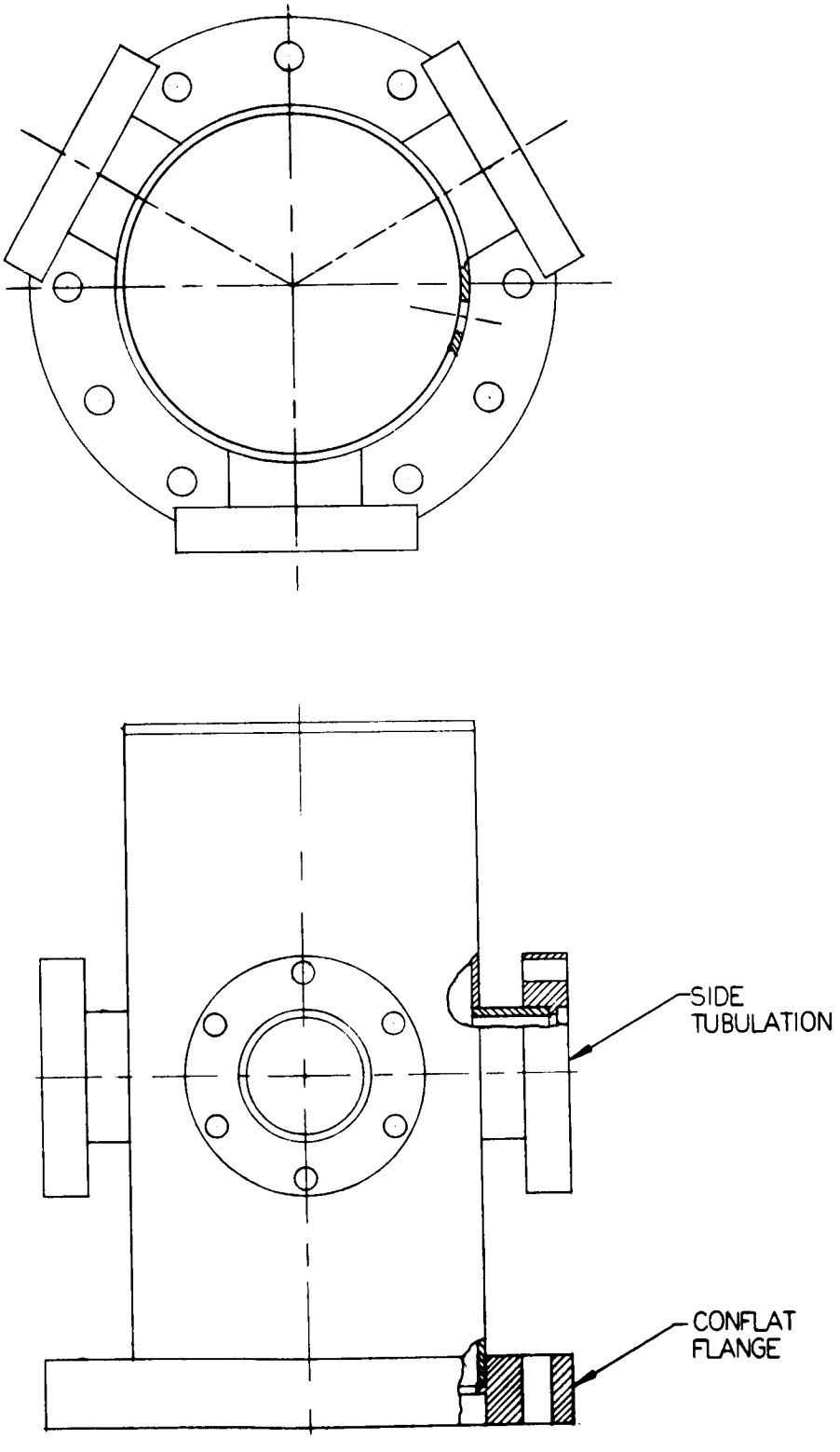

Figure 6. Test chamber.

the pressure in the test chamber above the plane of the gas inlet diffuser should be uniform.

Gas Inlet Diffuser. As shown in the drawing of Figure 7, the gas inlet diffuser consisted of only a few elements. The relatively small diameter gas entrance tube that brought gas into the test chamber had a heavy wall (welding wall) portion where it was welded to the test chamber. The open end of this tube had a weld shoulder to which a Kovar-pyrex graded seal was attached. The calibrated glass capillaries were connected to the pyrex of this graded seal. The closed end of the tube was welded to the small hollow cylindrical diffusion chamber.

Slots at the top and bottom of the gas entrance tube directed incoming gas molecules against the flat top and bottom surfaces of the diffusion chamber. After a number of collisions with the inside walls of the diffusion chamber, molecules would leave the chamber through one of 15 small gas exit holes that were drilled through the cylindrical side wall. The holes were spaced 22½ degrees apart and were located symmetrically with respect to the gas entrance tube. The function of the diffuser was to direct molecules symmetrically to the side wall of the test chamber so that the gas pressure developed at the plane of the diffuser would be fairly uniform.

Gas Inlet Chamber. The gas that was permitted to flow through the calibrated capillaries into the test chamber was drawn from a relatively small chamber where its pressure could be measured. Various

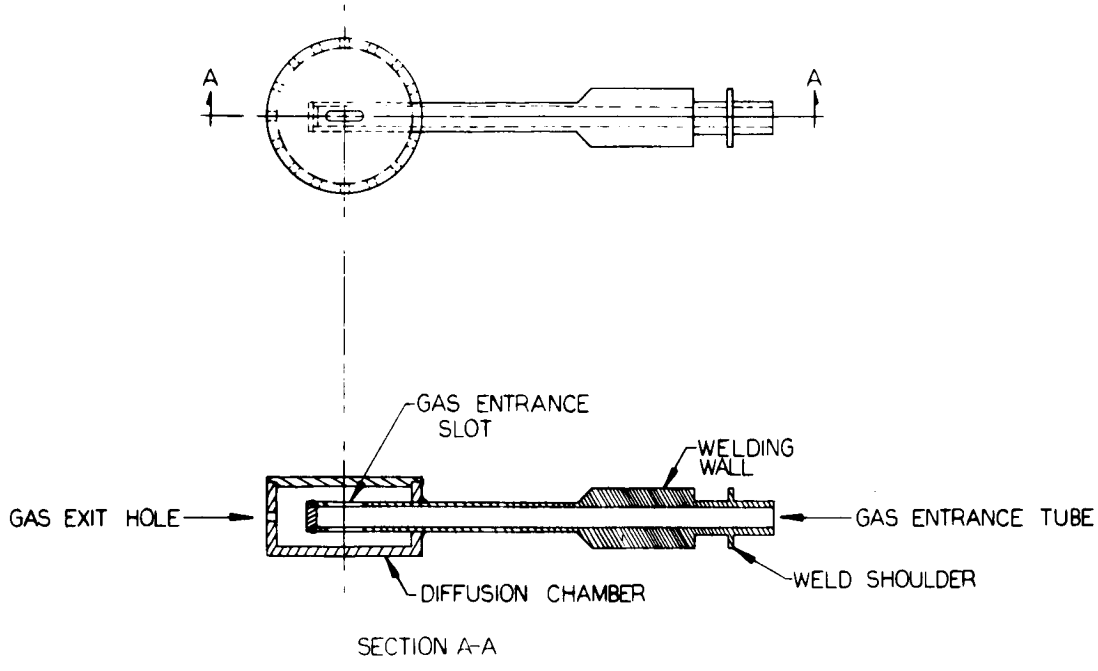

Figure 7. Gas inlet diffuser.

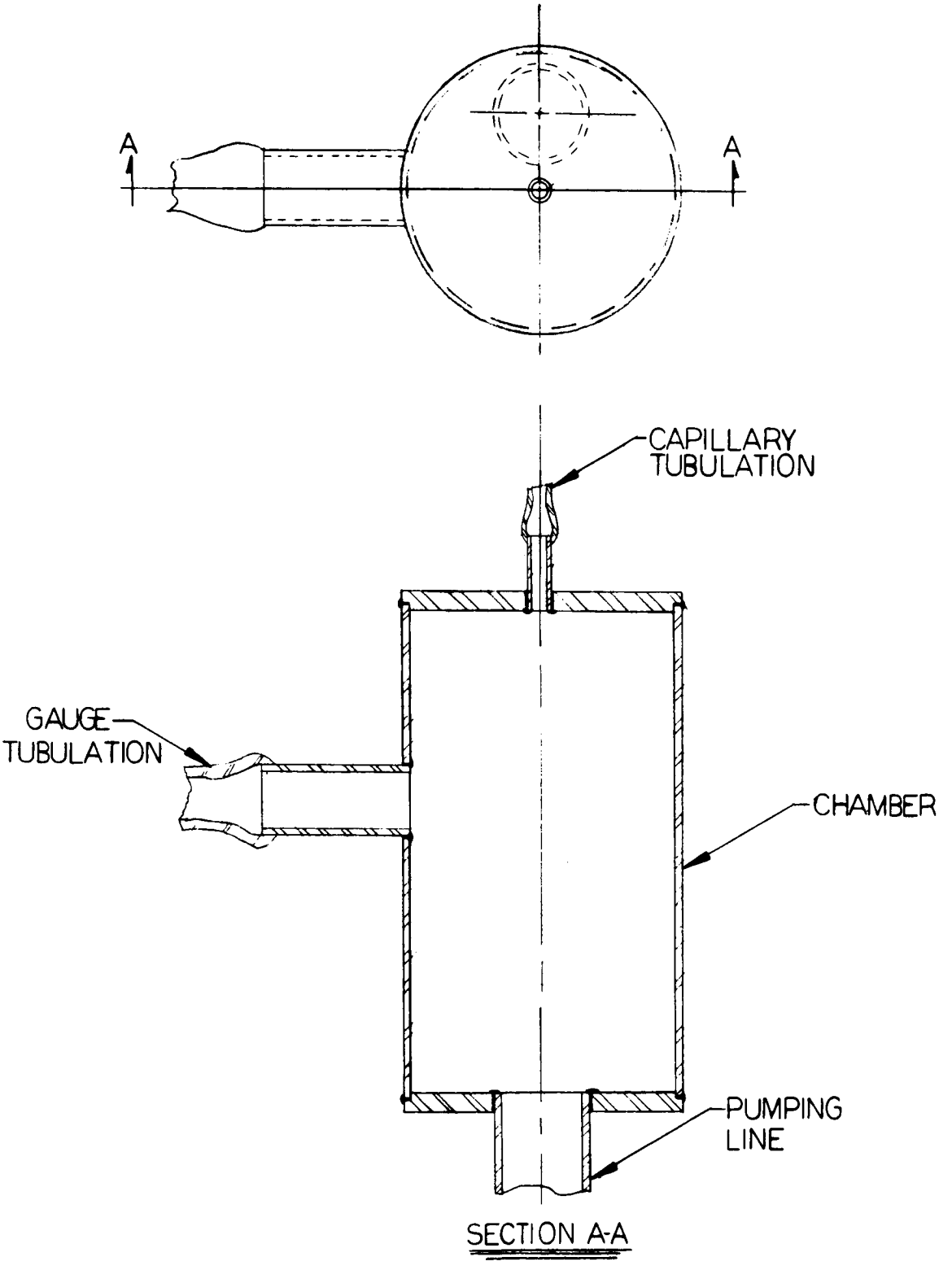

Figure 8. Gas inlet chamber.

gas pressures were established in the gas inlet chamber by varying the leak rate of the metal valve that separated the gas bottle from the pumping line connecting the gas inlet chamber and the gas introduction portion of the pumping system. The pumping line had a diameter of 1 inch above the insulated table top and terminated in a 2-3/4" O.D. ConFlat flange just below the table top. The pumping line below the table top was 1½ inches in diameter.

A hot filament gauge was connected to the gauge tubulation, a graded Kovar to pyrex seal, as shown in the figure. It was normally operated at reduced emission to minimize its pumping action. The capillary tubulation to the gas inlet chamber was also a Kovar-pyrex graded seal.

Isolation Cold Trap. The isolation cold trap proved to be a very useful and trouble-free component of the vacuum system. It acted efficiently to block the flow of mercury vapor in either direction through the trap and permitted pressure measurements to be made at the position of the trap.

Referring to Figure 9, it can be seen that the outer housing or shell of this component was generally cylindrical with a tapered upper portion and a flat-bottomed base. Two 1½" O.D. pumping tubulations were welded through the side wall of the shell so that they extended about the same distance inside the shell as outside. The tubulations were placed diametrically opposite one another and were flanged on

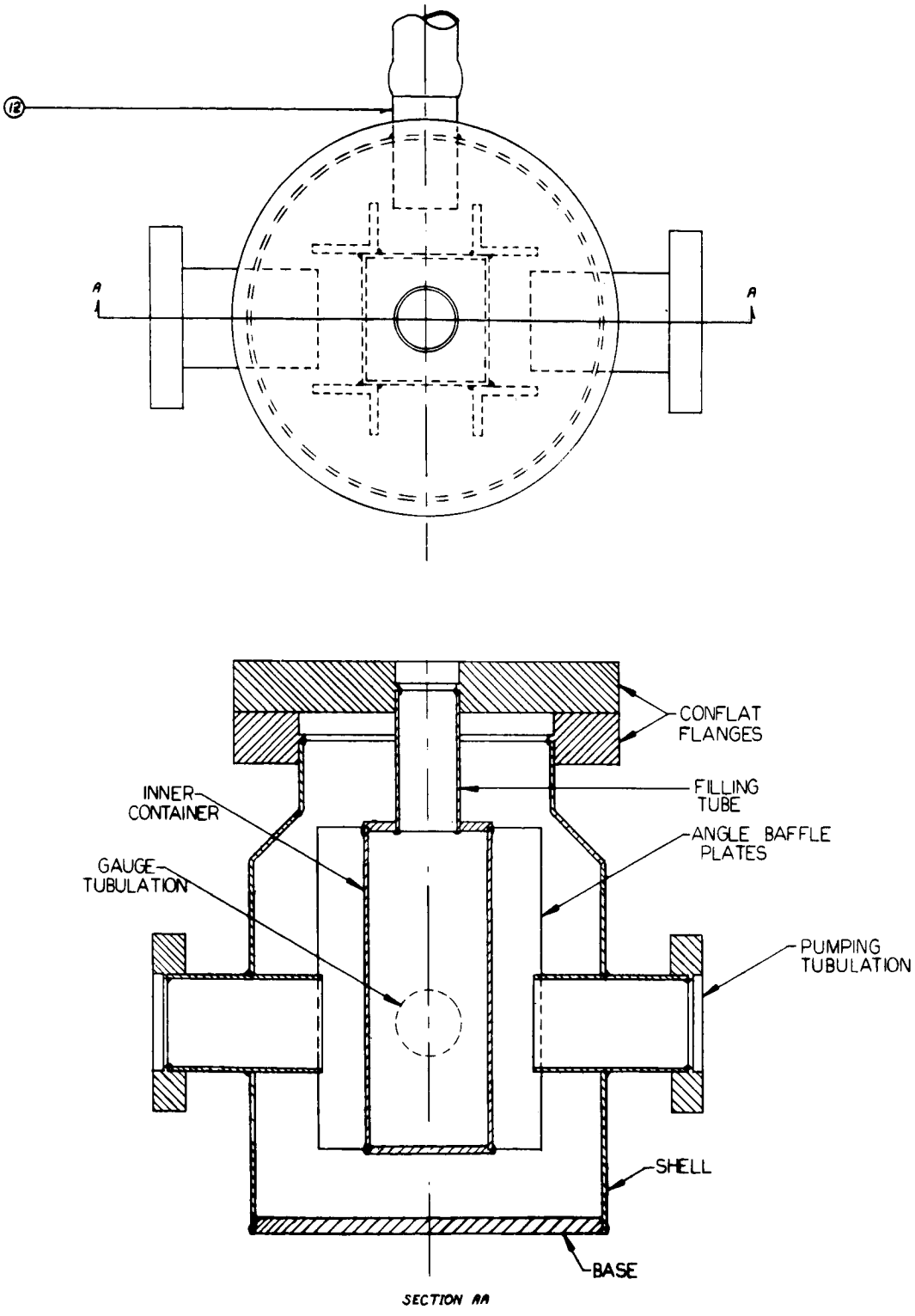

Figure 9. Isolation cold trap.

their outer ends with 2 3/4" O.D. ConFlat flanges. A Kovar-Pyrex graded seal was also welded through the sidewall of the shell at a position 90 degrees from either pumping tubulation.

A portion of square stainless steel tubing was used as the inner container. The square tubing (about 2"x2"x5") was closed at the bottom and connected to a cylindrical filling tube at the top. The filling tube had a small wall thickness to minimize its heat conduction and was welded to the top (cover) ConFlat flange.

Four stainless steel angle pieces 3/4"x1"x5" were tack-welded to the square liquid nitrogen inner container along the edges as shown. The angle pieces served as baffle plates to shield the inner ends of the pumping tubulations and the gauge tubulation from direct line-of-sight exposure to the uncooled shell or housing of the cold trap.

The capacity of the isolation cold trap inner container was about 300 cm^3. The filling tube served for both filling and venting the liquid nitrogen. There was never any difficulty with icing of the filling tube. A cover of marinite 36 was generally kept in position above the top flange of this cold trap.

Water-Cooled Baffle. In order to minimize the loss of mercury from the Consolidated Vacuum Corp. model MHG-40 mercury diffusion pump, it was decided to build a special cold water baffle. This baffle was designed to form a connecting link between the diffusion pump and the isolation cold trap and thus facilitate the mounting of the pump.

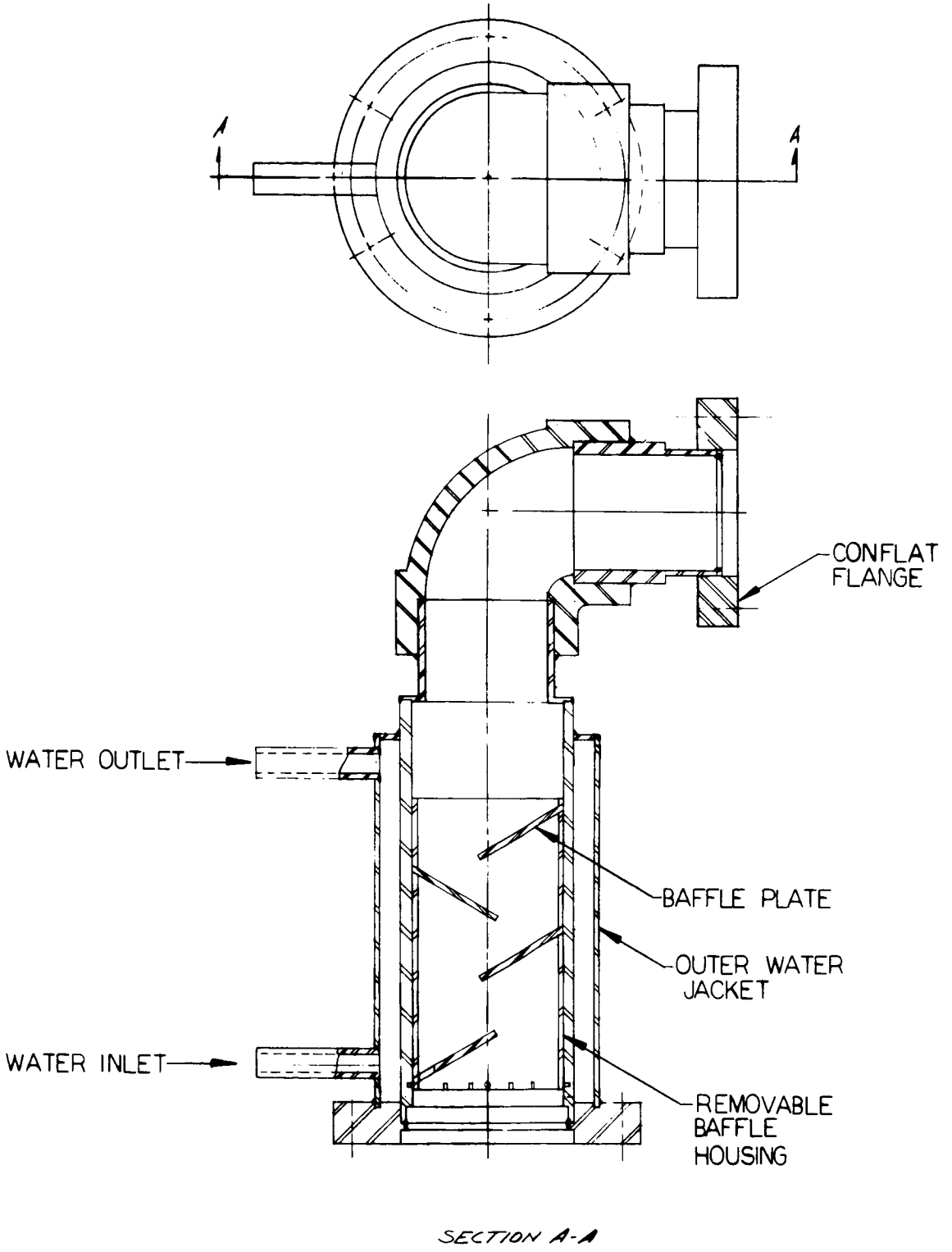

Figure 10. Water cooled baffle.

The actual baffle plates used were elliptical in shape and fitted into slots that were cut in a tubular baffle housing. The baffle housing was held in place with a removable pin so that it could be easily taken out for cleaning. The lowest baffle plate was slotted in the region adjacent to the baffle housing so that any liquid mercury that collected on this plate would be drained back to the diffusion pump. The baffle plates were cooled by conduction from the inner tube of the water jacket.

The lower flange of the water-cooled baffle was designed to mate with the flange of the diffusion pump. The upper flange of the baffle was a 2-3/4" O.D. ConFlat flange that mated with the pumping tubulation flange of the isolation cold trap.

3.2 CRYOPUMP-ION PUMP SYSTEM

3.2.1 Overall Design. The cryopump-ion pump system, as shown in the block diagram of Figure 11 and the photograph of Figure 12, was quite different from the mercury diffusion pump system just described. The ultra high vacuum part of the system consisted of five components: (1) a liquid helium cryopump; (2) a magnetron type ion pump; (3) a test chamber; (4) a bakeable UHV valve; and (5) a calibrated capillary tube. The UHV components were mounted on an insulated oven base and positioned so that they could be baked out by a roll-on type oven.

The fore-vacuum components used with this vacuum system consisted of a Varian Vac Sorb zeolite absorption type pump, a Varian Vacion sputter-ion pump, a fore-vacuum valve, an ionization gauge, and a gas bottle and adjustable leak.

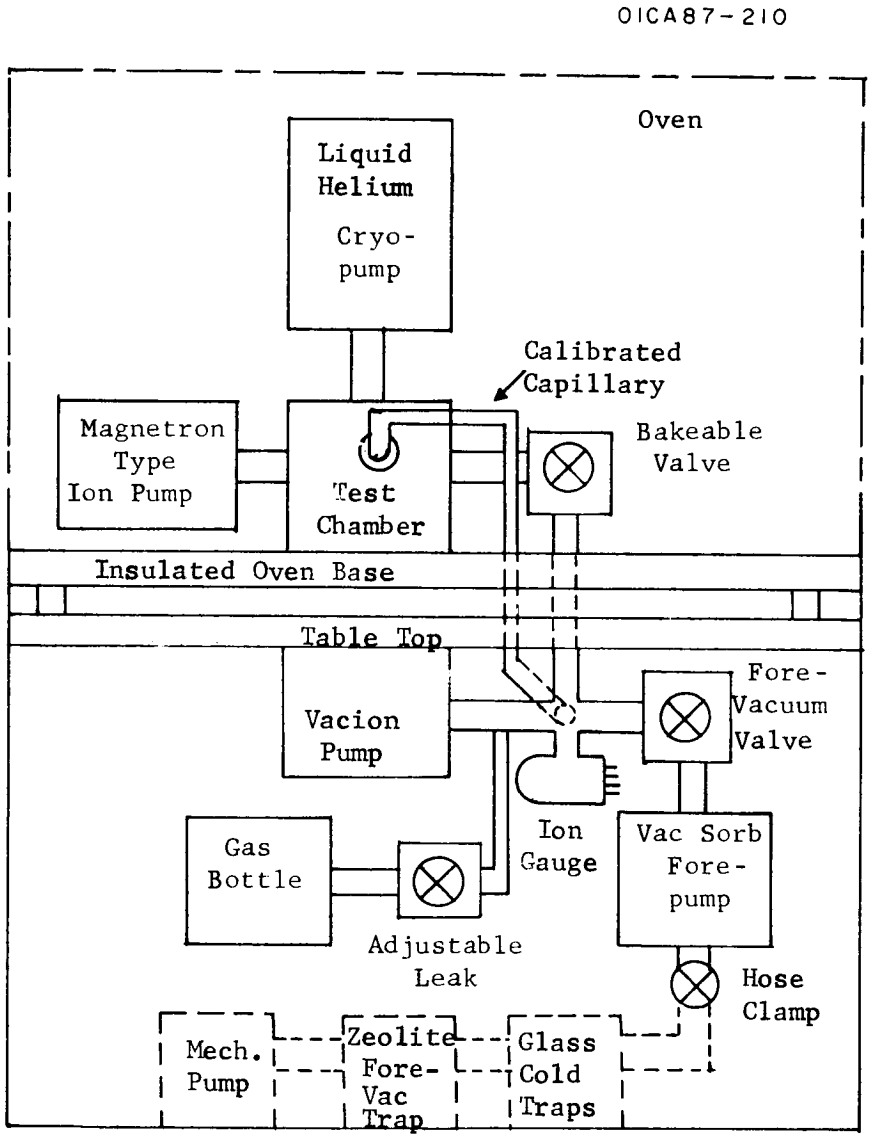

Figure 11. Block diagram of cryopump-ion pump system.

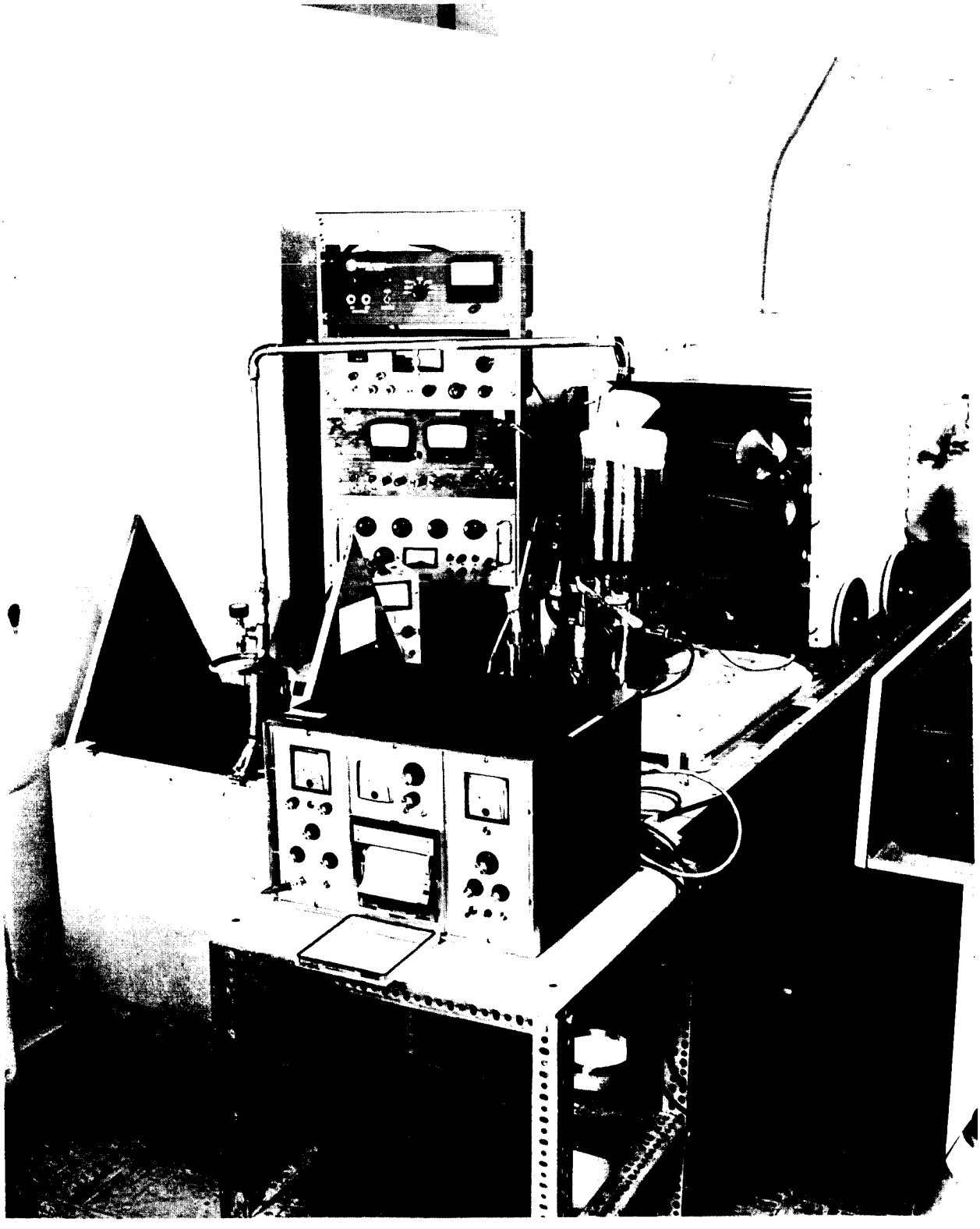

Figure 12. Photograph of cryopump-ion pump system.

In addition to the above components, some auxiliary equipment was used during the system bakeout period. The extra equipment included a rotary mechanical vacuum pump, a zeolite-charged fore-vacuum trap, two glass vacuum cold traps in series, and a rubber connection to the Vac Sorb pump. The rubber connection to the Vac Sorb pump could be closed off with a hose clamp. After bakeout, the fore-vacuum valve was closed to isolate the Vac Sorb pump and all the auxiliary equipment from the rest of the system. When the cryopump was being used, it was necessary to employ a liquid helium transfer line to fill the cryopump from a 25-liter liquid helium dewar.

The entire system was constructed to fit both above and below a standard laboratory table 30x84x34" high. The additional table length served to support the roll-on oven when it was not in use, as shown in Figure 12. A standard electronics rack housed the control units for the ion pumps and ionization gauges.

The liquid helium cryopump was mounted directly on top of the test chamber via a 6" O.D. ConFlat flange. The magnetron type ion pump was connected to one of the four side tubulations of the test chamber. There was adequate clearance between this ion pump and the insulated oven base for mounting the ion pump magnet. The weight of the magnet could have been carried by the pump, but it was thought best to provide a separate support for the magnet.

The bakeable UHV valve that isolated the test chamber, the cryopump, and the magnetron type ion pump from the rest of the system was a Varian 1-1/2" bellows sealed valve. It was mounted on the test chamber side tubulation directly opposite the ion pump. The third side tubulation of the test chamber contained a Varian UHV-14 nude, hot filament ionization gauge, while the fourth side tubulation of the test chamber was used for mounting either a mass spectrometer or a calibrated capillary tube. The connection to the capillary tube consisted of a short length of 3/8" diameter stainless steel tubing that extended inside the test chamber and was shaped to direct the flow of gas at the center of the chamber base.

The UHV bakeable valve above the oven base was connected via 1-1/2" O.D. tubing to one port of a stainless steel ConFlat flanged Tee fitting located just below the table top. A Vacion sputter ion pump and a second Varian 1-1/2" bakeable valve (fore-vacuum valve) were connected to the remaining two ports of the Tee fitting. A Veeco RG-75 hot filament ionization gauge, a glass tubulation to the gas bottle adjustable leak valve, and a glass tubulation to the calibrated capillary tube were attached to the Tee fitting via Kovar-Pyrex graded seals. The Varian Vac Sorb forepump was flanged directly to the fore-vacuum valve.

The Vac Sorb pump, after activation, was used to evacuate the remainder of the system. When the system pressure reached the 10^{-4} or 10^{-5} torr level, the Vacion pump was started and the Vac Sorb pump was valved off. The system pressure was then lowered by several decades, the

bakeable valve above the oven base was closed, and the magnetron ion pump was turned on. The liquid helium cryopump was activated to attain the lowest pressures.

The Vacion pump actually had a dual role in this system. It was used as a fore-pump to pre-evacuate the UHV portion of the system, and it was also used to maintain various gas pressures in the Tee fitting chamber. The gas pressure in the Tee chamber was measured with the Veeco gauge.

3.2.2 Component Design. As was the case for the mercury diffusion pump system, most of the components of the cryopump-ion pump system were unique and require a more detailed description. Assembly drawings of the components, with the major parts labelled, will be used to illustrate their design and construction.

Liquid Helium Cryopump and Cap. The design of the liquid helium cryopump was quite similar in several respects to the design of the non-level-sensitive cold traps. Referring to the drawing of Figure 13, it can be seen that this component had two liquid containers at the center of the assembly. The lower or "inner" container was a shortened version of the inner container that was used in the non-level-sensitive cold trap. It was held in position by two short horizontal tubulations that also served to fill it with liquid nitrogen when the pump was in operation. The upper or "helium" container was suspended from a relatively long, thin-walled fill tube to minimize the conduction of heat to the helium.

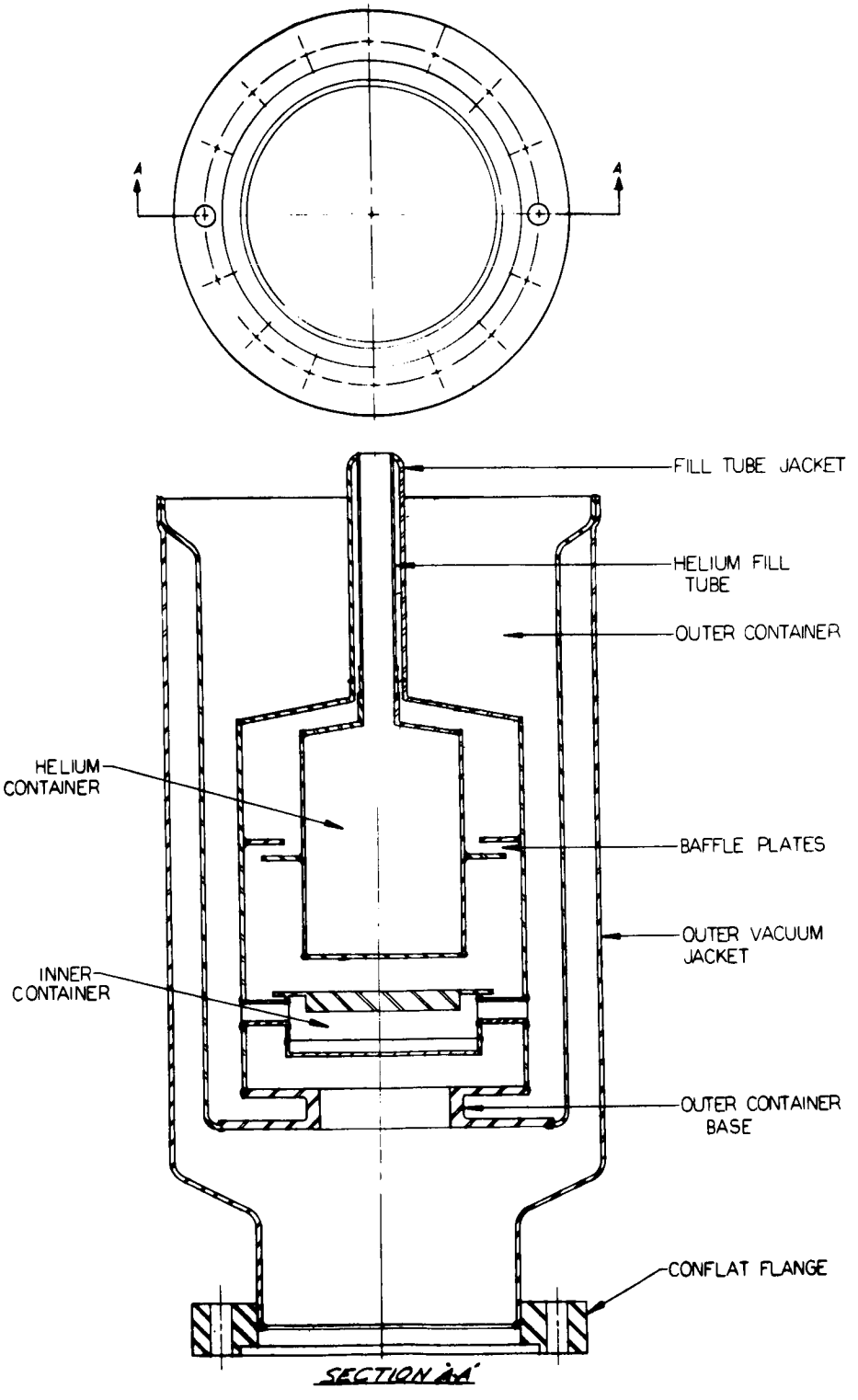

Figure 13. Liquid helium cryopump.

The liquid helium container was almost entirely surrounded by the liquid nitrogen that filled the outer container and the inner container. A relatively large amount of liquid nitrogen was required for the upper portion of the outer container. The same outer container base used for the non-level-sensitive cold traps was also used in the cryopump.

The helium container and its surrounding metal jacket were fitted with annular-shaped baffle plates that were spaced apart, but overlapped. The function of the baffle plates was to help recondense any atoms or molecules which might be desorbed from the top of the helium container when the liquid level became too low.

At first, it was planned to gold plate the helium container to increase its reflectivity, but it was finally decided to sacrifice helium consumption economy in order to test the pumping action of cooled stainless steel surfaces.

The cryopump was designed so that the various cylindrical elements would nest together. The overall height of the pump was just under 14 inches and its maximum diameter was 6-5/8 inches. The liquid helium capacity of the pump was about 240 cm^3.

In order to provide complete shielding of the liquid helium container in the cryopump, a cryopump cap was designed and constructed as illustrated in Figure 14. The cap would be slipped over the fill tube jacket of the cryopump so that its lower portion was submerged in the liquid nitrogen of the cryopump. At the same time, the inner container

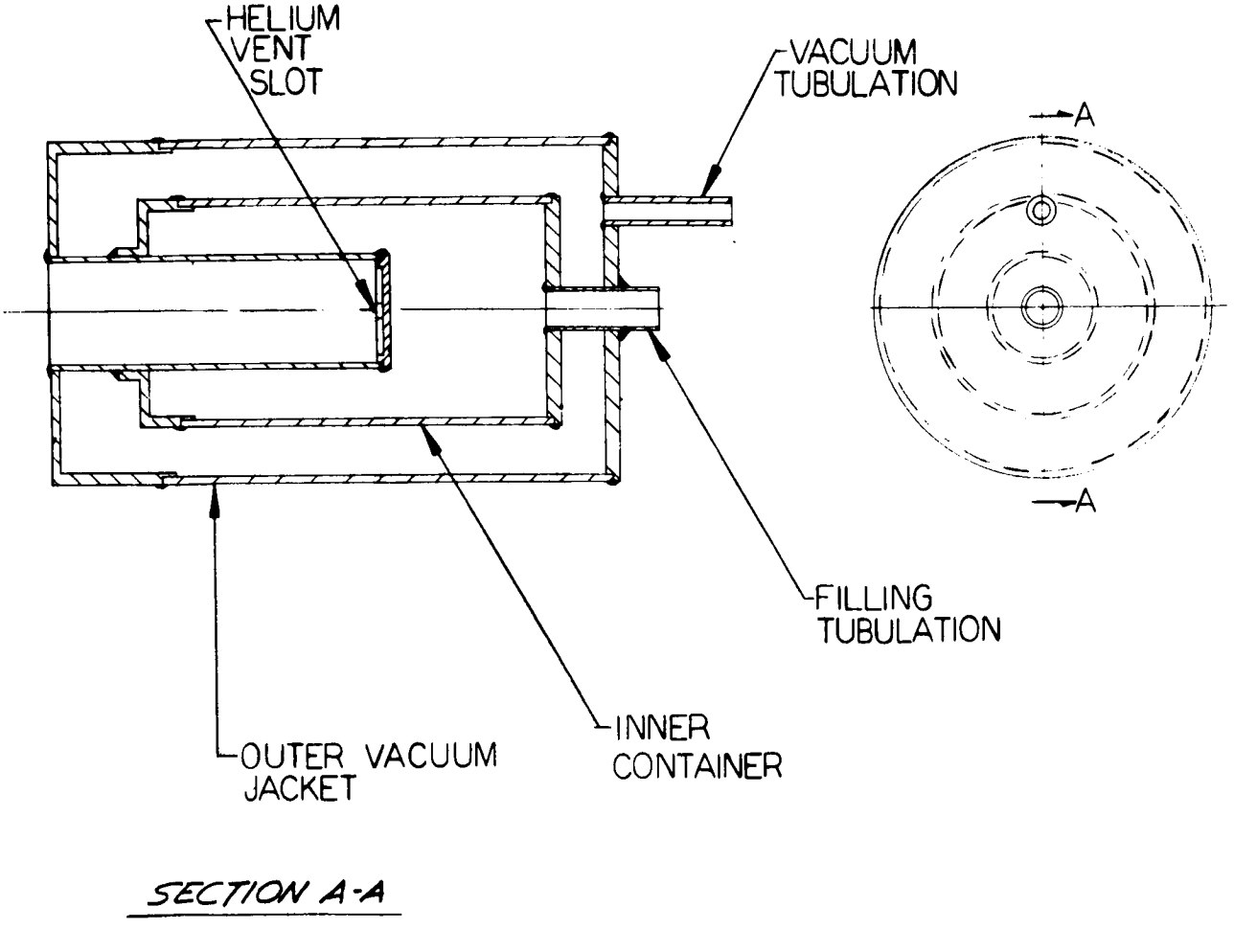

Figure 14. Cryopump Cap.

TABLE VI (CONT.)

MASS SPECTROMETER STUDIES OF THE MERCURY DIFFUSION PUMP SYSTEM

Time (Hr:Min)	Mass Number	Mass Peak Current (Amperes)	Change in Mass Peak (%)	Remarks
6:35	Took mass spectrum with 10 min. sweep, 0.25 Ma emission.			
	44	2.94×10^{-11}	+ 145	P_T(gauge off), P_B(gauge off)
	28	4.35×10^{-11}	- 51	Top NLS cold trap last filled
	18	1.35×10^{-11}	7	at 3:58. Note the beginning
	17	3.8×10^{-12}	---	of CO_2 desorption and the
	16	2.55×10^{-10}	1.9	decrease in the CO desorption.
	12	7×10^{-12}	22	The decrease in mass 12 probably
	Traces of masses 14 and 15 present			due to the smaller total amount of CO and CO_2.
7:05	Took mass spectrum with 10 min. sweep, 0.25 Ma emission.			
	44	9.2×10^{-10}	+3030	P_T(gauge off), P_B(gauge off)
	28 >	1×10^{-10}	---	Top NLS cold trap last filled
	22	2.6×10^{-11}	new peak	at 3:58. Note the very large
	18	1.45×10^{-11}	7.4	desorption of CO_2 from trap inner
	17	7×10^{-12}	84	container. It is possible that
	16+	3.0×10^{-10}	17.6	mass 22 is doubly ionized CO_2.
	16-	2.3×10^{-10}	new peak	Mass 16- is atomic oxygen from
	12	10.1×10^{-11}	1340	CO_2 dissociation. Mass 16+ is desorbed surface oxygen.
7:15	Took mass spectrum with 10 min. sweep, 0.25 Ma emission.			
	44	8.15×10^{-10}	11.4	P_T(gauge off), P_B (gauge off)
	28	2.5×10^{-10}	---	Top NLS cold trap last filled
	22	2.2×10^{-11}	15.4	at 3:58. The mass 19 peak
	19	8.0×10^{-12}	new peak	could be fluorine that had been
	18	1.5×10^{-11}	+ 3.4	trapped out over a long period
	17	not readable	---	of mass spectrometer operation.

TABLE VI (CONT.)

MASS SPECTROMETER STUDIES OF THE MERCURY DIFFUSION PUMP SYSTEM

Time (Hr : Min)	Mass Number	Mass Peak Current (Amperes)	Change in Mass Peak (%)	Remarks
				H_2O as the m.s. outgassing decreased (or its pumping increased).
5:00	Took mass spectrum with 10 min. sweep, 0.25 Ma emission.			
	44	1.45×10^{-11}	+ 12	P_T (gauge off), P_B (gauge off)
	28	3.35×10^{-11}	- 1.5	Top NLS cold trap last filled 3:58
	18	1.4×10^{-11}	0	Small amount of CO_2 desorbed
	17	not readable	- - -	from upper part of the top cold
	16	2.9×10^{-10}	+ 7	trap.
	12	5×10^{-12}	0	
5:30	Took mass spectrum with 10 min. sweep, 0.25 Ma. emission.			
	44	1.45×10^{-11}	0	P_T (gauge off), P_B (gauge off)
	28	3.20×10^{-11}	- 4.5	Top NLS cold trap last filled
	18	1.55×10^{-11}	+ 10.7	at 3:58. Lower NLS
	17	not readable	- - -	cold trap is being kept
	16	2.85×10^{-10}	- 1.7	filled. Not the small
	12	not readable	- - -	amount of H_2O desorbed from upper part of the top cold trap.
6:00	Took mass spectrum with 10 min. sweep, 0.25 Ma emission			
	44	1.2×10^{-11}	- 15.5	P_T (gauge off), P_B (gauge off)
	28	8.9×10^{-11}	+ 178	Top NLS cold trap last filled
	18	1.45×10^{-11}	- 6	at 3:58. Note the strong
	17	not readable	- - -	desorption of CO from the top
	16	2.6×10^{-10}	- 9	cold trap. Unexplained decrease
	12	9×10^{-12}	+ 80	in the mass 44, 18 and 16 peaks.

of the cap would be filled with liquid nitrogen through the filling tubulation. The space between the inner container and the outer vacuum jacket was evacuated via the vacuum tubulation and kept under vacuum by sealing it with rubber tubing and a hose clamp. As shown in the drawing, a vent slot permitted helium vapor to leave the helium container and bubble through the liquid nitrogen at the top of the cryopump. In this way, the helium vapor served to cool the fill tube jacket of the cryopump and thus reduced the loss rate of liquid helium.

Multiple Cell Magnetron Ion Pump. The housing or envelope of the multiple cell magnetron ion pump was fashioned from a pair of 6" O.D. ConFlat flanges. A 1½" O.D. tubulation was welded to one flange face (the inner flange) while the ceramic-metal cable end seals that connected to the anode and cathode of the pump were welded to the face of the other flange (the outer flange). The free end of the tubulation was later welded to a 2-3/4" O.D. ConFlat flange so that the pump could be easily attached to the test chamber.

There were eight (8) cylindrical, magnetron type unit cells in this pump. Eight separate anode cylinders were mounted adjacent to one another in a circular arrangement as shown in Figure 15. These anodes were held together by their close-packed geometry within the annular-shaped anode retainer. An electrical connection to the anode retainer or to any one anode was a connection to all of the anodes. The anode retainer was electrically insulated from the flange housing by means of eight ¼-inch diameter ceramic spheres.

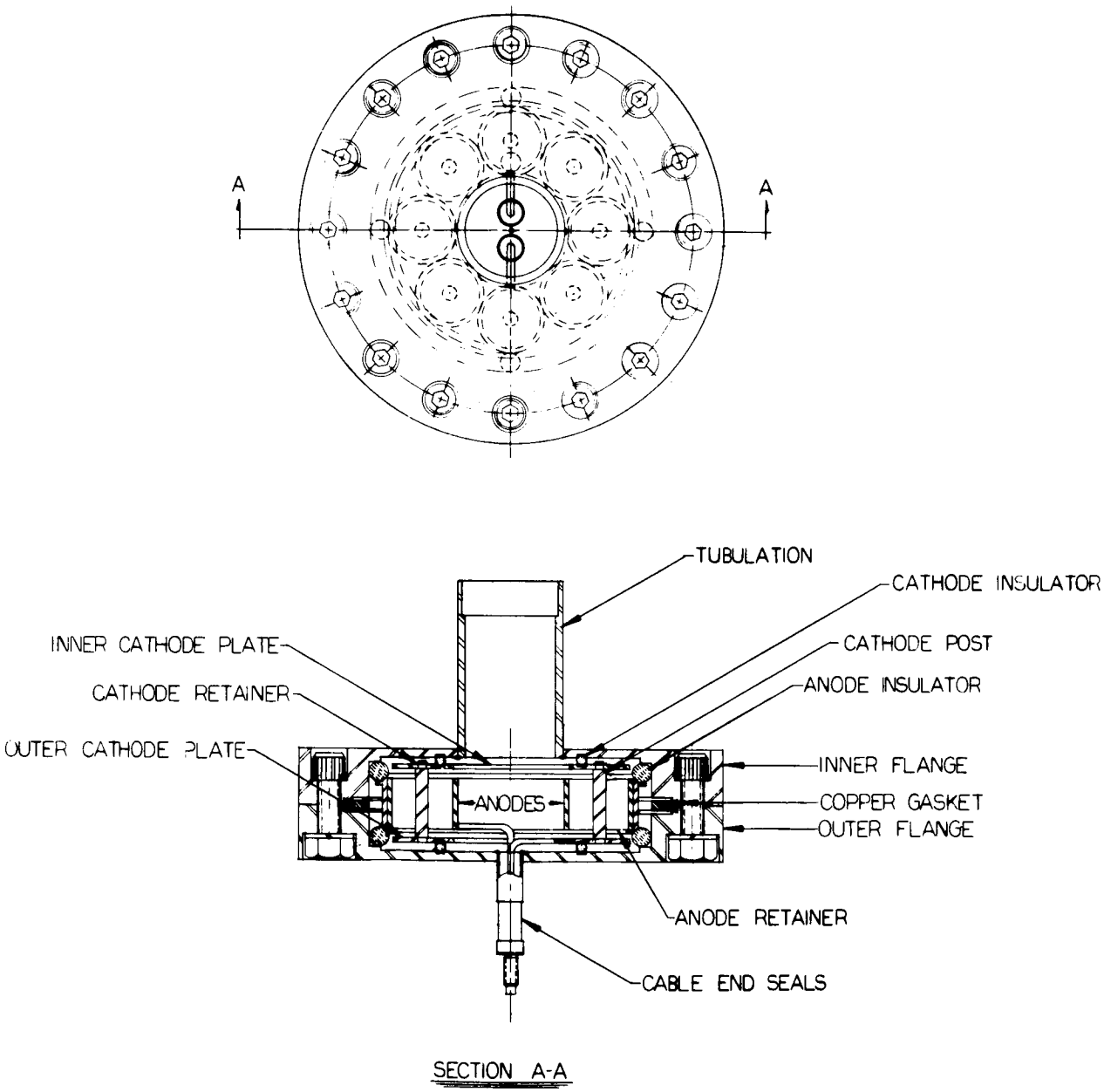

Figure 15. Multicell magnetron type ion pump.

The eight unit cells of the magnetron ion pump shared portions of the same cathode end plates which were fabricated in the form of annular disks. The cathode plates were spaced apart by eight cylindrical posts that were located at the axis of the eight anode cylinders. The cathode posts were locked to the cathode plates by means of small retainer clips. The entire cathode assembly of plates and posts was supported by eight 1/8-inch diameter ceramic spheres that rested on spot-faced portions of the inner and outer flanges. The pump components were machined to close tolerances so that they were locked in position when the ConFlat flanges were drawn up to a metal-to-metal contact position.

It can be appreciated that the magnetron ion pump design just described is demountable and can be easily modified. The cathode plates and posts can be interchanged with plates and posts of other materials. Thin titanium sheet material can be spot welded to the cathode plates and posts to convert to getter ion operation.

Indox V ceramic magnets of annular shape were used to provide the magnetic field for this pump. The magnets were placed adjacent to the faces of the flanges. The field strength of this magnet was 1030 gauss. A low carbon steel yoke provided a magnetic return path for the magnets.

Single Cell Magnetron Ion Pump. The single cell ion pump was essentially a larger scale version of a magnetron type cold cathode ionization gauge. The anode of this pump was a hollow cylinder about 2¼ inches in diameter and 1½ inches long. The cathode was spool-shaped

with end plates that were about 2 inches in diameter, a central cylindrical post ¼ inch in diameter, and an overall length of about 1-3/4 inches. The anode was supported by two heavy conductors that were welded to cable end seals. The cathode was supported by ¼" diameter spheres at either end of the spool.

The envelope of this ion pump was 4 inches in diameter and 2½ inches long. A U-shaped permanent magnet was used to provide a magnetic field of about 1000 gauss. As shown in the drawing of Figure 16, the tubulation was flanged with a 2-3/4" O.D. ConFlat flange. All metal elements of the ion pump were made of 304 stainless steel.

Test Chamber. The cryopump-ion pump system test chamber is illustrated in Figure 17. It consisted of a cylindrical housing or shell that was tapered at the top to fit a 6" O.D. ConFlat flange and was welded to a circular base at the bottom. Four side tubulations 1½ " in diameter and slightly more than 1" long were welded to the shell at 90 degreee intervals about 5" up from the base. Smaller 2-3/4" O.D. ConFlat flanges were attached to the ends of the side tubulations. The diameter of the chamber shell was 5½ inches and its overall height was about 8 inches. The test chamber was firmly attached to the oven base by means of an aluminum split-ring type clamp.

Roll-On Type Oven. The oven used with the cryopump-ion pump system was designed to roll over the ultra high vacuum portion of the system and rest on the oven base. The temperature of the oven was controlled by varying the power input to three pairs of strip-type heating elements.

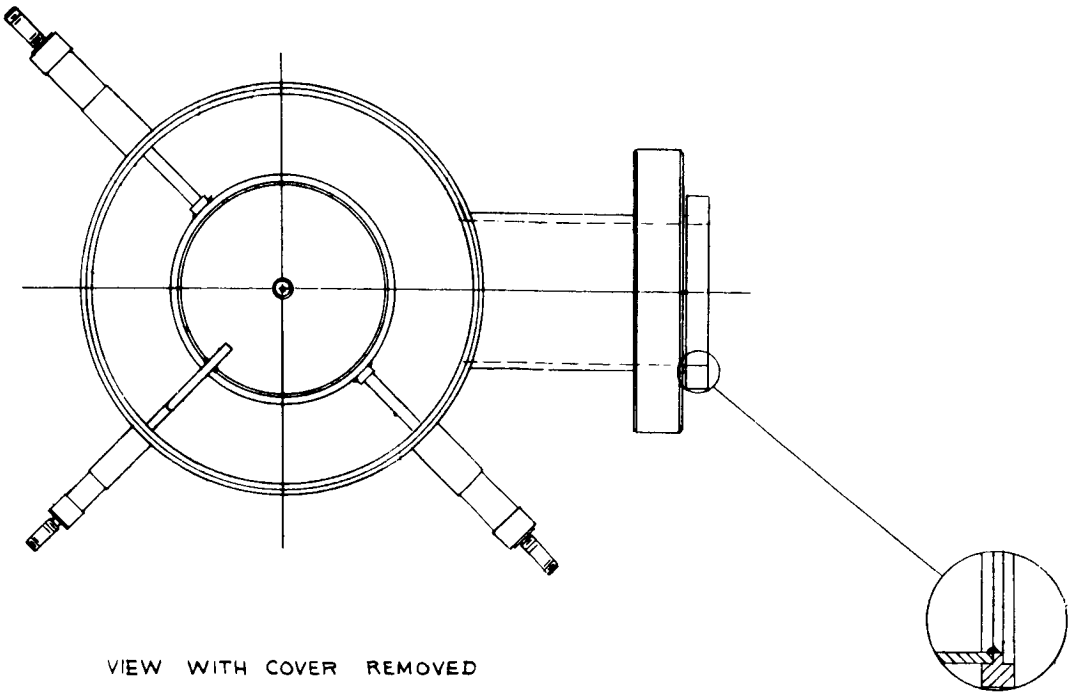

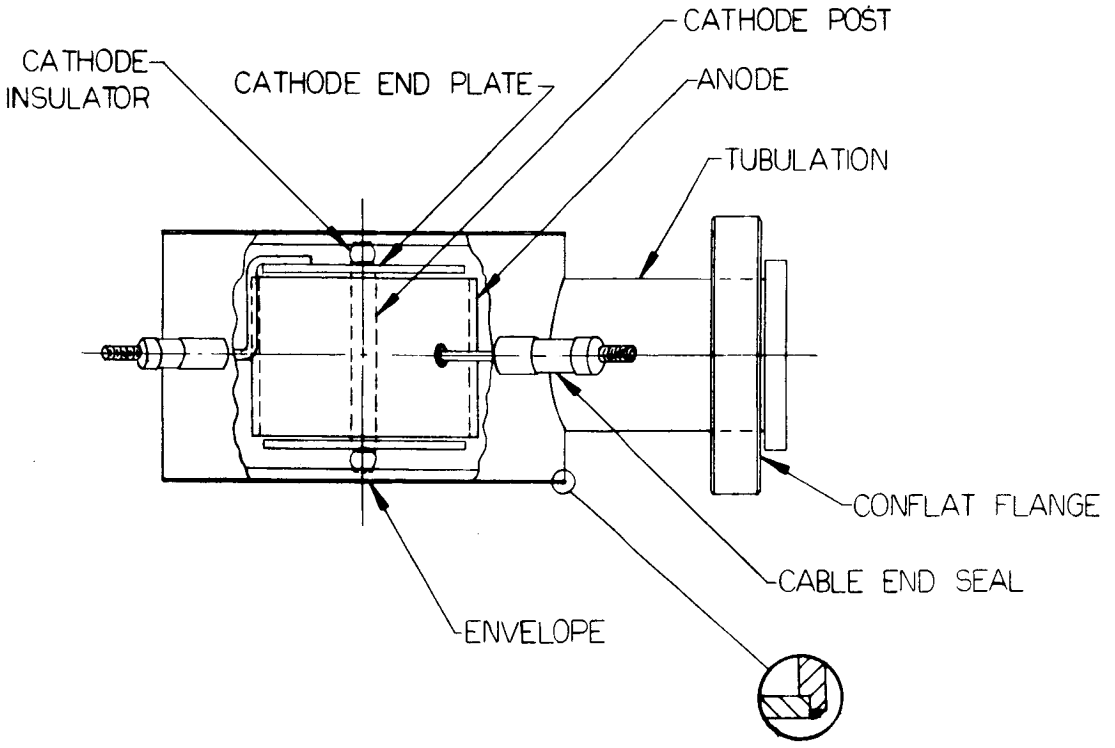

Figure 16. Single cell magnetron type ion pump.

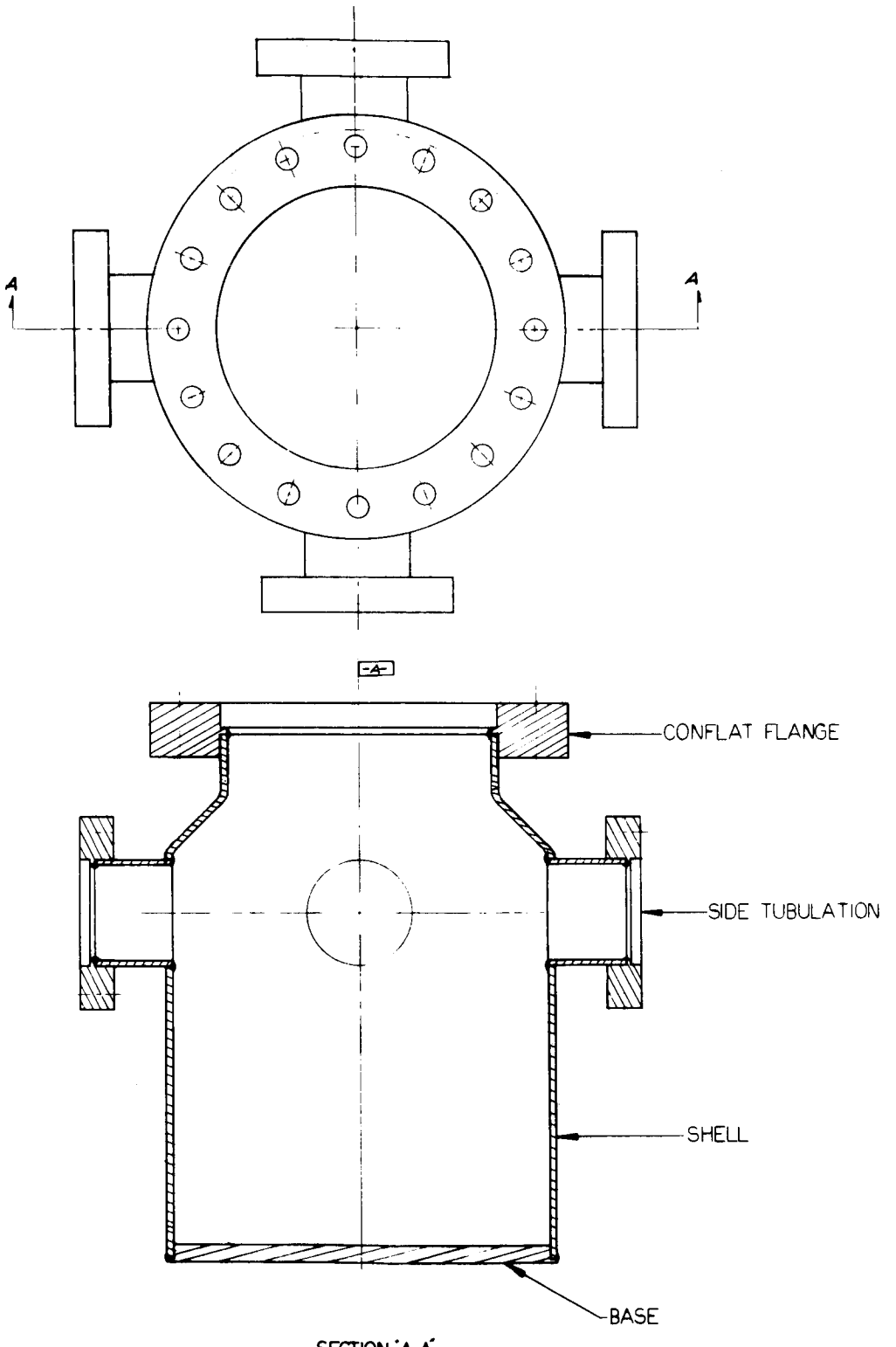

Figure 17. Cryopump-ion pump system test chamber.

Each pair of heaters had a separate switch which would apply power to the elements in series, parallel or singly. With power applied to the heaters, the oven temperature would increase until the heat loss just balanced the heat input. Since each heating element was rated for 1000 watts at 240 Volts input voltage, it was possible to apply 6 kw of power to this oven.

The oven was constructed of sheets of 1½ inch thick marinite 36, held together by hanger bolts embedded in the various edges. The bottom and one end of the enclosure were open. The interior dimensions of the oven were 24"x24"x21" wide. A 10" fan blade powered by a small 1/10 H.P. motor was used to circulate the air (or argon) within the oven. The motor was mounted outside the oven on a bracket. It was spaced well away from the oven wall, and an extension shaft was used to connect the motor shaft to the fan within the oven. A variac was used to control the speed of the motor. A mercury-in-glass thermometer was installed at the top of the oven.

The oven was mounted on four 8" diameter aluminum wheels so that it could be rolled along the table top. Movement of the oven was guided by an aluminum rail that was mounted on the table top and engaged by a bracket extending from the oven. The oven was rolled over the marinite oven base and then lowered so that it rested on the base. The open end of the oven was closed with another sheet of 1½ inch thick marinite 36.

4. SYSTEM OPERATING CHARACTERISTICS

4.1 MERCURY DIFFUSION PUMP SYSTEM

The earliest work performed with the mercury pump system involved checking for leaks that may have developed during the mounting and assembly of components, or which could exist at the demountable joints. Precautions were taken to tighten the ConFlat flanges uniformly until a metal-to-metal flange contact was established. The nuts and bolts used with the flanges must be well coated with molybdenum disulphide or they can never be removed after prolonged high temperature bakeout.

The system was pumped down with the booster pump into the low 10^{-7} torr pressure region, leak tested, and found to be tight. Experimentation with the various system components was then initiated to determine their characteristics.

4.1.1 Cold Trap Characteristics. The volumes of the isolation cold traps were measured and found to be about 310 cc. Liquid nitrogen loss rate tests were performed on these cold traps, and it was found that the liquid nitrogen level decreased at the rate of 2 inches per hour. Since the liquid nitrogen chambers are 4-3/4 inches deep, these traps would hold a charge of liquid nitrogen for about 2-1/2 hours. It was found convenient to fill these traps every hour.

The hot filament gauges that were connected to the isolation cold traps were kept unusually clean by the presence of the cold trap. Some

mercury vapor droplets were occasionally found in the gauges after long periods when the system was not in operation, but outgassing of the gauges cleaned them up sufficiently so that pressures of 1 or 2 x 10^{-8} torr could be measured. In operation, mercury droplets would be condensed on the baffle plates and the liquid nitrogen chamber walls. When operation of the system was terminated and the system vented, most of the mercury would drain downward to the base of the chamber and form a pool of mercury. When operation of the system was started again, the mercury at the bottom of the chamber would remain liquid, but this evidently did not affect the operation of the trap.

Before subjecting the system to bakeout, it was decided to test the operation of the non-level-sensitive cold traps and the UHV mercury diffusion pump. In the first experiment involving operation of the non-level-sensitive (NLS) cold traps, it was found that the liquid nitrogen level decreased 1¼ inch from the top level in 20 minutes, 2 inches in 35 minutes, and 3½ inches in 65 minutes (which placed the liquid nitrogen level below that of the inner chamber filling tubes located 3 inches below the top level). In a later experiment, it was found that the level of the liquid nitrogen in the outer container of the trap decreased 4½ inches in 105 minutes and was boiled off completely after 135 to 150 minutes. About 3 hours after a filling, the entire NLS cold trap--including the inner container -- would warm up sufficiently so that there was maximum desorption of gas from the trap. The NLS cold trap maintained a constant pressure in the system for about 2 hours (just

before the outer container ran out of liquid nitrogen). The NLS cold traps were routinely filled every 30 to 60 minutes. The filling operation was relatively slow when starting with the traps at room temperature, partly because of the narrow filling tubes that connected the inner chamber with the outer chamber and the positioning of these tubes at the same horizontal level.

During a later experiment, the entire system was baked and pumped down, with both NLS cold traps filled, until a hot filament Veeco RG-75 ionization gauge on the test chamber had reached its X-ray reading (an indicated pressure of 2.5×10^{-10} torr at 10 Ma. electron emission). At this time, the liquid nitrogen in the top trap was allowed to run out to see what sort of pressure could be maintained in the test chamber with only the single, lower NLS cold trap in operation.

As shown in Figure 18, the pressure in the test chamber was at the X-ray limit of the Veeco RG-75 gauge when the two non-level sensitive cold traps were filled and the experiment was started. About 1 hour and 45 minutes after filling the top trap (the bottom trap was kept filled), the system pressure began to rise. As will be shown in a later section, the first gas to be desorbed was found to be carbon monoxide. About 2½ hours after the filling, some cool air was blown into the outer container of the trap and there was a short additional desorption of gas which was most likely carbon dioxide. About 2 hours, 45 minutes after the filling, there was a very large desorption of gas from the inner container of the cold trap. The gas desorbed was most

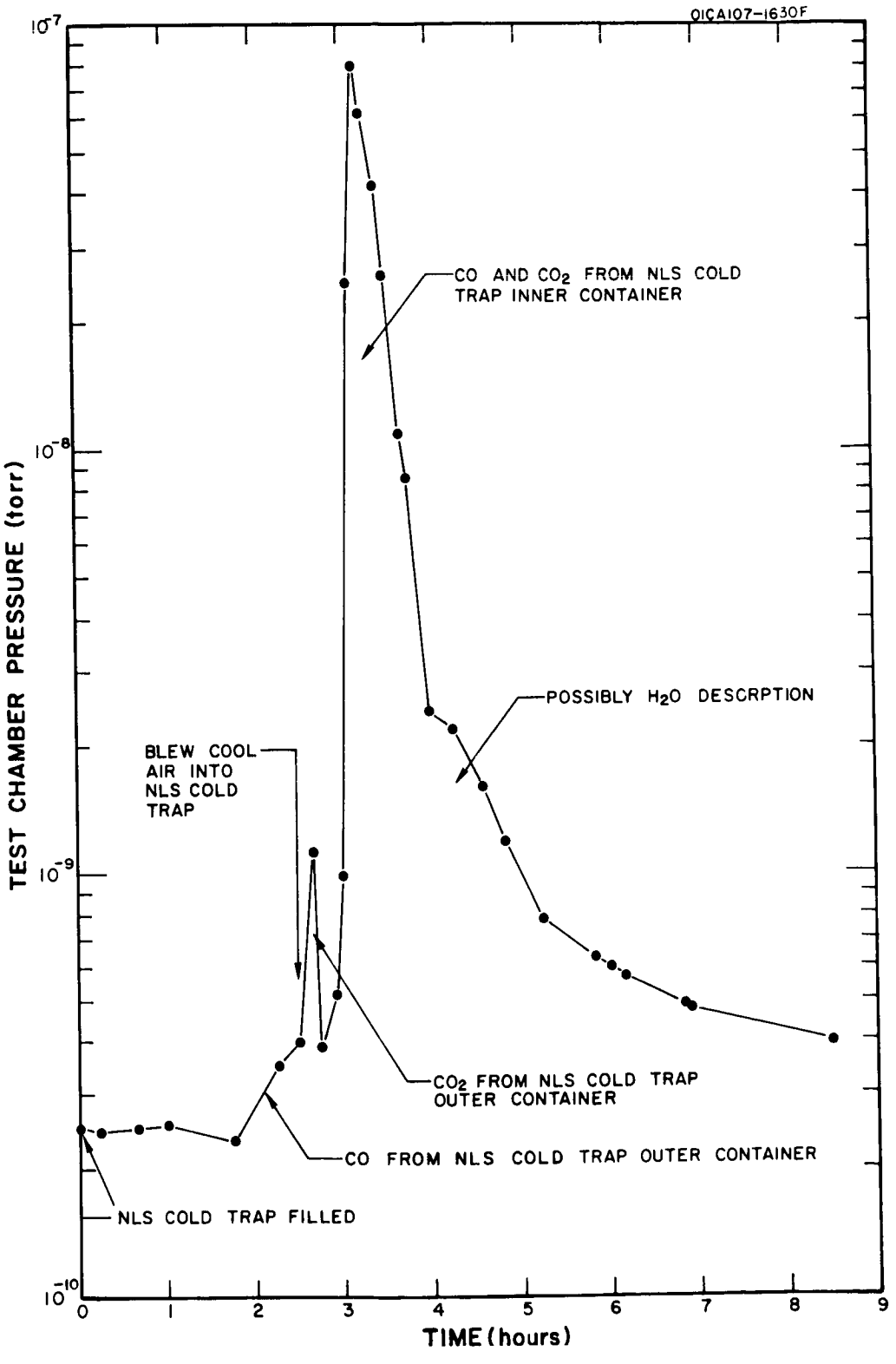

Figure 18. Gas desorbed from the upper non-level-sensitive cold trap as its liquid nitrogen evaporated.

likely both CO and CO_2. Four hours after the filling there was an additional desorption of gas. It is speculated that this last gas desorbed was water vapor.

Notice that 8½ hours after the upper trap was filled and then allowed to warm up to room temperature, the system pressure had returned to a level not very far above its starting level -- an indicated pressure of 4×10^{-10} torr (uncorrected for X-ray background). Fifteen and one half hours later (24 hours after filling the top cold trap), the indicated system pressure was 2.8×10^{-10} torr. This experiment (and other subsequent experiments), showed that a single non-level sensitive cold trap had sufficient mercury vapor trapping efficiency to permit pressures in the low 10^{-10} and high 10^{-11} torr region to be attained.

In another experiment, the mercury diffusion pump system was baked at 450°C for 30 hours. After the bake-out, only the lower NLS cold trap was filled. About 20 hours after the end of bake-out, a cold cathode gauge on the test chamber had a reading of 1.8×10^{-11} Amps at 4.0 Kv, corresponding to a pressure of 1.8×10^{-11} torr. This was the lowest pressure achieved with the use of only a single NLS cold trap.

4.1.2 UHV Diffusion Pump Characteristics. The effectiveness of the UHV mercury diffusion pump was established by two different methods. In the process of working with the pump, the acceptable range of heat input to the pump boiler was determined.

Prior to the initial operation of the UHV pump, the unbaked system had been under vacuum for several days with only the mechanical forepump and the MHG-40 backing diffusion pump operating. The test chamber pressure had stabilized at a value of 3.7×10^{-7} torr at the time the UHV diffusion pump was turned on with a heater current of 3 amperes (192 watts heat input). The graph of Figure 19 shows the pressure in the system after the UHV pump was turned on. There was no pumping action for the first 15 minutes. It was believed that the heat input was too low and so the heater current was increased to 4 amperes(341 watts heat input). Pumping action started 5 minutes later and the pressure dropped to a new, slowly decreasing plateau. This was the first evidence that the UHV diffusion pump would work. The cooling water flow through the pump at the time was 4 liters/minutes.

About 38 minutes after the UHV pump had been turn on, the heater current was increased from 4 to 4.5 amperes (431 watts heat input). This caused a temporary increase in pumping action and a dip in the pressure, but within 10 minutes, the effect was over and the pressure was back to the same plateau established earlier at 4 amperes of heater current. About 72 minutes after the pump had been turned on, the lower non-level sensitive (NLS) cold trap had run low (the level was down about 3½ inches from the top), and so it was filled. The upper NLS cold trap was empty at this time. Filling the cold trap caused no appreciable change in the pressure, indicating that the non-level sensitive design of the trap was effective.

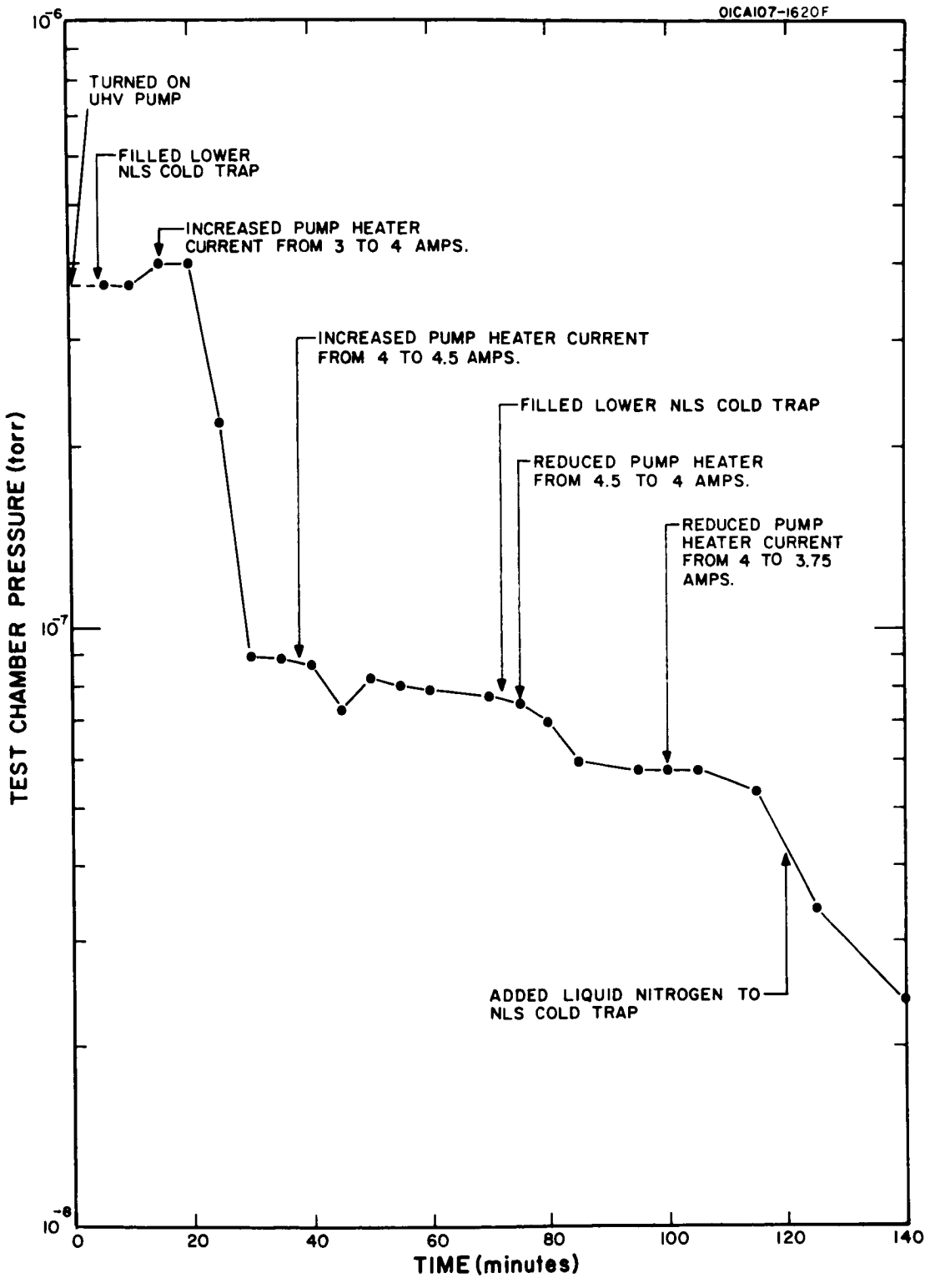

Figure 19. Time variation of pressure in the mercury diffusion pump system showing the effect of various heat inputs to the ultra high vacuum diffusion pump.

Three minutes after filling the lower cold trap, the pump heater current was reduced from 4.5 to 4 amperes, and the test chamber pressure decreased to a new, lower pressure plateau. Obviously, the net effective pumping speed was greater with 4 amperes of heating current than with 4.5 amperes. This effect could have been caused by a decreased outgassing of the mercury pumping fluid. When the pump heater current was reduced even further to 3.75 amperes (300 watts heat input), the system pressure decreased again. At this time, a small amount of liquid nitrogen was put into the empty upper NLS cold trap and the system pressure decreased considerably, indicating the presence of such condensables as H_2O and CO_2 in the system.

The experiment just described proved that the new UHV mercury diffusion pump would pump when its heat input ranged from 300 to 431 watts, with the best net pumping action occurring at 300 watts heat input to the pump boiler.

The second experiment that was performed to establish the effective pumping action of the UHV mercury diffusion pump involved turning off the backing diffusion pump and making the UHV pump do all of the pumping. The unbaked system had pumped overnight with only the backing diffusion pump on. The test chamber gauge was outgassed about 2 hours before the experiment started. Both non-level-sensitive cold traps were filled 10 minutes before the experiment started.

It can be seen from the graph of Figure 20 that 17 minutes after the UHV pump was turned on with a heater current of 3.75 amperes (300 watts

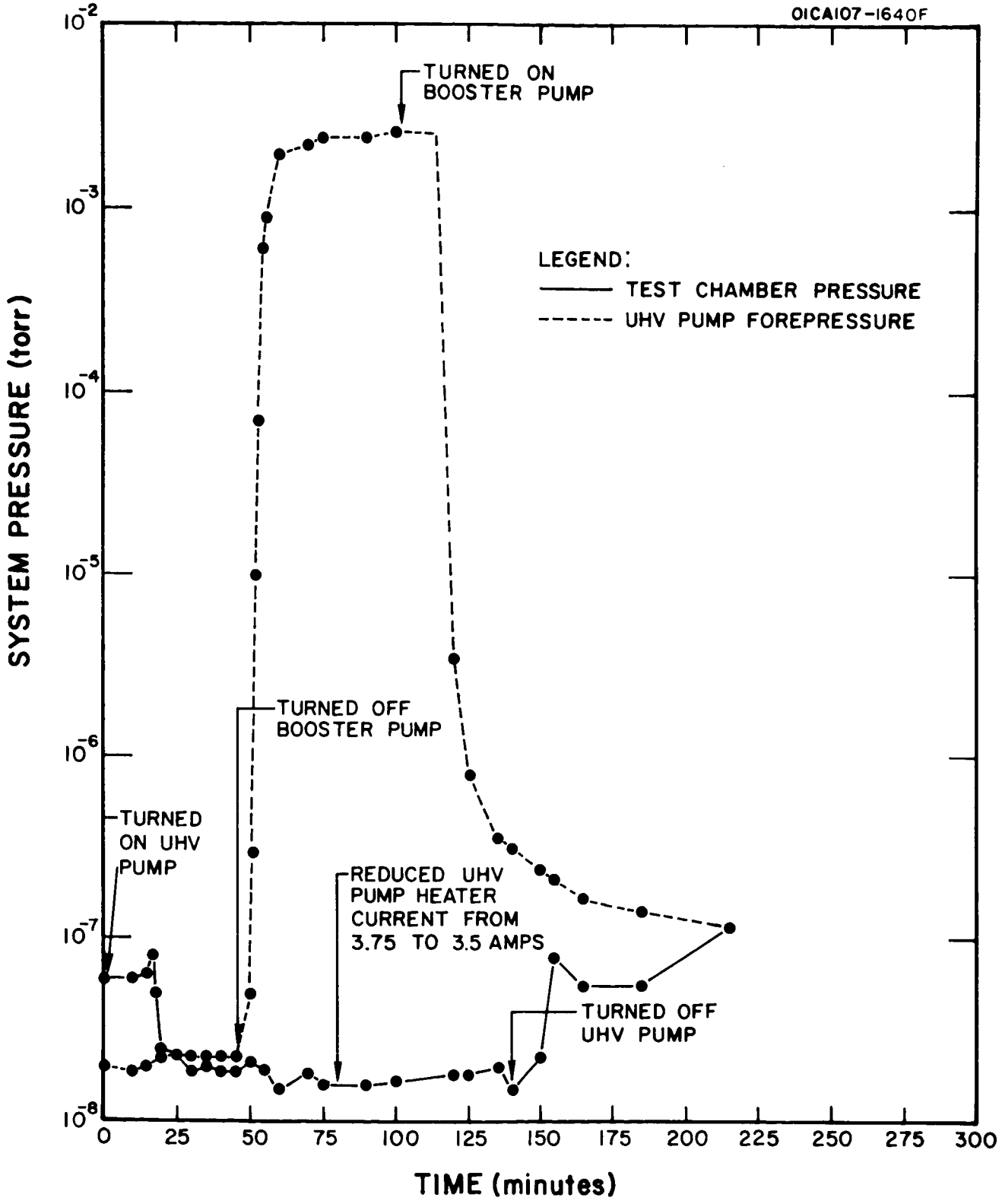

Figure 20. High pressure operation of the mercury diffusion pump system and its independence of ultra high vacuum diffusion pump forepressure.

heat input), the mercury outgassed, raising the test chamber pressure by about 30 percent. One minute later, the UHV pump began to pump and decrease the test chamber pressure. At the same time, the UHV pump forepressure was increased by about 15 percent, most likely because of the increased amount of gas now being furnished to the backing diffusion pump. After being on for 25 minutes, the test chamber pressure was reduced slightly below the forepressure, indicating a positive pumping action.

To further test the capability of the UHV pump, the backing diffusion pump was turned off, so that the UHV pump forepressure increased into the 10^{-3} torr region. The change in forepressure, as can be seen in Figure 20, had no discernable effect on the test chamber pressure. It must be concluded that the UHV pump speed was constant and independent of its forepressure at least over the range from 2.3×10^{-8} to 2.5×10^{-3} torr. Another way of describing the above result would be to say that the UHV pump could maintain a pressure differential of at least 10^{5} for the residual gases that were present in the unbaked metal system.

When the UHV pump heater current was reduced from 3.75 amperes (300 watts) to 3.5 amperes (260 watts heat input), there was a small but steady increase in the test chamber pressure, indicating a decrease in the pumping speed. It appeared that a heat input of 260 watts was marginal for good pump operation. After the backing diffusion pump was turned on again and warmed up, the forepressure began to decrease, rapidly at first, but then more slowly. The UHV pump was turned off, and the

test chamber pressure started to rise rapidly after about 10 minutes. When the test chamber pressure reached a level that was about ¼ or 1/3 of the forepressure, the pressure rise stopped and the test chamber pressure remained well below the forepressure for about an hour. It is most likely that the top jet of the UHV pump stopped pumping after 10 to 15 minutes, but the lower jet continued to pump for almost an hour.

Measurements made at the walls of the UHV pump boiler showed that the walls adjacent to the cone heater reach temperatures over 500°C (with 300 watt heat input), while the walls at the outside of the pump boiler only reach temperatures of the order of 120°C. There is undoubtedly a temperature gradient in the mercury within the boiler. The amount of mercury vaporized and condensed per unit time, that is, the mass flow through the pump jets, could be determined approximately by watching the mercury spill over the top of the mercury return line and U-tube vapor trap. For normal pump operation, there was spill-over of mercury every 5 to 10 seconds. It is estimated roughly that about 0.5 cc of mercury was returned to the boiler during each spill-over. Hence, the range of mass flow through the two pump jets varied from about 2/3 to 4/3 gram/sec.

4.1.3 High Temperature Bake-out Procedure. In order to obtain pressures below about 1×10^{-9} torr in the mercury diffusion pump system, it was necessary to bake the system. After some preliminary bakeouts at 250°C and 400°C for a few hours, and finally an overnight bakeout at 400°C, a more or less routine procedure for bakeout at 450°C (or above) was adopted.

To prepare the system for bakeout, the driver heads of the Granville Phillips Type C UHV valves were removed and bake-out clamps were attached. The UHV diffusion pump water flow was stopped and the pump was drained. Heating tapes were installed on the pumping lines joining the UHV diffusion pump and its isolation cold trap and the gas inlet pumping line from a position just below the table top to its isolation cold trap. The oven was lowered over the system until it rested on the insulated table top, and it was then locked in position. A mercury-in-glass thermometer was inserted into the lower portion of the oven through a small hole in the insulated table top. The two isolation, cold traps were filled about every half hour during the entire bakeout procedure.

The general objective of system bakeout was to heat system components to the highest practicable temperature while maintaining the lowest possible pressure. The heating of the system was accomplished in a series of steps, the temperature being raised for each step. The length of time devoted to each step depended on the reaction of the system. After each temperature increase, the system pressure would increase at first. Sufficient time was allowed for the pressure to rise to a maximum and then decrease to a value that appeared to be a quasi-equilibrium value.

The system bakeout was actually carried out in three phases. During the first phase, the entire system was being baked. This was the longest and major portion of the bakeout cycle. For the second phase, the oven was raised to a position just above the UHV diffusion pump,and the base of the oven was closed off with a demountable oven base. When the UHV

pump had cooled sufficiently it was turned on and allowed to pump while the remainder of the system was at a high temperature. For the third phase, the oven was riased again to a position just above the lower NLS cold trap and was closed off again with the demountable oven base. When the lower NLS cold trap had cooled, it was filled with liquid nitrogen. Bakeout was continued until the system pressure was as low as desired. The oven was then turned off and raised above the system. Various gauges on the test chamber were either outgassed or placed directly into operation at this time, and the system was allowed to cool. The upper NLS cold trap was filled with liquid nitrogen as soon as it had cooled sufficiently to minimize thermal shock.

Table I below is a schedule for one particular high temperature bakeout that may be considered fairly typical. Starting with the system under vacuum, the oven temperature was raised progressively in steps. Note that the time is listed in terms of hours (first two digits) and minutes. All pressures are in torr units, all temperatures in degrees centigrade, and all currents in amperes.

4.1.4 Measurement of Pumping Speed For Nitrogen. Since the system was all assembled, it was decided to make an over-all measurement of the pumping speed at the gauge tubulations of the test chamber. The effective pumping speed at the gauge tubulations had to be known before flow type, pressure-reduction gauge calibrations could be made. The experimental results of the pumping speed measurement could be compared with the theoretical values obtained from kinetic theory via calculations of

TABLE I

SCHEDULE OF A TYPICAL HIGH TEMPERATURE BAKEOUT
OF THE UHV MERCURY DIFFUSION PUMP SYSTEM

Time (Hr:Min)	Backing Diffusion Pump Pressure P_B(Torr)	Gas Introduction System Diffusion Pump Pressure P_G(Torr)	Oven Control Temperature Setting T_C(°C)	Oven Thermometer Reading T_O(°C)
00:00	9.4×10^{-8}	8.4×10^{-8}	0	23
00:20	Heater tape on UHV pump foreline energized			
00:30	1.05×10^{-7}	---	0	23
00:50	1.8	1.1×10^{-7}	100*	23
00:55	2.1	1.2	100	110
01:15	2.6	1.2	100	110
	Heater tape on gas inlet pumping line energized			
01:25	2.6×10^{-7}	1.3×10^{-7}	200*	118
01:45	3.1	2.1	200	200
02:00	1.3×10^{-6}	2.0	200	200
02:45	4.1×10^{-7}	2.0	300*	204
03:10	7.0	2.4	300	298
05:30	6.0	2.2	400*	312
06:10	3.8×10^{-6}	7.4	400	390
06:55	2.0	4.0	425*	394
07:20	3.1	4.9	450*	420
07:50	4.0	5.2	450	440
16:20	1.9	4.8	450	434
17:10	1.9	4.7	475*	435
17:20	2.4	5.7	475	458
17:45	2.95	5.7	475	458
18:00	3.0	5.7	475	458
18:30	3.0	5.7	475	457
19:00	2.85	5.4	475	455
19:30	2.80	5.2	475	455

*Indicates that oven temperature was changed.

TABLE I (Continued)

Time (Hr:Min)	Backing Diffusion Pump Pressure P_B(Torr)	Gas Introduction System Diffusion Pump Pressure P_G(Torr)	Oven Control Temperature Setting T_C(°C)	Oven Thermometer Reading T_O(°C)
19:50	2.75×10^{-6}	5.0×10^{-7}	300*	454
21:30	5.5×10^{-7}	3.2	475*	300
	Oven raised to first stage position			
22:00	6.6×10^{-7}	3.0×10^{-7}	475	440
22:55	1.3×10^{-6}	3.2	475	454
22:40	1.5	3.1	475	456
	Cooling water flow to UHV pump turned on			
	Turned on the UHV pump			
23:10	1.7×10^{-6}	3.1×10^{-7}	475	455
23:30	1.65	3.0	475	455
	Heater tape on UHV pump foreline de-energized			
23:55	1.55×10^{-6}	2.9×10^{-7}	475	455
24:10	1.55	2.9	300*	455
24:50	4.7×10^{-7}	2.55	300	300
	Oven raised to second stage position			
25:00	4.0×10^{-7}	2.55×10^{-7}	475*	300
25:20	6.0	2.65	475	452
25:35	8.3	2.7	475	458
	Started to force cool the lower NLS cold trap			
26:05	9.0×10^{-7}	2.75×10^{-7}	475	459
	Started to fill the lower NLS cold trap			
26:40	8.2×10^{-7}	2.75×10^{-7}	475	460
28:10	8.4	2.8	475	458
28:45	9.5	2.55	300*	458

* Indicates that oven temperature was changed.

TABLE I (Continued)

Time (Hr:Min)	Backing Diffusion Pump Pressure P_B(Torr)	Gas Introduction System Diffusion Pump Pressure P_G(Torr)	Oven Control Temperature Setting T_C(°C)	Oven Thermometer Reading T_O(°C)
29:05	5.6	2.2	300	370
	Heating tape on gas inlet pumping line de-energized			
29:20	3.3×10^{-7}	1.4×10^{-7}	0*	306
	Oven raised completely above system			
30:00	Turned on the two cold cathode gauges			

Time (Hr:Min)	Backing Diffusion Pump Pressure P_B(Torr)	Gas Introduction System Diffusion Pump Pressure P_G (Torr)	#1 Cold Cathode Gauge Current I_1(Amperes)	#2 Cold Cathode Gauge Current I_2(Amperes)
30:05	1.6×10^{-7}	1.1×10^{-7}	1.0×10^{-9}	4.2×10^{-9}
30:40	1.6	4.6×10^{-8}	3.2×10^{-10}	1.3
31:20	1.4	3.5	1.3	2.2×10^{-10}
32:15	1.15	3.5	3.5×10^{-11}	7.8×10^{-11}
	Started to fill the upper NLS cold trap			
33:00	1.10×10^{-7}	3.5×10^{-8}	5.4×10^{-12}	2.8×10^{-12}

system conductance and the diffusion pump speed.

Essentially, the two gauge method was used to measure pumping speed. If gas is flowed through a tubulation (capillary or orifice) of known vacuum conductance into a region where it is being pumped away, and the pressure is measured at either end of the tubulation, then the rate at which the gas is being pumped can be determined. The amount of gas Q (in torr liters/sec) passing through the capillary is

$$Q = C(P_{G.I.} - P_T) \tag{1}$$

The rate at which gas is pumped away is given by the expression

$$Q = SP_T \tag{2}$$

where S liters/sec is the effective pumping speed at the position where the lower test chamber pressure P_T torr is being measured. The vacuum conductance of the capillary tubulation is C liters/sec. and the pressure at the higher pressure (upstream) end of the capillary tubulation is $P_{G.I.}$ torr (gas inlet chamber pressure). At equilibrium, the rate at which gas is pumped out of the test chamber must equal the rate at which it flows in, and so combining equations (1) and (2) yields

$$S = \frac{C(P_{G.I.} - P_T)}{P_T} \tag{3}$$

The mercury diffusion pump system was prepared for nitrogen pumping speed measurements by attaching a 1-liter flask of spectroscopically pure

nitrogen gas to the gas bottle value and baking the system for 5 hours at 400°C. When cooled, the pressure in the test chamber was below the X-ray limit of the Veeco RG-75 hot filament gauge used to measure its pressure, P_T torr. The background pressure in the gas inlet chamber was 6.6×10^{-8} torr at the time that the seal-off on the nitrogen gas bottle was broken, and a gas pressure of 7.90×10^{-5} torr was established in the test chamber. At equilibrium, the test chamber pressure P_T was 2.45×10^{-9} torr. Using a value of $C = 6.98 \times 10^{-4}$ liters/sec as calculated from the dimensions of the capillary for nitrogen gas at 25°C, and correcting the reading of the test chamber gauge for its X-ray background, a value of S = 25.2 liters/second was obtained.

The gas bottle valve was then opened further to increase the nitrogen pressure in the gas inlet chamber until a pressure of $P_{G.I.} = 8.30 \times 10^{-4}$ torr was established. After about one hour, the test chamber pressure stabilized at a value $P_T = 2.40 \times 10^{-8}$ torr. Substituting these pressure values and the conductance value listed above in Equation (3) yielded a pumping speed value of S = 24.4 liters/second.

It is of interest to compare the above measured values of total effective pumping speed at the test chamber with the calculated value. The calculated pumping speed of the UHV mercury diffusion pump -- based on the dimensions of the top jet, the pump barrel, and a Ho coefficient of 0.400, as has been found applicable for a pump of this design -- was 220 liters/sec. The flange-to-flange conductance of each non-level-sensitive cold trap was calculated to be 54.2 liters/sec. The conductance

of the test chamber from the flange to the gauge ports is about 510 liters/sec. Thus the effective calculated speed of the pump at the gauge ports would be 23.5 liters/sec. Hence, the experimental values of pumping speed that were found were in good agreement with the computed value.

4.1.5 Vacuum Gauge Calibration Procedure. The mercury diffusion pump system could be used to calibrate vacuum gauges by either direct comparison with a primary standard such as a McLeod gauge, direct comparison with a secondary standard calibrated Bayard Alpert gauge or mass spectrometer, or flow type, pressure reduction calibration in which a known pressure was established in the test chamber.

In order to become familiar with the application of the system to vacuum gauge calibration, a combination flow type, pressure reduction calibration and comparison calibration against a Bayard Alpert gauge and a mass spectrometer was performed. There was no attempt made to achieve very accurate results, since the emphasis was on operational procedure and system limitations. A primary standard McLeod gauge was not used to measure the pressure of the gas inlet system, as would be the case for accurate calibration work. The secondary standard Bayard Alpert gauge had not been previously calibrated against a McLeod gauge. Lastly, the system background pressure was much higher than it would normally be for low pressure calibration work.

The gas selected for the gauge calibration experiment was nitrogen. Actually, for purposes of comparison calibration with a mass spectrometer, this was not a good choice because of the relatively large background of CO (mass 28). Argon, for example, would have been a better choice. However, nitrogen was convenient because it could be assumed that the Bayard Alpert gauge readings, using the manufacturer's calibrations, were approximately correct.

The gauges to be calibrated were connected to the test chamber with the shortest possible tubulations. Metal gauges were welded directly to ConFlat flanges. The system was then baked overnight at 350°C.

Calibration work should not be started until the pressures in the test chamber and the gas inlet chamber have reached their lowest levels. When the lowest pressures are to be achieved with the mercury diffusion pump system, all hot filament gauges and mass spectrometers must be turned off, and the pressure must be monitored with a cold cathode gauge. Cold cathode gauges can be calibrated at very low pressures using a flow type, pressure reduction technique. Calibration of a hot filament gauge at very low pressures is difficult because outgassing from the gauge itself raises the system pressure and the pressure within the gauge envelope. The use of nude ion gauges and high speed pumping systems could overcome this low pressure limitation.

After system pressures had stabilized at their lowest, background levels, readings of all the gauges were recorded,and nitrogen gas flow from a one liter flask of reagent grade gas was initiated. It was found that there was a transient period of 1½ to 2 hours before equilibrium pressures were established in the test chamber and the gas inlet reservoir. The cold traps were filled every 15 to 30 minutes during the transient period. Readings of the gauge on the gas inlet chamber and the gauge being calibrated were recorded. When the pressure in the test chamber was high enough, a secondary standard Bayard Alpert gauge and/or

a mass spectrometer were turned on so that comparison readings could be made. This would normally be done when the test chamber pressure reached the 10^{-9} torr region. After each set of readings, the gas bottle valve was opened further to increase the system pressure for the next calibration point.

The test chamber pressure P_T that was established by a flow of gas through a capillary of conductance C from the gas inlet chamber, having a pressure $P_{G.I.}$, was computed from Equation (3) of the preceeding section, which can be rearranged to yield:

$$P_T = \frac{C}{S+C} P_{G.I.} \cong \frac{C}{S} P_{G.I.} \qquad (3)$$

Since the capillary conductance C was at least 4 orders of magnitude less than the effective pumping speed S, the simplified expression on the right of Equation (3) above was used in the computation.

A test chamber which has a residual (background) pressure P_o and is subject to the influx of known amounts of gas Q_i will attain various values of pressure P_i corresponding to the gas flows. This is expressed mathematically as:

$$P_i = P_o + \frac{Q_i}{S} \qquad (4)$$

The changes or increments of pressure can be expressed in terms of the gas flow increments:

$$\Delta P_i = P_{i+1} - P_i = \frac{1}{S}(Q_{i+1} - Q_i) = \frac{\Delta Q_i}{S} \qquad (5)$$

For relatively small pressure changes, one can assume that the sensitivity constant of the gauge being calibrated does not change much, so that one can express ΔP_i in terms of the gauge current increment ΔI_i in a linear fashion:

$$\Delta P_i = K_i \, \Delta I_i \qquad (6)$$

Since ΔP_i is given by Equation (5) in terms of ΔQ_i, and since ΔI_i is measured directly, one can easily determine the gauge constants K_i. If the gauge is linear, then the gauge constants will all be equal. Non-linearities in the gauge current-pressure characteristic will lead to a series of non-equal constants K_i.

The total pressure in the test chamber at any time is the sum of the residual pressure P_o and the pressure increments ΔP_i:

$$P = P_o + \Delta P_1 + \Delta P_2 + \ldots = P_o + \sum_{i=1} \Delta P_i \qquad (7)$$

The residual pressure P_o can be determined by using an extrapolated value of the gauge constant. The extrapolated value K_o is obtained by plotting the values of K_i as a function of the gauge current I_i and extrapolating this curve to the value I_o. In the case of magnetron type cold cathode ionization gauges, the values of K_i as a function of I_i lie on a straight line in a log log plot, and the determination of K_o is straightforward.

As an example of the use of the mercury diffusion pump system for vacuum gauge calibration, consider the results shown in Figure 21 and Tables II and III. The three calibration points at the lower pressures were obtained via the flow type, pressure reduction technique described. The data on which the curves are based are displayed in Tables II and III. Notice that the last two values of the flow-calculated test chamber pressure P_i differ considerably from the readings of the comparison Bayard Alpert gauge. The errors in the flow calculated values stem from incorrect readings of the gas inlet chamber pressures $P_{G.I.}$ at pressures above 10^{-3} torr. If the gas inlet chamber pressures had been measured with a McLeod gauge, there would have been no difficulty. However, as pressures of 10^{-2} torr are approached in the gas inlet chamber, it is possible for the gas flow through the capillary tube to lose its molecular flow characteristics. Ideally, the pressure in the gas inlet chamber should never go above 1×10^{-3} torr. Higher pressures could be obtained in the test chamber by increasing the capillary conductance or decreasing the effective pumping speed at the test chamber. The vapor valve could be used to perform the latter function.

The small insert graph in Figure 21 indicates the manner in which the gauge constant K_o was obtained. The data in Table II are self-explanatory and were tabulated as a convenient way of calculating the test chamber pressures according to the preceeding equations.

The three calibration points in Figure 21 at the higher pressures were obtained from the readings of the comparison Bayard Alpert gauge.

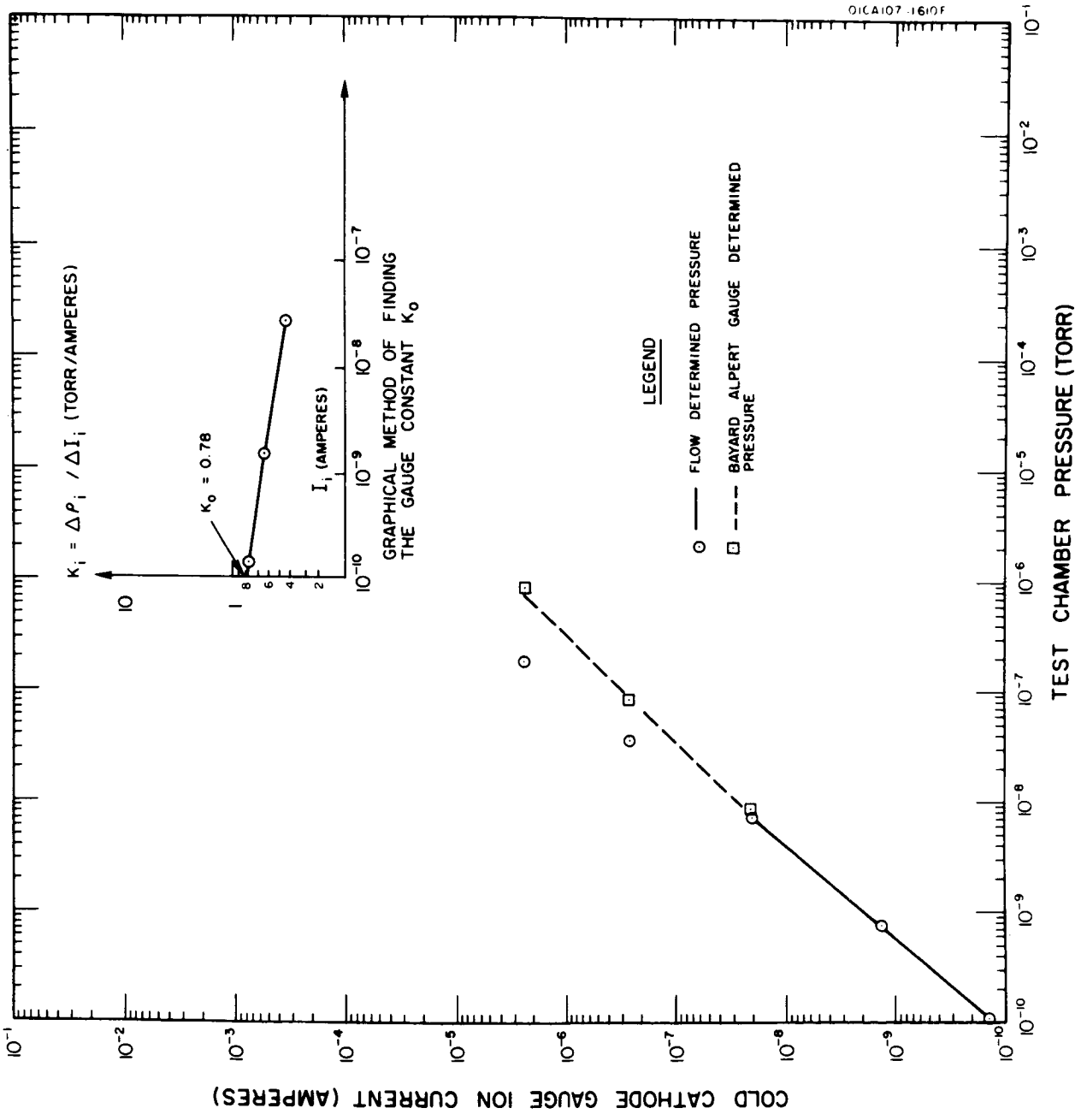

Figure 21. Calibration curve for a cold cathode ionization gauge as derived from both flow type, pressure reduction measurements and direct comparison data.

TABLE II

DATA REDUCTION FOR THE FLOW TYPE CALIBRATION OF A COLD CATHODE IONIZATION GAUGE FOR NITROGEN GAS

Gas Flow Increment i	C.C. Gauge Current I_i (Amp.)	Gas Inlet Chamber Pressure $P_{G.I.}$ (Torr)	Gas Flow $Q_i = C^{\dagger} P_{G.I.}$ (Torr ℓ/sec)	Gas Flow Increment ΔQ_i (Torr ℓ/sec)	Pressure Increment $\Delta P_i = \Delta Q_i / S^{*}$ (Torr)	C.C. Gauge Current Increment ΔI_i (Amp.)	Gauge Constants K_i (Torr/Amp.)	Flow Calculated Pressure P_i (Torr)
0	1.40×10^{-10}	1.40×10^{-7}	0	---	---	---	$^{\ddagger}7.8\times10^{-1}$	1.09×10^{-10}
1	1.35×10^{-9}	2.35×10^{-5}	1.64×10^{-8}	1.64×10^{-8}	6.51×10^{-10}	1.21×10^{-9}	5.38×10^{-1}	7.60×10^{-10}
2	2.04×10^{-8}	2.60×10^{-4}	1.81×10^{-7}	1.65×10^{-7}	6.55×10^{-9}	1.90×10^{-8}	3.45×10^{-1}	7.31×10^{-9}
3	2.59×10^{-7}	$^{**}1.25\times10^{-3}$	8.72×10^{-7}	6.91×10^{-7}	2.74×10^{-8}	2.39×10^{-7}	1.15×10^{-1}	3.47×10^{-8}
4	2.40×10^{-6}	$^{**}6.55\times10^{-3}$	4.56×10^{-6}	3.69×10^{-6}	1.46×10^{-7}	2.14×10^{-6}	6.81×10^{-2}	1.81×10^{-7}

$^{*}S$ = 25.2 ℓ/sec, effective system pumping speed at the gauge

$^{\dagger}C$ = 6.98×10^{-4} ℓ/sec, capillary vacuum conductance

**These readings were too high to be measured accurately

‡Value taken from graphical extrapolation

TABLE III

COMPARISON OF MERCURY DIFFUSION PUMP
SYSTEM TEST CHAMBER NITROGEN PRESSURE VALUES

Gas Flow Increment i	Flow Calculated Pressure P_i (Torr)	Veeco RG-75P Ionization Gauge Reading P_{BA} (Torr)	Gen. Elec. Partial Pressure Analyzer I_{MS} (Amp.)	Partial Pressure Analyzer Sensitivity I_{MS}/P_{BA} (Amp/Torr)
0	1.09×10^{-10}	---	$^{*}4.1 \times 10^{-10}$	---
1	7.60×10^{-10}	---	$^{*}3.1 \times 10^{-10}$	---
2	7.31×10^{-9}	$^{\dagger}8.03 \times 10^{-9}$	$^{**}1.45 \times 10^{-9}$	0.180
3	3.47×10^{-8}	$^{\dagger}8.12 \times 10^{-8}$	$^{**}2.03 \times 10^{-8}$	0.250
4	1.81×10^{-7}	$^{\dagger}8.35 \times 10^{-7}$	$^{**}1.95 \times 10^{-7}$	0.235

*Primarily outgassing CO

**Corrected for background of 2.0×10^{-10} ampere

†Corrected for X-ray reading of 2.5×10^{-10} torr

Notice that the current-pressure relationship for the cold cathode gauge that was calibrated was linear in the region above 10^{-8} torr and non-linear below 10^{-8} torr. This sort of behavior appears to be characteristic of magnetron type cold cathode ionization gauges. The sensitivity of the gauge in the linear region was about 3 amperes/torr. At a pressure of 1×10^{-10} torr, the sensitivity had fallen to about 1.3 amperes/torr.

Table III lists the various comparable values of test chamber pressure as determined by the flow technique, readings of a Bayard Alpert gauge, and readings of a mass spectrometer. The BA gauge readings were corrected for X-ray background and the mass spectrometer readings were corrected for background mass 28 peak. The last column of the table lists the mass spectrometer sensitivities for nitrogen as determined by the Bayard-Alpert gauge readings. It can be seen from the table that the mass spectrometer was probably still outgassing at the time that the first gas flow increment was established. Notice the relatively good agreement between the flow calculated pressure and the direct comparison reading of the Veeco RG-75P gauge after the second gas flow increment was established. The mass spectrometer (partial pressure analyzer) sensitivity values of about ¼ amperes/torr for nitrogen seem rather low and are probably due to decreased multiplier gain.

4.1.6 Recycling Capability of the Diffusion Pump System. After the entire vacuum system was baked and the UHV diffusion pump was operated with the non-level-sensitive cold traps filled, the test

chamber pressure very quickly went into the 10^{-11} torr region or lower. Under certain circumstances, it might be necessary to turn off the UHV diffusion pump and permit the NLS cold trap to warm up. The test chamber pressure, under these conditions, would most certainly rise into the 10^{-7} or 10^{-8} torr regions. If, now, the UHV pump was turned back on again and the NLS cold traps filled, would the system pressure return to the 10^{-11} torr level?

In order to test the system ultra high vacuum recycling capability, the system was first baked at high temperature, and brought into the 10^{-11} torr region in the usual way. A flow of nitrogen gas was then established to raise the test chamber pressure to a value of 4.25×10^{-10} torr. The UHV pump was turned off, and the two NLS cold traps were permitted to warm up. However, the backing diffusion pump and the gas introductory system diffusion pump were kept operating, and the two isolation cold traps were kept filled with liquid nitrogen overnight.

After the UHV pump and NLS cold traps had been inoperative for about 18 hours, the lower NLS cold trap was filled with liquid nitrogen, and the test chamber Veeco gauge was turned on. The initially measured test chamber pressure was 1.9×10^{-8} torr and was decreasing due to outgassing of the gauge. When the Veeco gauge read 1.3×10^{-8} torr, about 35 minutes after it was turned on, the UHV pump was started. About 40 minutes after the pump was started, the test chamber pressure was 6.3×10^{-9} torr and decreasing. About 2 hours after starting the UHV pump, the pressure was 4.1×10^{-9} torr, about a decade higher than on

the previous day. There was every indication that the pressure would continue to decrease until it reached its former level.

When the nitrogen gas flow into the gas inlet system was stopped, the test chamber pressure began to decrease fairly rapidly. After about 2 hours of pumping, the pressure had dropped from 4×10^{-9} torr to 1.2×10^{-9} torr, again with every indication of a continuing decrease into the 10^{-10} torr region. Unfortunately, the experiment had to be stopped at this time, but on the basis of the data taken, it seemed certain that the pressures obtained earlier would at least be closely approached after a sufficiently long pumping period.

4.2 CRYOPUMP-ION PUMP SYSTEM

After a few initial difficulties with flanges that were not properly bolted, a bakeable valve that had a weld leak, and a weld leak in the cryopump, the new system was placed in operation. The earliest work with the cryopump-ion pump system involved the development of an effective bakeout procedure. After this, the multiple cell magnetron type ion pump was operated,and its voltage-current characteristic for background gas was determined. In later experiments, the multiple cell ion pump current output and pumping speed vs. pump voltage were determined for nitrogen gas. The cryopump was operated with liquid helium several times to obtain pressures in the 10^{-10} torr region and below. Finally, the single cell ion pump was tested at low pressures, and measurements were made of the residual gas in this closed system.

4.2.1 Liquid Helium Cryopump Characteristics. The volumetric capacity of the cryopump for the liquid nitrogen used to shield the liquid helium container and also remove such gases as water vapor, carbon dioxide, and hydrocarbons, was 2200 cm^3. It was found that the initial loss rate of the pump for liquid nitrogen was about 1 inch per hour with a ¼-inch thick asbestos board covering the top of the liquid nitrogen section of the pump. At this rate, liquid nitrogen would evaporate from the upper, large volume portion of the pump in about 3 hours. The loss rate for the lower, narrow annular region of the pump was about 2 inches per hour, so that the liquid nitrogen in this region would also last about 3 hours. Thus the total holding time for a single filling of liquid nitrogen was of the order of 6 hours.

The holding time for a single filling of liquid helium was about 2½ hours, with the cryopump cap in position. It can be seen that the helium holding period was compatible with the liquid nitrogen loss rate at the upper part of the pump, so that liquid nitrogen did not have to be added to the cryopump after initial filling, if this was not convenient.

The inherent pumping speed of the liquid helium container within the cryopump was quite high. The effective surface area of the container was of the order of 200 cm^2. Assuming a condensation coefficient of unity, the pumping rate of this surface would just be equal to the molecular impingement rate i.e., the pumping speed for molecules having a maxwellian distribution would be about 11.6 liters/sec per cm^2 of

surface area for nitrogen gas. Thus the speed of the liquid helium pumping surface would be over 2000 liters/sec.

Unfortunately, the inherently high pumping speed of the liquid helium container surface was limited by the vacuum conductance of the entrance configuration of the cryopump. The vacuum conductance in question was calculated to be about 62 liters/sec. The effective pumping speed for molecules having a unity condensation coefficient would then be about 60 liters/sec.

The effective speed of the cryopump for molecules of water, carbon dioxide and some hydrocarbons could be much greater than 60 liters/sec since these gases could be pumped by the shielding liquid nitrogen cooled parts of the pump. The conductance of the entrance tubulation to the pump was 540 liters/sec. The liquid notrogen cooled surface facing the entrance tubulation had a surface area of about 200 cm^2, so the pumping speed for those gases condensible at 77°K with a condensation coefficient of unity would also be about 2,000 liters/sec. The effective pumping speed for these gases would be about 425 liters/sec. Carbon dioxide would not be pumped until its partial pressure increased above the low 10^{-8} torr level[9] unless, of course, it was being cryotrapped by other gases. The saturation vapor pressure of methane at 77°K is close to 10 torr, and so this gas would not be pumped at low pressures by the liquid nitrogen cooled surfaces. The saturation vapor pressure of hydrogen at 4.2°K is about 1×10^{-7} torr and partial pressures of hydrogen less than this value could exist in the cryopump. However,

in the presence of water vapor, it is possible that cryotrapping of hydrogen would occur.[10] The point to be made in this discussion is that the pumping speed of the cryopump was different for the various residual gases present -- varying from zero for helium to a maximum of about 425 liters/sec for water vapor. Most of the so-called permanent gases such as nitrogen, carbon monoxide, argon, and oxygen would be pumped with a maximum speed of about 60 liters/sec.

In the first experiment involving the filling of the cryopump with liquid nitrogen and liquid helium, it was found that filling the cryopump with liquid nitrogen reduced the test chamber pressure by about a factor of three. The filament of the test chamber ion gauge had burned out and so exact system pressures cannot be listed. However, the multiple cell ion pump was operating and its current readings were roughly proportional to the pressure. The ion pump was operated at an anode voltage of 2700 volts. It was shown in a later experiment that the pump current did not vary linearly with pressure for this anode voltage, but rather decreased in sensitivity as the pressure decreased, at least for pressures between 10^{-8} and 10^{-7} torr. Keeping the latter fact in mind, the change in pressure in the system due to addition of liquid helium to the cryopump, which corresponds to an ion pump current change from 6.6×10^{-7} amps to 4.2×10^{-10} amps, might only represent about two orders of magnitude change in the system pressure.

In a second experiment using liquid nitrogen and helium in the cryopump, the nude ion gauge mounted in the test chamber gave fairly

accurate readings of the system pressure. With the multiple cell magnetron type ion pump operating at 2500 volts,and the cryopump at room temperature, the nude ion gauge indicated a pressure of 7.5×10^{-8} torr,while the ion pump current was 1.5×10^{-6} amperes (ion pump sensitivity of 20 amps/torr at this pressure). About 25 minutes after liquid nitrogen had been added to the cryopump, the nude ion gauge read a pressure of 3.5×10^{-8} torr, and the ion pump current was 5.6×10^{-7} amps (sensitivity of 16 amps/torr). About 8 minutes after liquid helium was introduced into the cryopump, the nude gauge read a pressure of 3.6×10^{-10} torr, two decades lower than its last reading. The ion pump current had decreased to 2.6×10^{-9} Amps (sensitivity of 7.2 amps/torr). Fifteen minutes after putting liquid helium into the cryopump, the nude ion gauge yielded its lowest reading of 2.5×10^{-10} torr,while the ion pump current decreased to 2.0×10^{-9} amps.

At this time, a flow of nitrogen gas into the test chamber was started and was increased slowly in several steps. During this process, an attempt was made to refill the cryopump with liquid helium. Evidently, the helium transfer line had warmed up, and the refill attempt only succeeded in flashing off all of the liquid helium.

Using the last values of the pressure attained in the gas inlet "Tee" and in the test chamber before the loss of the liquid helium, the pumping speed of the cryopump for nitrogen gas was calculated to be 87.4 liters/sec. This value has the right order of magnitude, but has no great accuracy since both values of pressure mentioned above were still changing.

4.2.2 Magnetron Type Ion Pumps. The initial operation of the multiple cell magnetron type ion pump was carried out with the test chamber under vacuum as a result of the pumping action of the VacIon pump in the forevacuum part of the system. A highly regulated power supply (J. Fluke, model 408A) was used to supply the voltage to the pump anodes. A Keithley model 600 electrometer was used to measure the ion pump cathode current.

The ion pump discharge first started at an anode voltage of 2100 volts. Strong outgassing from the electrode surfaces was observed as the anode voltage was slowly increased in 100 volt steps. By varying the voltage from about 2 to 4 Kv it was found that there was a maximum ion pump current at a voltage 2.7 Kv and so the anode voltage was set at this value. About 2 hours after the pump had first been turned on, the bakeable valve separating the test chamber and UHV part of the system from the Vac Ion pump and the forepressure part of the system was closed. The new ion pump then pumped the closed UHV portion of the system by itself, slowly reducing its pressure.

A few days after the eight cell magnetron type ion pump was turned on, it was decided to vary the pump voltage and monitor the pump current and the system pressure. Since the nude gauge on the system had a burned-out filament, the bakeable UHV valve was opened so that the Vac Ion pump current could be used as a measure of the system pressure. As will be shown later, the 8 liter/sec Vac Ion pump had a pumping speed that was over five times greater than the magnetron type pump (which contained

no titanium). Thus, the major pumping in the system was being done by the Vac Ion pump.

Starting with a voltage of 4.0 Kv, the voltage on the magnetron type ion pump was decreased in steps of 500 volts, and readings of the pump current and the Vac Ion pump "pressure" were taken. The results of this experiment are shown in Figure 22. The current-voltage characteristic of the magnetron type multicell pump, as shown, was found to be typical of this pump for both residual system gases and pure nitrogen gas. The variation of the system pressure (as measured by the Vac Ion Pump) with the multicell pump voltage, however, was not typical, as will be shown shortly. The system pressure should have a minimum value somewhere in the vicinity of the maximum multicell pump current. In this experiment, there was a maximum pressure (or rather a maximum value of Vac Ion pump current) when the multicell pump current was a maximum.

The multicell pump has its lowest pumping speed at a voltage of 4.0 Kv as will be shown later, so that the pressure indication of 3×10^{-8} torr as shown by the Vac Ion pump for multicell pump voltages of 4.0 and 3.5 Kv must represent the base pressure attainable with only the Vac Ion pump in operation. When the multicell pump voltage was decreased from 3.5 to 3.0 Kv, both pump currents increased greatly. The assumption that the multicell pump outgassed more strongly when its current was greater is in contradiction to its established net effective pumping speed.

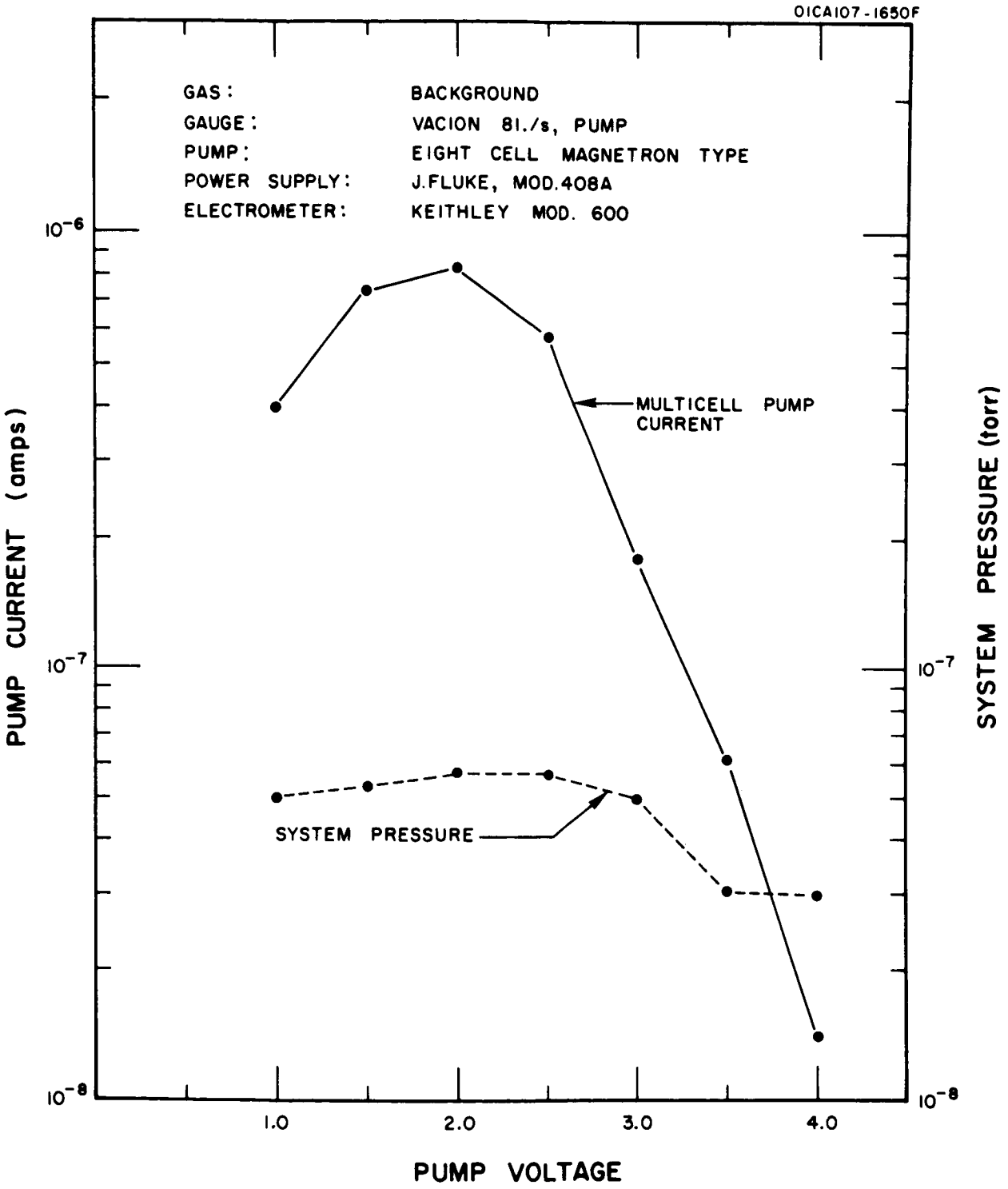

Figure 22. Current-voltage characteristic of the multicell magnetron type ion pump for background gas.

There are two possible explanations for the variation of the system pressure curve in Figure 22. The first, and simplest, is that the liquid nitrogen that was present in the cryopump at the time the experiment was made ran out at a time when the pump voltage was changed from 3.5 to 3.0 Kv. The second explanation is that there was an interaction between the two ion pumps. One example of this would be the collection by the Vac Ion pump of positive ions produced in the magnetron type pump. However, this occurrence is rather unlikely because of the physical positioning of the two pumps. Whatever the explanation, this experiment should be repeated to see if it is a real phenomenon or just an accidental occurrence.

The pumping speed of the multicell magnetron type ion pump for nitrogen gas was measured on two different occassions and similar results were obtained each time. The method used was to take readings of the test chamber pressure with and without nitrogen gas flow. The amount of nitrogen flowed into the chamber was computed on the basis of measured gas inlet pressures and the calculated conductance of a flow limiting capillary tube. This procedure was repeated for a complete series of magnetron ion pump voltages, and the pump currents as well as the test chamber pressures were recorded for each value of pump voltage. Nitrogen gas was admitted to the test chamber at two different pressure levels in these experiments. The data obtained for the background gas and the two different nitrogen pressures are displayed in graphical form in Figures 23, 24, and 25.

Notice that in the figures just mentioned, the variation of the net pumping speed of the multicell ion pump with changes in pump voltage are

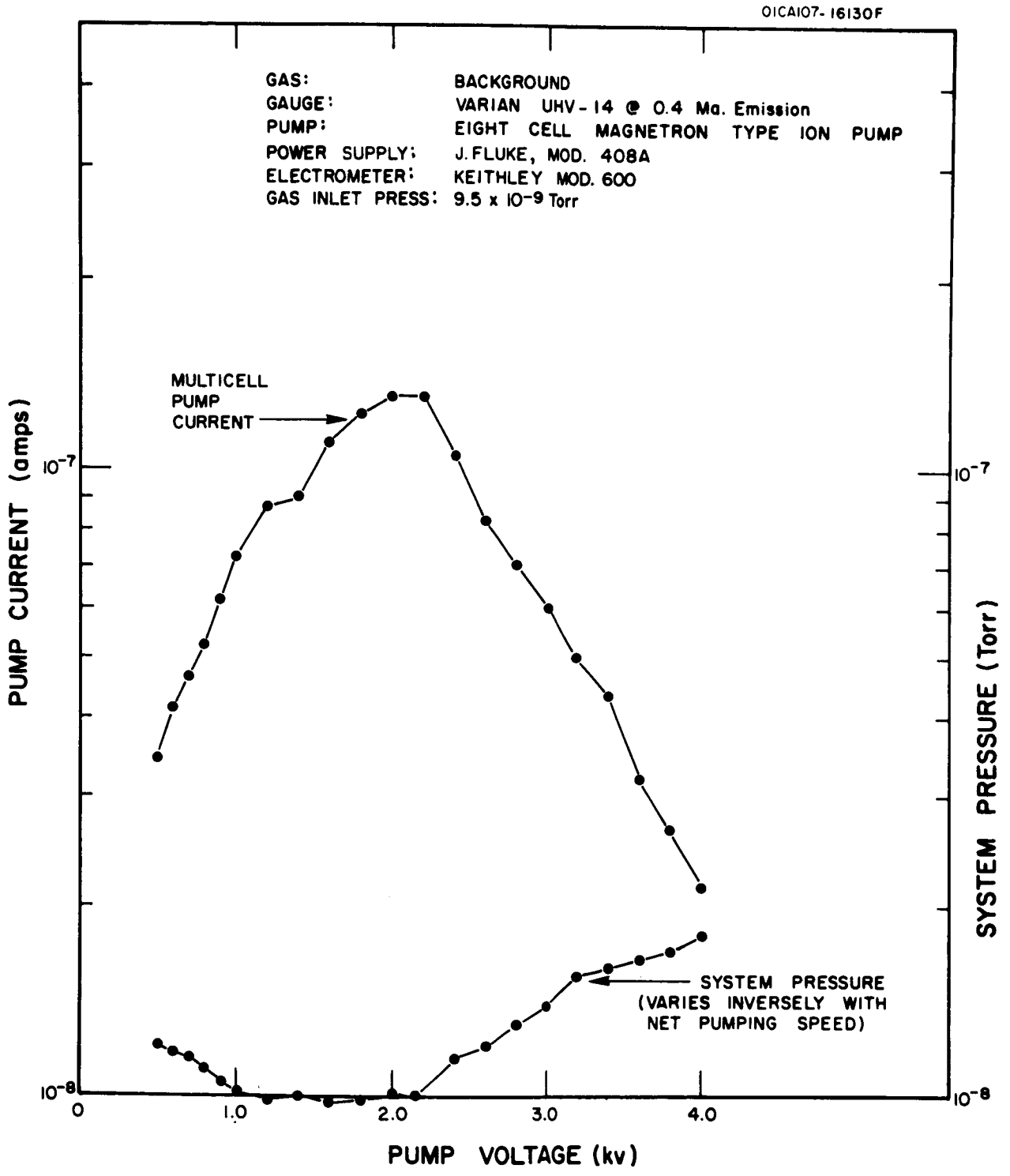

Figure 23. Current-voltage characteristic and pumping effect of the multicell magnetron type ion pump for background gas.

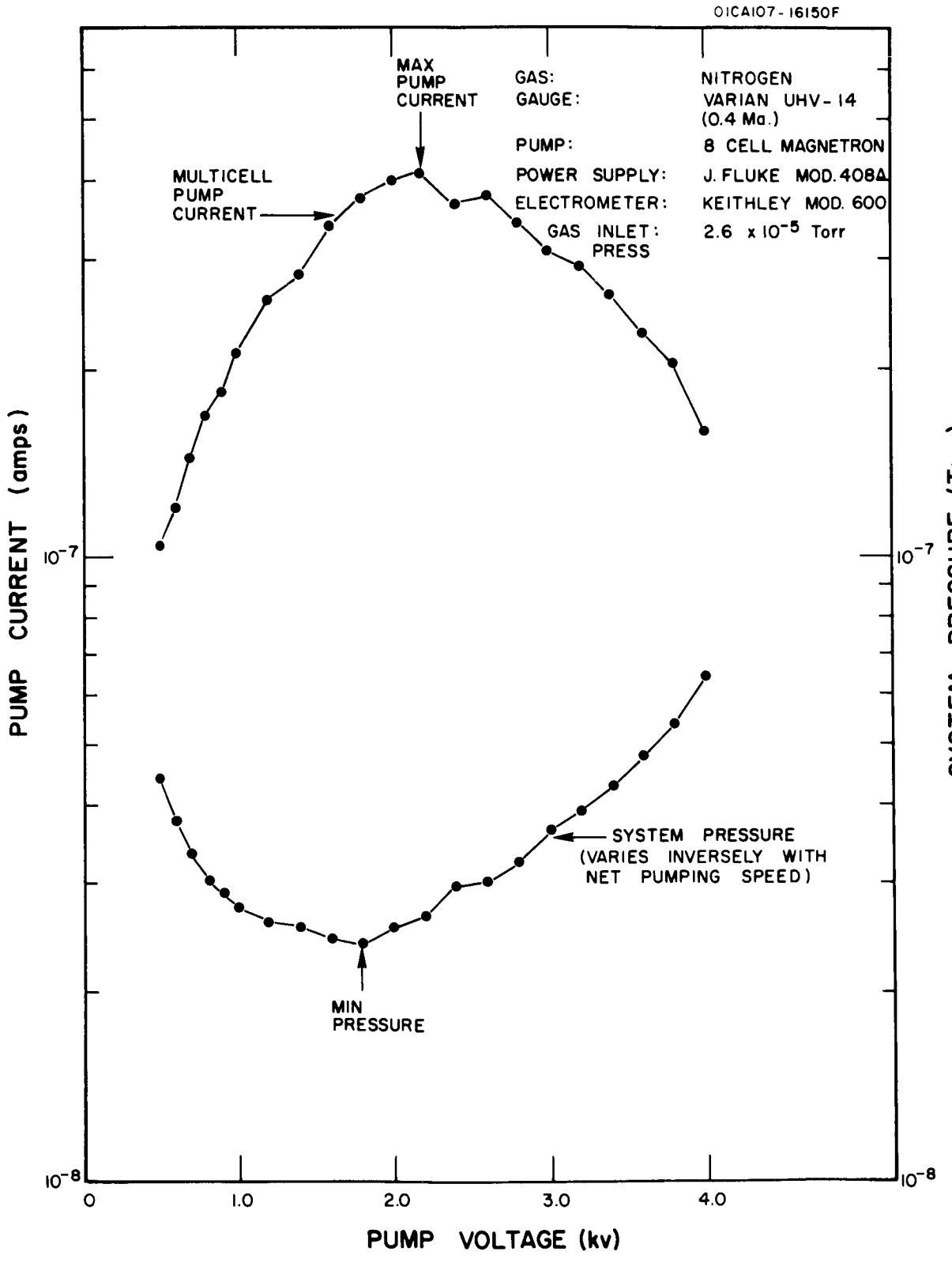

Figure 24. Current-voltage characteristic and pumping effect of the multicell magnetron type ion pump for lower pressure nitrogen gas.

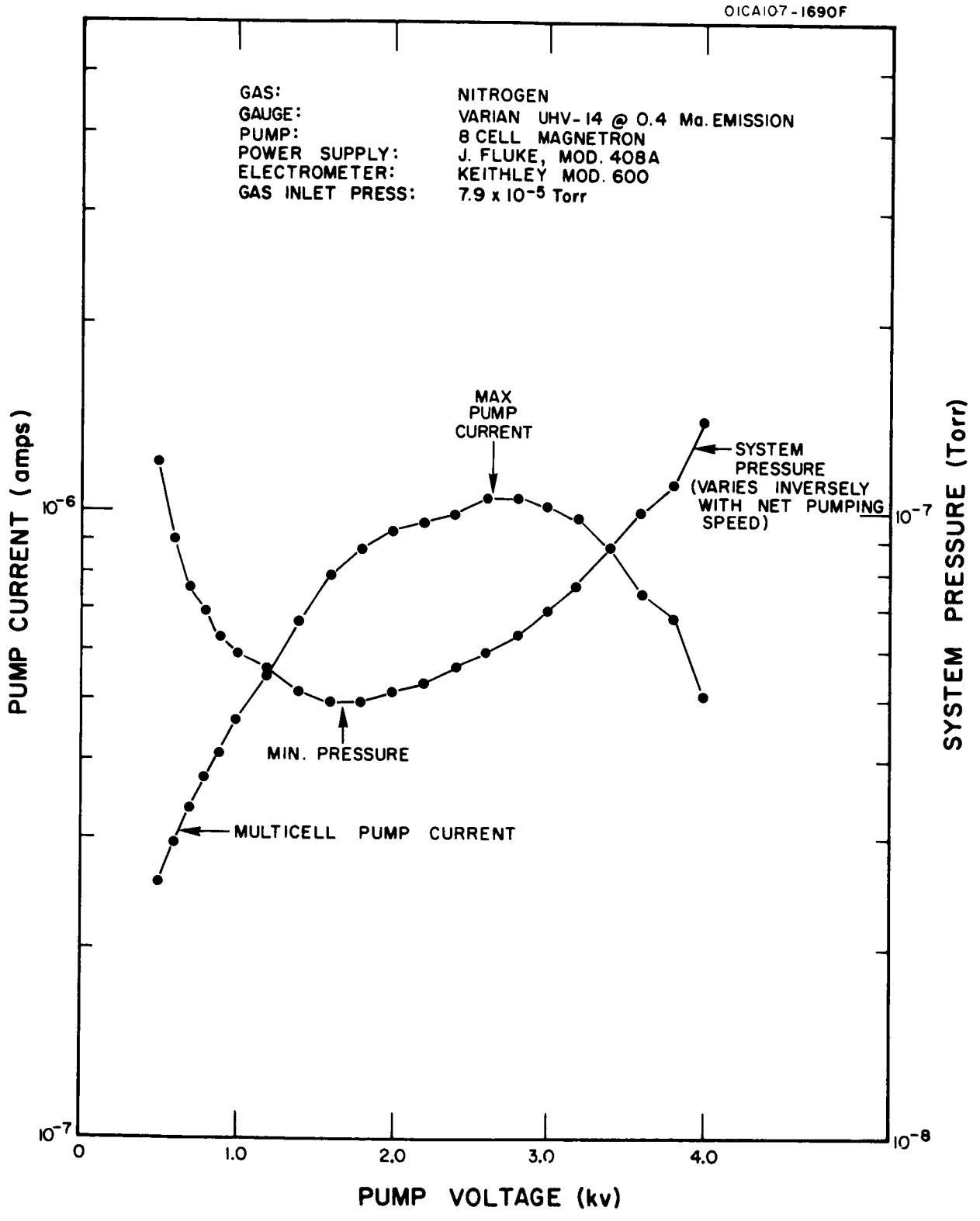

Figure 25. Current-voltage characteristic and pumping effect of the multicell magnetron type ion pump for higher pressure nitrogen gas.

immediately evident from the system pressure vs pump voltage curves. Since the system pressure varies inversely with the net pumping speed of the ion pump, the minimum in the system pressure vs. anode voltage pumping curves indicates the pump voltage at which maximum pumping occurred. The anode voltage for maximum net pumping ranged between 1.6 and 1.8 Kv. The maximum pumping speed measured was 1.38 liters/sec at an anode voltage of 1.8 Kv.

In addition to yielding pumping speed values, the data taken provide pressure calibrations for the multicell pump at the various pump voltages. Calibration curves (pump current vs. system pressure) for pump voltages of 1, 2, 3, and 4 Kv are shown in Figure 26. As can be seen from these curves, the current-pressure relationship is linear for a pump voltage of 1.0 Kv (unity slope on the log log plot), but is non-linear for the higher voltages.

Another way of providing data about the characteristics of an ion pump are to plot values of the ratios of pump current to system pressure I/p, and the ratios of the product of pumping speed and system pressure to pump current SP/I.[11] The values of I/p give the current sensitivity of the pump in amperes per torr and indicate the strength of the discharge (number of positive ions produced per unit time, amount of sputtering, etc.). Generally, one would expect maximum values of pumping to be associated with maximum values of I/p. The values of SP/I give the gas throughput per unit current flow in the pump and indicate the pumping efficiency.

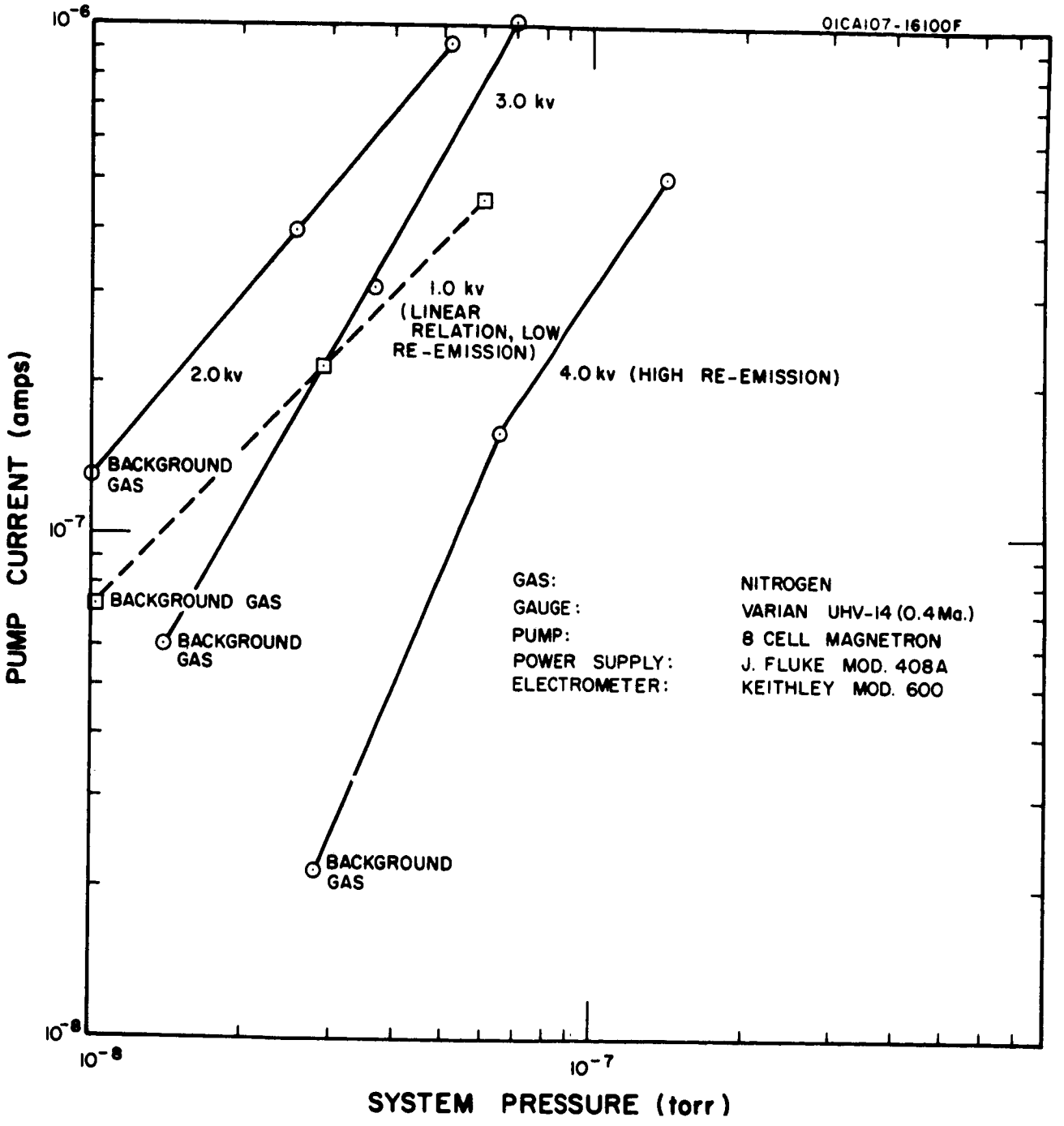

Figure 26. Current-pressure characteristics of the multicell magnetron type ion pump for nitrogen gas.

Values of the pumping speed S, the discharge intensity I/p, and the pumping efficiency SP/I are listed in Table IV for the nitrogen experiment performed. In general, the pumping speed increased with the discharge intensity I/p. The linearity of the pump current as a function of pressure when the anode voltage was 1 Kv is evident from the fairly constant values of I/p for this voltage. Notice that the discharge intensity was a maximum at 2 Kv, but the pumping efficiency was a minimum. The latter two quantities are always inversely related. Since there are 3.5×10^{19} molecules per torr liter and 6.2×10^{18} singly charged ions per coulomb, the ratio of the number of ions collected N_i to the number of molecules pumped N_m is

$$\frac{N_i}{N_m} = \frac{6.2 \times 10^{18}}{3.5 \times 10^{19}} \quad \frac{I}{SP} = \frac{0.177}{SP/I} \tag{8}$$

For the case of the low and high anode voltages of 1.0 and 4.0 Kv, respectively, the pumping efficiency was high, and the number of ions required to pump a single gas molecule approached unity. For the intermediate anode voltages of 2.0 and 3.0 Kv, it required at least two ions for each molecule pumped.

The curves of Figures 23, 24, and 25 show a most interesting phenomenon, namely the non-coincidence of the maximum pump current and the maximum net pumping speed. The multicell magnetron type ion pump was a more or less true ion pump -- as contrasted with a getter-ion pump. A getter-ion pump contains titanium or some similar active metal that

TABLE IV

CHARACTERISTIC BEHAVIOR OF THE MULTICELL MAGNETRON TYPE ION PUMP FOR NITROGEN GAS

Anode Voltage V (Kv)	Gas Inlet Pressure $P_{G.I.}$ (torr)	Pump Current I (Amps)	System Pressure P (torr)	Pumping Speed S(ℓ/sec)	Discharge Intensity I/P(Amps/torr)	Pumping Efficiency SP/I ($\frac{torr\,\ell}{sec,amp}$)
	*9.5×10^{-9}	7.25×10^{-8}	*1.02×10^{-8}	- - -	7.11	- - -
1	2.6×10^{-5}	2.15×10^{-7}	2.75×10^{-8}	1.00	7.81	0.128
	7.9×10^{-5}	4.60×10^{-7}	5.95×10^{-8}	1.08	7.73	0.140
	*9.5×10^{-9}	1.30×10^{-7}	*1.00×10^{-8}	- - -	13.0	- - -
2	2.6×10^{-5}	4.00×10^{-7}	2.55×10^{-8}	1.14	15.7	0.0727
	7.9×10^{-5}	9.30×10^{-7}	5.15×10^{-8}	1.32	18.0	0.0731
	*9.5×10^{-9}	6.00×10^{-8}	*1.40×10^{-8}	- - -	4.29	- - -
3	2.6×10^{-5}	3.10×10^{-7}	3.65×10^{-8}	0.82	8.49	0.0962
	7.9×10^{-5}	1.02×10^{-6}	6.95×10^{-8}	1.00	14.6	0.0681
	*9.5×10^{-9}	2.15×10^{-8}	*1.80×10^{-8}	- - -	1.19	- - -
4	2.6×10^{-5}	1.60×10^{-7}	6.45×10^{-7}	0.40	2.48	0.162
	7.9×10^{-5}	5.10×10^{-7}	1.40×10^{-7}	0.46	3.64	0.126

* Background Gas

can combine chemically via sputtering with active gas molecules. A true ion pump, ideally, should pump gas only by the mechanism of ionization and burial of ions in the pump cathode.

The explanation of the non-coincidence of maximum pump current and maximum net pumping speed must depend on the phenomenon of re-emission of previously pumped molecules. In a true ion pump, the presence of re-emission should be quite evident at all times, as it appears to be in the multicell magnetron ion pump. In a getter-ion pump, re-emission may not be as noticeable because most of the pumping takes place by gettering action.

As the anode voltage of the magnetron type pump was increased beyond about 1.5 Kv, re-emission of previously pumped molecules (or possibly a sputtering and release of other gases in the pump cathode) caused the net pumping speed to decrease. Thus, as the discharge intensity was increasing to a maximum with increasing anode voltage, the net pumping speed was actually decreasing due to the release of more gas than was being pumped. This behavior, of course, is reflected in the data of Table IV.

All true ion pumps exhibit a saturation effect. After a finite number of molecules have been pumped, the net speed of the pump decreases considerably. Generally, monolayer coverage of a surface with pumped or trapped molecules is considered to constitute saturation. There are approximately 1×10^{15} molecules/cm^2 in a monolayer, and since the geometrical surface area of the cathodes in the multicell pump was

about 120 cm^2, at least 1.2×10^{17} molecules would have to be pumped before saturation was reached. If it is assumed that each ion formed is pumped, then operation at a pressure of 1×10^{-8} torr with an ion current of about 1×10^{-7} amperes would lead to saturation in 2¼ days of operation. Such a pump, operating in combination with a cryopump at a pressure of 1×10^{-10} torr, would not saturate for 225 days.

Although the nitrogen pumping speed experiment as described was not sufficient to saturate the multicell pump, the system had been in operation and the multicell pump had been pumping background gas at a pressure of about 1×10^{-8} torr for a few weeks prior to the experiment. It is most likely that the pump cathode was partially saturated with background gas at the time the experiment was started.

The initial operation of the single cell magnetron type ion pump took place after the cryopump-ion pump system had been baked at temperatures above 240°C for 6 hours, of which 2 hours was spent at temperatures above 300°C, up to a maximum of 345°C. The permanent magnet used with this pump had a magnetic field of 900 gauss.

The single cell ion pump did not start until a voltage of 3.5 kv was placed on the anode. There was very little outgassing from this pump, its pumping action starting almost immediately. The pressure in the system at the time was in the low 10^{-6} torr region. After the ion gauge which measured the test chamber pressure had been outgassed, and the single cell pump had been in operation for a few hours at 4.0 kv, its sensitivity at a test chamber pressure of 6×10^{-8} torr was about 10 amperes/torr.

The variation of the single cell ion pump current with anode voltage for the background gas present in the closed system was determined in a separate experiment. The pressure in the system was measured with a nude Bayard-Alpert type gauge for each setting of the pump anode voltage. As before, the system pressure was inversely proportional to the net pumping speed of the single cell ion pump. The results of this experiment are plotted in the graph of Figure 27.

As can be seen from the figure, the pump sensitivity increased with increasing anode voltage over the range from 500 volts to 4.6 kv. As the discharge intensity increased, so too did the net pumping speed, so that the system pressure fell monatomically with increasing pump voltage. At a system pressure of 3×10^{-8} torr (at an anode voltage of 4.0 kv) the pump sensitivity was about 10 amperes/torr. Re-emission of molecules could not be detected in this experiment since the pump current did not exhibit a maximum for the voltage range covered. However, the current-voltage characteristic appeared to be levelling off at a voltage of 4.5 kv, and there is no doubt that higher anode voltages would begin to produce smaller pump currents.

The pumping speed of the single cell magnetron type ion pump was not measured. However, a comparison of the residual pressures attained with both magnetron type pumps indicated that the pumping speed of the single cell pump was less than that of the multicell pump.

During an experiment in which liquid helium was added to the cryopump, it was found that the single cell ion pump voltage had to be

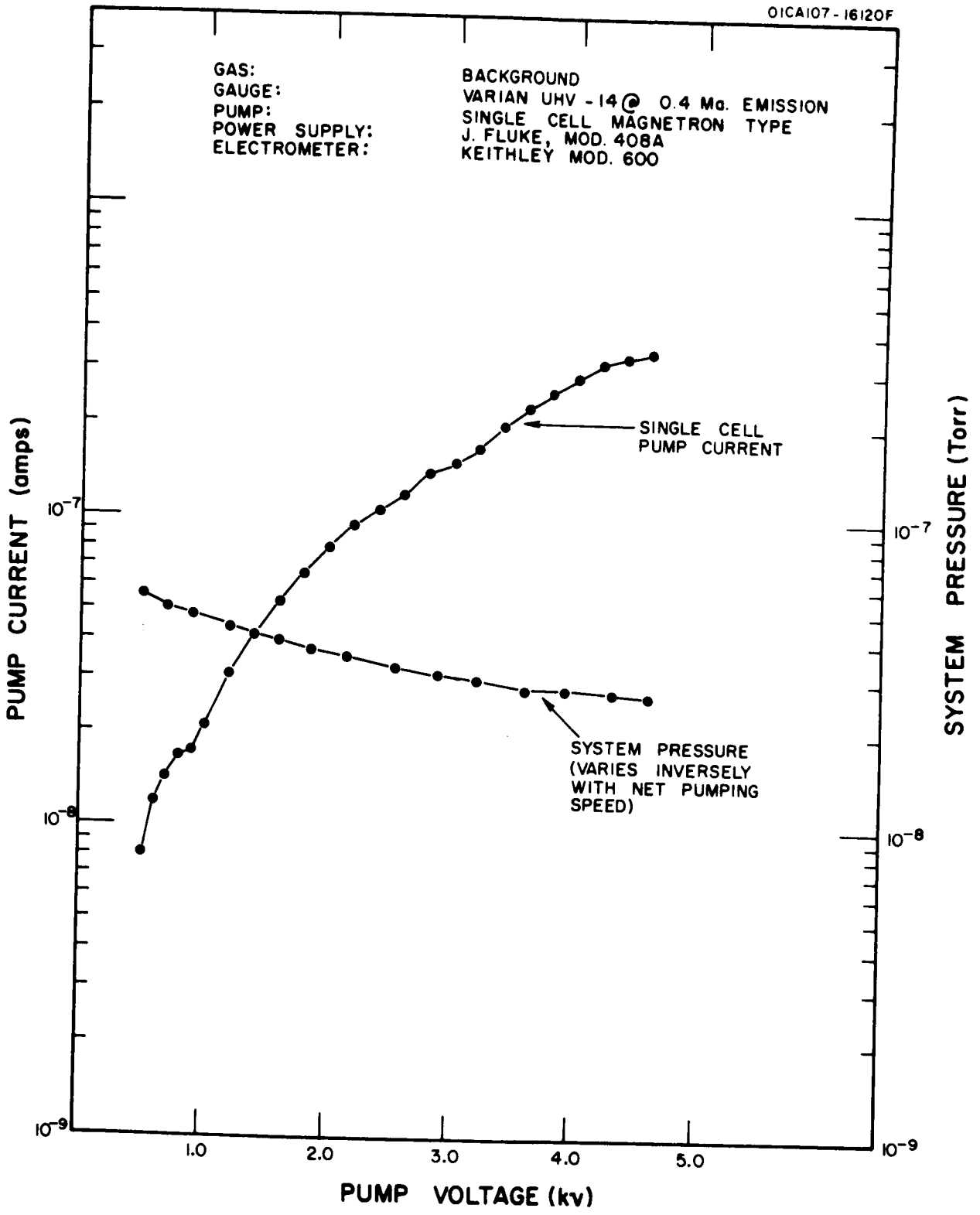

Figure 27. Current-voltage characteristic and pumping effect of the single cell magnetron type ion pump for background gas.

reduced from 4.0 kv to 3.0 kv or less in order to follow the system pressure variations and yield a pump current in the 10^{-10} ampere region consistent with the system pressure (as measured with the nude hot filament ionization gauge). It is not known whether the pump current readings of about 1×10^{-8} torr at 4.0 kv were caused by pump outgassing at the higher voltage or by leakage or cold field emission. The lowest single cell ion pump current reading obtained was a value of 3.3×10^{-10} amperes at an anode voltage of 3.0 kv. The system pressure as measured by the nude Varian gauge was 1.2×10^{-10} torr at 0.04 Ma emission (uncorrected) at this time. The actual pressure in the system was estimated to be in the high 10^{-11} torr region.

4.2.3 Bakeout Procedure. The procedure for baking the cryopump-ion pump system was somewhat complicated by the use of three separate pumps for this operation. A mechanical vacuum pump was first used to rough out the entire system through a zeolite charged foreline trap and a dry ice trap. The mechanical pump was then used to maintain a low pressure in the zeolite absorption type pump while it was baked. After the absorption forepump had been baked overnight, it was isolated from the mechanical pump and cooled to liquid nitrogen temperature. The system oven was then energized, and the foreline getter-ion pump was also heated, the pressure in the system being maintained in the 10^{-4} to 10^{-5} torr region by the pumping action of the chilled zeolite absorption pump. The system pressure was monitored by the hot filament gauge connected to the foreline "Tee" section.

After the UHV portion of the system had been baked for at least several hours at temperatures up to 350°C, the foreline getter-ion pump (Vacion pump) was allowed to cool down and was then turned on. After some time, the absorption type pump was valved off, and the getter-ion pump was used by itself for the last phase of the bakeout cycle.

When the UHV part of the system had cooled, the various gauges and pumps attached to the test chamber were turned on and permitted to outgas into the getter-ion pump. Once the magnetron type pumps had been operated under voltage for an hour or two, the bakeable valve separating the UHV and foreline parts of the system could be closed. The magnetron type pump would then be pumping the UHV part of the system by itself.

A typical bakeout schedule for the cryopump-ion pump system is shown in Table V. Notice that although the entire procedure took about 30 hours, the system was baked only about 6 hours at temperatures over 240°C, and only 2 hours at temperatures over 300°C. The maximum oven temperature reached during this bakeout was 345°C. At the latter temperature, the system pressure was 1.4×10^{-4} torr, a relatively high pressure. Temperatures above 350°C were not attained because the system pressure would have been high enough to cause oxidation of all internal metal surfaces. As will be pointed out later, the limitation of system bakeout temperature imposed a limit on the system outgassing rate and hence limited the ultimate pressure that could be attained.

TABLE V

SCHEDULE OF A TYPICAL BAKEOUT
OF THE CRYOPUMP-ION PUMP SYSTEM

Time (Hr : Min)	System Pressure (torr)	Vacion Pump Temp. (°C)	Oven Temp. (°C)
00:00	$< 1x10^{-3}$	0	0
	Turned on absorption pump heating mantle.		
	Mechanical pump on. UHV part of system is isolated		
00:45	$38x10^{-3}$	0	0
5:10	$110x10^{-3}$	0	0
15:30	$65x10^{-3}$	0	0
17:00	$63x10^{-3}$	0	0
	Turned off absorption pump heating mantle.		
	Isolated absorption pump from mechanical pump.		
17:50	$8x10^{-3}$	0	0
19:00	$8x10^{-3}$	0	0
	Started to cool the absorption pump with liquid nitrogen.		
19:10	$< 1x10^{-3}$		
	Turned on the hot filament forepressure gauge		
19:15	$6.2x10^{-5}$	0	0
20:00	$2.4x10^{-5}$	0	0
	Turned on oven. Each pair of heating elements set at "Low" position.		
20:45	$6.0x10^{-5}$	0	124
21:15	$4.4x10^{-5}$	0	140
	Vacion pump heating mantle turned on.		
21:30	$8.5x10^{-5}$	220	150
	Center pair of oven heating elements changed from "Low" position to "High" position.		
22:15	$9.1x10^{-5}$	288	240
22:50	$9.8x10^{-5}$	300	274

TABLE V (Continued)

Time (Hr : Min)	System Pressure (torr)	Vacion Pump Temp. (^{o}C)	Oven Temp. (^{o}C)
23:30	1.5×10^{-4}	302	300
	Turned off the Vacion pump heating mantle.		
23:50	1.8×10^{-4}	- - -	310
24:00	2.1×10^{-4}	- - -	317
	Started the Vacion pump.		
24:10	1.3×10^{-4}	- - -	320
	Vacion pump reading was 1.5×10^{-4} torr.		
	The Vacion pump is still hot to the touch.		
25:20	1.4×10^{-4}	- - -	345
	Center pair of oven heating elements changed from "High" position to "Low" position.		
25:40	9.0×10^{-5}	- - -	306
28:10	1.6×10^{-5}	0	237
	Vacion pump reading was 3×10^{-5} torr		
28:45	1.3×10^{-5}	0	230
	Vacion pump reading was 2.3×10^{-5} torr		
	Isolated the absorption pump from UHV system.		
	Turned off the oven heaters.		
28:50	2.7×10^{-6}	0	225
	Vacion pump reading was 1.0×10^{-5} torr		
	Warmed up the absorption pump and removed desorbed gas with the mechanical pump.		
31:00	3.6×10^{-7}	0	80^{o}C
	Vacion pump reading was 3.5×10^{-7} torr		

4.2.4 Oven. The inexpensive "roll-on" type oven that was constructed for the cryopump-ion pump system proved to be quite satisfactory. The oven was relatively easy to install and remove. The oven fan was vibration free, quiet, and adjustable in speed. Temperature at various points within the oven could be easily measured with a mercury-in-glass thermometer. A small gas fitting was installed through the oven wall so that an inert gas such as argon could be flowed into the oven enclosure. At oven temperatures above 250°C, the use of argon gas minimized external oxidation of the system.

The connection of the oven heaters in pairs located symmetrically on either side wall proved to be a good arrangement. The three pairs of heaters, each with its own switch, furnished nine different heat inputs. Additional heat inputs could be obtained if symmetry of heating was abandoned.

In the short table below, the nine symmetrical heating combinations are listed together with some equilibrium temperatures that were obtained when the oven was empty. The symbols O, L, and H stand for off, low, and high switch positions, respectively.

Switch Position	O O L	O L L	L L L
Equilibrium Temp.	165°C	220°C	260°C
Switch Position	O O H	O L H	L L H
Equilibrium Temp.	-----	346°C	-----
Switch Position	O H H	L H H	H H H
Equilibrium Temp.	422°C	440°C	-----

5. RESIDUAL GAS ANALYSIS

5.1 DIFFUSION PUMP SYSTEM

Multiple mercury diffusion pump systems that are operating at low pressures seem to have a characteristic residual gas mass spectrum. The gas species that were usually found to be present in both the metal diffusion pump system described herein and in similar Venema type glass mercury diffusion pump systems were CO_2^{44}, CO^{28}, H_2O^{18}, OH^{17}, O^{16}, C^{12}, and H_2^{2}. None of the ordinary atmospheric components such as A, O_2, N_2, Ne, or He was ever present in detectable amounts at system pressures of the order of 10^{-10} torr. Mercury vapor was never detected in the metal system.

In the metal mercury diffusion pump system operating at 10^{-10} torr or below, atomic oxygen was always found to be the largest mass peak present. In terms of the current output of the mass spectrometer, the mass peaks listed according to their magnitude were O, CO, H_2O, CO_2, C, and H_2. The OH peak is grouped with the H_2O peak in the above listing.

A typical residual gas spectrum for the metal mercury diffusion pump system operating at a pressure in the low 10^{-10} torr region is shown in Figure 28. The mass spectrometer used was the General Electric metal envelope partial pressure analyzer (Model 22PT110). The largest mass peak in the spectrum, atomic oxygen, appeared to be completely unrelated to the system pressure, as will be shown shortly. It has been postulated

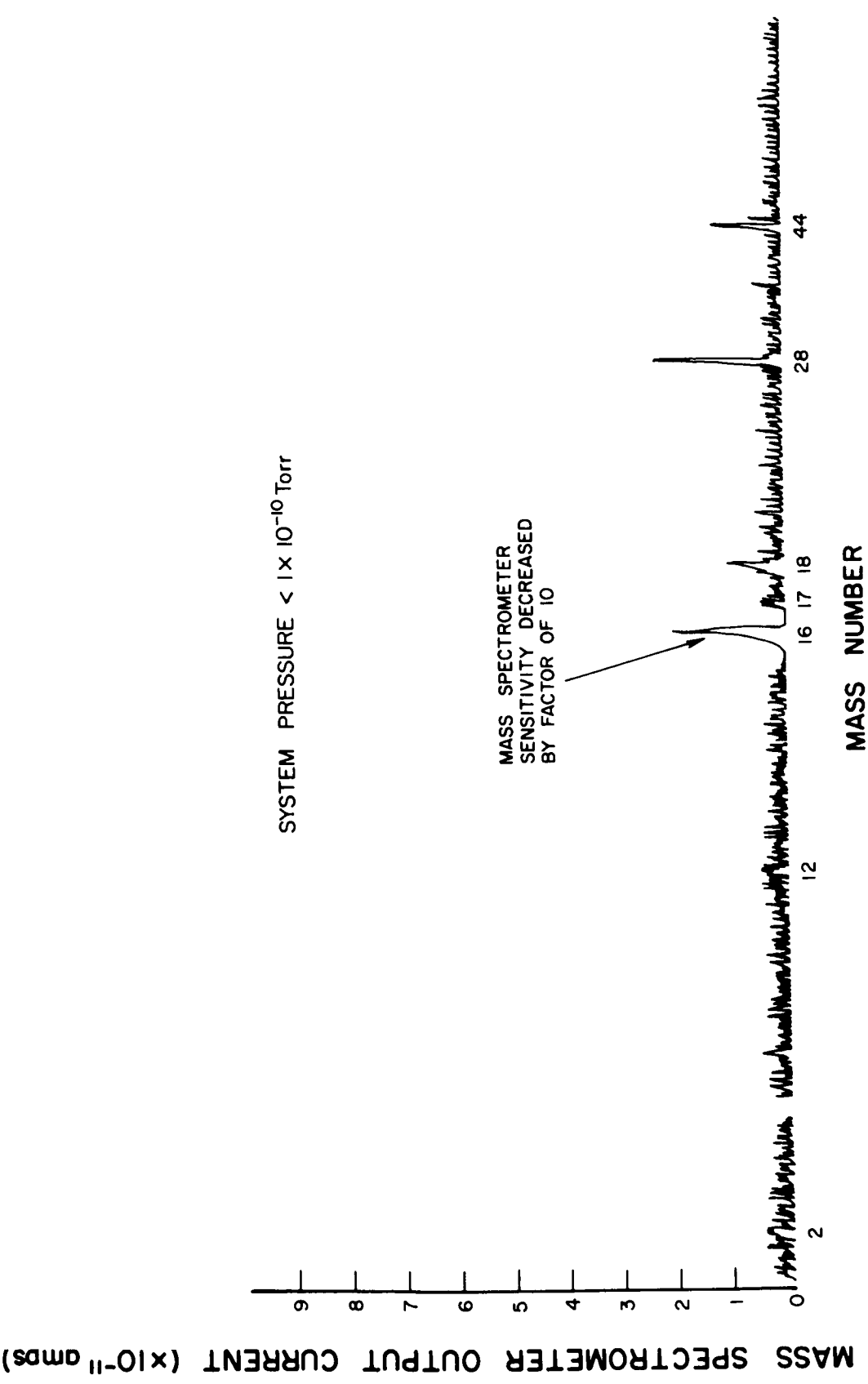

Figure 28. Typical residual gas mass spectrum of the mercury diffusion pump system at a pressure below 1 x 10^{-10} torr.

that atomic oxygen such as that found in this mass spectrum derives from electron bombardment of the mass spectrometer grid cage[14]. Certain other masses, such as fluorine F^{19}, and chlorine Cl^{35} and Cl^{37} are also sometimes seen in low pressure mass spectra. We have found that fluorine and chlorine were not detectable in the spectra until bakeout temperatures of 350°C or higher were used.

A residual gas spectrum of a vacuum system is most useful when the sources of each gaseous component can be determined. Toward this end, a series of changes and perturbations were made in a number of elements of the system -- including the mass spectrometer itself. Table VI lists the changes that were made and their effect on the residual gas spectrum.

A study of the data presented in Table VI leads one to a number of important conclusions. In the General Electric partial pressure analyzer that was used to study the system residual gas spectrum, the speed of the sweep affected the amplitudes of the strip chart recorded mass peaks. Mass peak amplitudes were definitely smaller for sweeps that were less than 10 minutes in duration. Possibly the limitation here was the limited speed of response of the d.c. amplifier or strip chart recorder. Sweep speeds of 30 minutes or more were judged to be too long to obtain comparable values of low and high masses when conditions in the system were changing.

It was found that the mass spectrometer, in common with hot filament ionization gauges, outgassed heavily, especially at higher emission currents. The use of a smaller emission current reduced the outgassing

TABLE VI

MASS SPECTROMETER STUDIES OF THE MERCURY DIFFUSION PUMP SYSTEM

Time (Hr : Min)	Mass Number	Mass Peak Current (Amperes)	Change in Mass Peak (%)	Remarks
00:00	Test Chamber Pressure, P_T, = 2.5×10^{-10} torr at 10 Ma emission Backing Diffusion Pump Pressure, P_B = 1.2×10^{-7} at 10 Ma emission Turned on Filament of Mass Spectrometer. P_T increased to 9.5×10^{-10} torr and then started to decrease. Adjusted M.S. filament emission to 1.0 Ma at 70 Volts.			
00:55	Filled both non-level-sensitive cold traps. P_T = 3.25×10^{-10} torr, P_B = 8.5×10^{-7} torr			
1:05	Took Mass Spectrum using a 3 Minute sweep. P_T = 3.3×10^{-10} torr, P_B = 8.0×10^{-7} torr			
	44	1.5×10^{-10}		m.s. filament emission 1.0 Ma at 70 Volts.
	28	3.8×10^{-10}		
	18	2.05×10^{-10}		
	17	5.5×10^{-11}		
	16	7.9×10^{-10}		
	12	5.8×10^{-11}		
1:15	Took Mass Spectrum using a 10 minute sweep, 1.0 Ma emission. P_T = 3.3×10^{-10} torr			
	44	1.7×10^{-10}	+ 13.3	Increase in all mass peaks due to longer sweep time.
	28	4.0×10^{-10}	5.3	
	18	2.25×10^{-10}	9.7	
	17	6.0×10^{-11}	9.1	
	16	8.4×10^{-10}	6.3	
	12	6.4×10^{-11}	8.6	

TABLE VI (CONT.)

MASS SPECTROMETER STUDIES OF THE MERCURY DIFFUSION PUMP SYSTEM

Time (Hr : Min)	Mass Number	Mass Peak Current (Amperes)	Change in Mass Peak (%)	Remarks
1:30	Turned off the backing diffusion pump hot filament gauge.			
1:55	Took Mass Spectrum with 10 min. sweep, 1.0 Ma emission. $P_T = 3.2 \times 10^{-10}$ torr, P_B (gauge off)			
	44	1.6×10^{-10}	- 5.9	Note the slight decrease in
	28	3.95×10^{-10}	0.8	the test chamber pressure P_T.
	18	2.3×10^{-10}	+ 2.2	
	17	6.0×10^{-11}	0	
	16	9.3×10^{-10}	+ 10.7	The increase in the 16 peak
	12	6.4×10^{-11}	0	evidently had no effect on pressure P_T.
2:10	$P_T = 3.2 \times 10^{-10}$ torr at 10 Ma emission. Turned off the test chamber gauge.			
3:00	Took mass spectrum with 10 min. sweep, 1.0 Ma emission.			
	44	1.4×10^{-10}	- 14.4	P_T (gauge off), P_B (gauge off)
	28	3.75×10^{-10}	6.6	Note the decrease in all
	18	2.05×10^{-10}	13.9	mass peaks except mass 12.
	17	6.0×10^{-11}	8.3	Test chamber glass hot
	16	9.0×10^{-10}	3.2	filament gauge produced
	12	6.4×10^{-11}	0	mostly CO_2 and H_2O.
3:12	Reduced m.s. filament emission from 1.0 Ma to 0.5 Ma.			
3:30	Took mass spectrum with 10 min. sweep, 0.5 Ma emission			
	44	5.7×10^{-11}	- 59.9	P_T (gauge off), P_B (gauge off)
	28	1.25×10^{-10}	66.8	Note the decrease in all mass
	18	5.7×10^{-11}	71.9	peaks of 60 to 70 percent.
	17	1.9×10^{-11}	68.3	(except for mass 16) for only

TABLE VI (CONT.)

MASS SPECTROMETER STUDIES OF THE MERCURY DIFFUSION PUMP SYSTEM

Time (Hr : Min)	Mass Number	Mass Peak Current (Amperes)	Change in Mass Peak (%)	Remarks
	16	5.85×10^{-10}	34.9	a 50% decrease in emission
	12	1.7×10^{-11}	73.8	current. This implies a decreased outgassing of the m.s. filament at 0.5 Ma, emission and indicates that most of the gas comes from the mass spectrometer.
3:40	Reduced m.s. filament emission from 0.5 to 0.25 Ma.			
3:58	Filled both non-level-sensitive cold traps			
4:00	Took mass pectrum with 10 min. sweep, 0.25 Ma emission.			
	44	1.6×10^{-11}	- 71.9	P_T (gauge off), P_B (gauge off)
	28	3.4×10^{-11}	72.6	For a second reduction of
	18	1.95×10^{-11}	63.2	electron emission by 50%,
	17	6.6×10^{-12}	65.3	There was again a general
	16	2.8×10^{-10}	52.2	decrease of 60 to 70 percent
	12	5×10^{-12}	70.6	in all mass peaks except 16.
4:29	Filled the lower non-level-sensitive (NLS) cold trap. Will permit the level of the top NLS cold trap to run low.			
4:30	Took mass spectrum with 10 min. sweep, 0.25 Ma emission.			
	44	1.3×10^{-11}	- 19	P_T (gauge off), P_B (gauge off)
	28	3.4×10^{-11}	0	Top NLS cold trap last filled
	18	1.4×10^{-11}	- 28	at 3:58.
	17	not readable	- - -	There seems to be a correlation
	16	2.75×10^{-10}	- 1.8	between mass peaks 28 and 12.
	12	5×10^{-12}	0	Note the reduction in CO_2 and

TABLE VI (CONT.)

MASS SPECTROMETER STUDIES OF THE MERCURY DIFFUSION PUMP SYSTEM

Time (Hr : Min)	Mass Number	Mass Peak Current (Amperes)	Change in Mass Peak (%)	Remarks
	16+	3.2×10^{-10}	+ 6.7	The CO_2 desorption is
	16-	2.0×10^{-10}	- 13.0	decreasing.
	12	7.8×10^{-11}	23	
7:30	Took mass spectrum with 10 min. sweep, 0.25 Ma emission.			
	44	3.4×10^{-10}	- 58.4	P_T (gauge off), P_B (gauge off)
	28	1.5×10^{-10}	40	Top NLS cold trap last filled
	22	1.05×10^{-11}	52.3	at 3.58.
	19	4×10^{-12}	50	Note that all masses decreased
	18	1.6×10^{-11}	+ 67	40 or 50 percent except
	17	5×10^{-12}	- - -	water vapor. This is
	16+	3.0×10^{-10}	- 6.2	probably the beginning
	16-	1.2×10^{-10}	40	of water vapor desorption
	12	3.6×10^{-11}	54	from the top cold trap.
7:50	Made mass spectrometer search for helium. No mass peak greater than the noise level of 1 or 2×10^{-12} amperes was found.			
	Took hydrogen mass spectrum with 1 min. sweep, 0.25 Ma emission			
	2	1.2×10^{-11}	- - -	The hydrogen mass peak is usually about 5 or 6×10^{-12} amperes. The larger peak here is probably due to desorption of water.
22:50	The system had been pumping overnight with only the lower NLS cold trap being filled. Turned on the mass spectrometer and adjusted the filament emission to 0.25 Ma. The test chamber pressure increased from			

TABLE VI (CONT.)

MASS SPECTROMETER STUDIES OF THE MERCURY DIFFUSION PUMP SYSTEM

Time (Hr : Min)	Mass Number	Mass Peak Current (Amperes)	Change in Mass Peak (%)	Remarks
	4.8×10^{-10} torr at 10 Ma. emission to about 3×10^{-9} torr, then started to decrease.			
23:05	Took mass spectrum with 10 min. sweep, 0.25 Ma. emission			
	44	1.35×10^{-11}		$P_T = 5.1\times10^{-10}$ torr, $P_B = 7\times10^{-8}$ torr. The top NLS cold trap is empty.
	28	2.7×10^{-11}		
	18	1.0×10^{-11}		
	17	2×10^{-12}		
	16	2.3×10^{-10}		
	12	$< 5\times10^{-12}$		
	2	4.8×10^{-12}		
	Searched for doubly ionized mercury at mass number 100, but found none.			
23:45	Turned off the backing diffusion pump ion gauge.			
24:00	Filled the lower NLS cold trap with liquid nitrogen. $P_T = 5.1\times10^{-10}$ torr at 10 Ma. emission.			
25:15	Took mass spectrum with 19 min. sweep, 0.25 Ma. emission			
	44	7.0×10^{-11}	+ 419	$P_T = 3.65\times10^{-9}$ torr at start
	28	4.9×10^{-11}	81.4	$P_T = 4.2\times10^{-9}$ torr at end
	18	1.4×10^{-11}	40	Lower NLS cold trap last
	17	6×10^{-12}	200	filled at 24:00.
	16	2.25×10^{-10}	2.2	Note the increase in all
	12	1.1×10^{-11}	- - -	masses except mass 16.
25:45	Took separate mass spectrum of hydrogen, 10 min sweep, 0.25 Ma. emission.			
	2	4.65×10^{-12}	- 3.1	$P_T = 4.4\times10^{-9}$ torr at 10 Ma.

TABLE VI (CONT.)

MASS SPECTROMETER STUDIES OF THE MERCURY DIFFUSION PUMP SYSTEM

Time (Hr : Min)	Mass Number	Mass Peak Current (Amperes)	Change in Mass Peak (%)	Remarks
				Effectively no change in hydrogen.
25:55	Filled the lower NLS cold trap with liquid nitrogen.			
26:45	$P_T = 5.2 \times 10^{-10}$ torr at 10 Ma. Started to fill the upper NLS cold trap with liquid nitrogen.			
27:55	Took mass spectrum with 10 min. sweep, 0.25 Ma. emission.			
	44	1.25×10^{-11}	- 82	$P_T = 3.3 \times 10^{-10}$ torr at 10 Ma.
	28	3.0×10^{-11}	39	This mass spectrum, when
	18	1.25×10^{-11}	10.7	compared with the 23:05
	17	not readable	- - -	mass spectrum, indicates that
	16	2.15×10^{-10}	4.4	the ion gauge at the test chamber
	12	not readable	- - -	and the mass spectrometer do not always see the same gas components.
28:05	Turned on a heating tape that covered about 188 cm^2 of the test chamber 304L stainless steel surface.			
28:25	Took mass spectrum with 10 min. sweep, 0.25 Ma. emission.			
	44	1.8×10^{-11}	+ 44	$P_T = 4.0 \times 10^{-10}$ at 10 Ma.
	28	3.0×10^{-11}	0	Chamber temperature = 340°C.
	18	1.65×10^{-11}	32	Note the increase in CO_2
	17	6×10^{-12}	- - -	and H_2O. Carbon monoxide
	16	2.15×10^{-10}	0	and atomic oxygen were
	12	6×10^{-12}	- - -	unchanged.
28:40	Took separate mass spectrum of hydrogen, 1 min. sweep, 0.25 Ma. emission.			

TABLE VI (CONT.)

MASS SPECTROMETER STUDIES OF THE MERCURY DIFFUSION PUMP SYSTEM

Time (Hr : Min)	Mass Number	Mass Peak Current (Amperes)	Change in Mass Peak (%)	Remarks
	2	7.3×10^{-12}	- - -	$P_T = 7.0 \times 10^{-10}$ torr at 10 Ma. Chamber Temperature = 360°C.
28:45	Turned off the heating tape and cooled test chamber with a flow of room temperature air.			
29:00	Took separate mass spectrum of hydrogen, 1 Min. sweep, 0.25 Ma. emission.			
	2	6.5×10^{-12}	- 11	$P_T = 3.5 \times 10^{-10}$ torr at 10 Ma. Chamber temperature = 55°C The increase in H_2 at 360°C could be due to the increase in water vapor

-- and any subsequent ion pumping. One difficulty with the reduced emission of this particular instrument was the absence of a provision to make the emission reading meter more sensitive so that reduced emission currents could be accurately adjusted and monitored. By reducing the emission current in steps from 1.0 ma to 0.5 ma and then from 0.5 ma to 0.25 ma., it was shown that the mass peaks decreased by 60 to 70 percent for each 50 percent reduction in the emission, indicating outgassing of the ion source. The one exception in the above experiment was the behavior of mass peak 16, atomic oxygen. For the first 50 percent reduction in emission current, the atomic oxygen peak decreased only 35 percent. For the second 50 percent reduction in emission current, the atomic oxygen peak decreased by 52 percent.

In another experiment, the backing diffusion pump hot filament ionization gauge was turned off. About 25 minutes later, the test chamber gauge indicated a lower pressure by at least 3 percent while the mass spectrum showed an increase in the mass 16 peak of almost 11 percent, although the CO_2 peak decreased by about 6 percent. The atomic oxygen peak (16) seemed to have no connection with the indicated test chamber pressure.

When the test chamber hot filament ionization gauge was turned off, the mass spectrum showed decreases for all mass peaks except carbon (mass number 12). The small residual carbon peak, seemed unrelated to the partial pressures of CO_2 and CO. Carbon dioxide and water vapor were reduced by the largest amount, about 14 percent each, indicating

that these were the major outgassing products of the hot filament glass ionization gauge.

After the mass spectrometer filament emission was reduced to 0.25 ma., a further decrease in the CO_2 and H_2O peaks was recorded while at the same time there was no change in the CO and the C mass peaks. The latter two peaks appeared to be related.

As the top non-level-sensitive cold trap was allowed to run out of liquid nitrogen and warm up, there was first a small 12 percent desorption of CO_2 (about 1 hour after filling) and then a small 11 percent desorption of H_2O (about 1½ hours after filling) from the upper part of the top cold trap. About 2 hours after filling the cold trap, there was a large desorption of CO. The carbon mass peak also increased considerably, but the CO_2, H_2O, and O mass peaks decreased by 5 to 15 percent. It is speculated that some of the adsorption sites vacated by the CO molecules were filled by CO_2 and H_2O molecules. About 2½ hours after filling the cold trap, the beginning of CO_2 desorption become evident. Water vapor content decreased by 7 percent, again possibly by adsorption on vacated CO_2 adsorption sites. The CO desorption decreased. Three hours after filling the top cold trap, there was a very strong desorption of CO_2, presumably from the cold trap inner container. Doubly ionized CO_2 appeared in the mass spectrum, and for the first time, a twin atomic oxygen peak appeared. The higher mass peak of the pair, labelled mass 16+, was identified as the anomalous atomic oxygen that

had been present all along. This peak was believed to arise from desorption at some surface (most likely the grid cage) of the ion source that is bombared by electrons. It may possibly derive from dissociation of an oxide layer. The lower mass peak of the oxygen pair, labelled mass 16-, was believed to be atomic oxygen arising from dissociation of the CO_2. About 3 hours and 15 minutes after filling the top cold trap, a peak of mass number 19 appeared on the mass spectrum. This was believed to be fluorine. Three and one-half hours after filling the top trap, there was evidence of the start of water vapor desorption. A search was made for helium gas, but none was found. The hydrogen mass peak was about twice its normal magnitude--which could have been due to increased water vapor desorption.

In the next series of experiments, the system was operated with only the lower NLS cold trap being filled. A search was made for doubly ionized mercury at mass number 100, but none was found. It was then decided to let the single, lower NLS cold trap run low. One hour and 15 minutes after the cold trap had been filled to the brim, the test chamber pressure had increased from 5.1×10^{-10} torr to about 4×10^{-9} torr. The mass spectrum showed a general increase of all masses except mass 16. Carbon dioxide exhibited the largest percentage increase, followed by carbon monoxide and water vapor in that order. A separate mass spectrum taken 30 minutes later showed no increase in the system hydrogen background.

The last experiment performed involved heating a sizeable portion of the 304L stainless steel test chamber with heating tape to a

temperature of 340°C. The mass spectra taken before and after the heating showed a 44 percent increase in CO_2 and a 32 percent increase in H_2O. Notably, there was no change in the CO mass peak (nor the O mass peak). The hydrogen mass peak increased by about 11 percent due to the heated portion of the test chamber. Very roughly, the heating caused the test chamber pressure to double - an increase in pressure of about 1×10^{-10} torr. In accordance with this measurement and an exponential dependence of outgassing on temperature, it is clear that outgassing of the stainless steel does not limit the ultimate pressure attainable in the system.

Other, less methodical experiments with the metal mercury diffusion pump system confirmed the general system behavior just described. In addition, some of the other experiments that were made added new bits of information about the system and its pressure measurement. For example, the hot filament gauge on the test chamber was turned on and off, at intervals of about 30 minutes. When the gauge was turned on after being off for 30 minutes, there was an increase in its reading to about twice its normal value. An attempt was made to correlate the "pressure rise" in the ion gauge with increased peak heights in the mass spectrum, but actually there was a small decrease in all the peaks of the residual gas mass spectrum. One explanation of this phenomenon is that turning the gauge on caused electron bombardment and ionization of adsorbed gas at the grid of the gauge. The positive ions created at the surface were collected in the normal fashion at the collector and appeared to indicate a pressure rise. On the other hand, the cleaning

of the grid and the normal pumping action of the gauge caused the general pressure in the system to decrease.

In the cold cathode gauge calibration experiment, the system had been baked overnight at 350°C. The background mass spectrum, taken with the cold cathode gauge on and the hot filament test chamber gauge off, showed masses 19½, 35, and 37 to be present. It is speculated that the higher temperature, longer bakeout caused the impurity masses of fluorine (19½), and chlorine (35,37) to diffuse to the surface from the interior of some elements within the mass spectrometer. At the end of the gauge calibration experiment, the pressure in the test chamber was almost 8.35×10^{-7} torr and slowly decreasing. There was a strong flow of nitrogen gas through the system. A mass spectrum was taken, and the system pressure had decreased to 7.6×10^{-7} torr five minutes after the spectrum was completed. Five minutes later, the system pressure had decreased to 7.0×10^{-7} torr. The cold cathode gauge was turned off, and the system pressure increased to 7.45×10^{-7} torr, indicating a gauge pumping action. A mass spectrum taken at this time with the cold cathode gauge off showed an increase in the CO_2 mass peak of 37 percent, but a decrease in the Carbon peak of 13.5 percent. The cold cathode gauge must have been pumping and dissociating CO_2 generated elsewhere in the system.

After the mercury diffusion pump system had been under vacuum for about a month, it was noticed that the test chamber pressure seemed to be rising slowly, day by day. The pressure was in the 10^{-9} torr region

when there was a general power failure in the laboratory for 35 or 40 minutes. When the power was restored, the system pumps were turned on, and the system pressure recovered to the 10^{-7} torr region. About one week after the power failure, a mass spectrum was taken of the residual gas in the system. The test chamber pressure at the time was 6×10^{-7} torr. The spectrum showed the usual background gases with a large enhancement of water vapor. The water vapor was evidently not being removed from the system by the action of the diffusion pumps or the NLS cold traps because another mass spectrum taken the following day showed no appreciable change in the large amount of residual water vapor present. The two mass spectra, when compared closely, did show that the CO and CO_2 content of the system did increase with time, and this increase could account for the slow rise in system pressure just prior to the power failure. It is believed that the power failure caused the large increase in residual water vapor.

5.2 CRYOPUMP-ION PUMP SYSTEM

The first operation of the mass spectrometer with the cryopump system took place after the system and spectrometer had been baked for six hours at temperatures as high as 345°C. The first mass spectrum was taken with no refrigerants in the cryopump and only the Vacion pump operating in the closed system. The test chamber pressure was 5.2×10^{-8} torr as read by a nude ion gauge operated at a reduced emission of 0.4 Ma. The mass spectrum showed many more mass peaks than appeared at a similar pressure in the mercury diffusion pump system. The masses present in this

initial mass spectrum were 44, 40, 37, 30, 29, 28, 27, 26, 25, 19½, 18, 17, 16, 15, 14, 13, 12 and 2. Those mass peaks which could be identified with a reasonable amount of confidence were 44, CO_2; 40, A; 30, 29, 28, 27, 26, 25, C_2H_6; 28, CO, N_2; 18, 17, H_2O; 16, 15, 14, 13, 12, CH_4; and 2, H_2.[15,16] A second mass spectrum was taken about 40 minutes later under approximately the same conditions except that the test chamber pressure had decreased to 4.75×10^{-8} torr. The largest peak in the spectrum was hydrogen (mass peak current = 2.4×10^{-9} Amps). The next largest peak was ethane, carbon monoxide, and nitrogen (mass peak current = 5.2×10^{-10} amps). Water vapor was the third largest peak (mass peak current = 2.2×10^{-10} amps), and methane and atomic oxygen combined to yield the fourth largest peak (mass peak current = 1.3×10^{-10} amps).

The single cell magnetron type ion pump was turned on at an anode voltage of 4.0 Kv. After it had been on for a few minutes, the bakeable valve separating the UHV and forepressure portions of the system was closed. About 15 minutes later, the pressure in the test chamber had decreased to a value of 3.90×10^{-8} torr, and a mass spectrum was taken. The mass spectrum showed essentially the same masses that had been found for the Vacion pumped system although the magnetron ion pump contained no titanium. A search was made for helium gas, but none was found.

After the single cell ion pump had been operating for several weeks pumping just the UHV part of the system, the pressure in the test chamber was 2.7×10^{-8} torr as measured with the nude ion gauge. There were no

refrigerants present in the cryopump. Turning on the mass spectrometer caused the system pressure to rise momentarily, but within 85 minutes, the pressure in the system had decreased to 2.4×10^{-8} torr, indicating that the mass spectrometer was pumping. Ten minutes after the mass spectrometer was turned on, a mass spectrum of the residual gas was made. The mass peaks that appeared in the spectrum are listed in the first column of Table VII under the heading "initial spectrum". About 90 minutes after this spectrum was taken, the single cell, magnetron type ion pump was turned off and the system pressure began to rise. Ten minutes after the ion pump had been turned off, the system pressure was 1.0×10^{-7} torr and a second mass spectrum was made. In the same manner, mass spectra were also taken 2 hours and 40 minutes and 5 hours and 35 minutes after turning off the ion pump. The mass spectra obtained are listed in Table VII. The experiment was performed in an attempt to determine what gases were being pumped or evolved by the ion pump.

A study of Table VII indicates that at least one gas which had previously been pumped was now being re-emitted. This gas was argon, mass 40. Its partial pressure in the system continually increased after the ion pump was turned off. It is interesting to note that carbon dioxide, mass 44, was generally conspicuous by its low partial pressure in the ion-pumped system. It can be seen that its partial pressure hardly increased at all when the ion pump was turned off. Under ordinary conditions with the ion pump operating, mass peak 28 seemed to be a combination of CO, N_2, and C_2H_6 (for system pressures of the order of 10^{-8} torr). When the ion pump was turned off, the increase in mass 28

TABLE VII

EFFECT OF TURNING OFF THE SINGLE CELL MAGNETRON TYPE ION PUMP IN THE CLOSED CRYOPUMP - ION PUMP SYSTEM

Time	Initial Spectrum -1:30	*(Hr : Min) 00:10	(Hr : Min) 4:40	(Hr : Min) 5:35
System Pressure	2.7×10^{-8} torr	1.0×10^{-7} torr	2.45×10^{-7} torr	3.9×10^{-7} torr
Mass Number	**Mass Peak Height (Amperes)	Mass Peak Height (Amperes)	Mass Peak Height (Amperes)	Mass Peak Height (Amperes)
44	1×10^{-11}	1.5×10^{-11}	- - - -	2×10^{-11}
40	9.10^{-12}	3.0×10^{-11}	4×10^{-11}	7×10^{-11}
30	5×10^{-12}	1.5×10^{-11}	- - - -	- - - -
29	6.5×10^{-12}	2.5×10^{-11}	4×10^{-11}	1×10^{-11}
28	$> 1\times10^{-10}$	5.2×10^{-10}	6.05×10^{-9}	1.35×10^{-8}
27	1.7×10^{-11}	4×10^{-11}	1×10^{-10}	- - - -
26	1.1×10^{-11}	3×10^{-11}	5×10^{-11}	- - - -
19½	6.5×10^{-11}	1×10^{-11}	- - - -	2×10^{-11}
18	8.3×10^{-11}	9.5×10^{-11}	8×10^{-11}	9×10^{-11}
17	3.4×10^{-11}	5.7×10^{-11}	5×10^{-11}	5.5×10^{-11}
16	6.3×10^{-11}	$> 1\times10^{-9}$	2.4×10^{-9}	3.4×10^{-9}
15	4.1×10^{-11}	$> 1\times10^{-9}$	1.7×10^{-9}	2.25×10^{-9}
14	1.25×10^{-11}	4.3×10^{-10}	3.75×10^{-10}	5.35×10^{-10}
13	8×10^{-12}	2.2×10^{-10}	1.6×10^{-10}	2.3×10^{-10}
12	1.75×10^{-11}	1.0×10^{-10}	6.05×10^{-10}	1.22×10^{-9}
2	2.2×10^{-9}	2.15×10^{-9}	1.9×10^{-9}	2.65×10^{-9}

* Ion Pump was turned off at 00:00

** Mass Spectra taken at 1.0 Ma emission at 70 V., 10 Min. Sweep.

appeared to be primarily an increase in carbon monoxide. This is a reasonable occurrence since the nude ion gauge in the system as well as the mass spectrometer were undoubtedly generating carbon monoxide. The mass 19½ impurity appeared to vary little with time and the same was true for the water vapor mass peaks (18 and 17). It is most likely that the 19½, 18, and 17 mass peaks all derived from the ion source of the mass spectrometer. The methane in the system seemed to increase to a new higher equilibrium pressure that was about 30 times greater than its original pressure with the ion pump operating. It is speculated that a major portion of the methane originated in the nude ion guage and was being effectively pumped by the magnetron ion pump. The increase in the methane content of the system would naturally lead to a small increase in the system hydrogen content. However, there was no increase in the system hydrogen content for at least 2 hours and 40 minutes after turning off the ion pump, in fact there was a slight decrease. The approximately 40 percent increase in the system hydrogen content that occurred at the end of the experiment is explained by the assumption that hydrogen pumping continued after the discharge stopped.(17)

The last few residual gas experiments were performed to show the effects of turning off the nude ion gauge, filling the cryopump with liquid nitrogen, and, finally, filling the cryopump with liquid helium. Table VIII shows the results of turning off the nude ion gauge, filling the cryopump with liquid nitrogen, and turning the nude ion gauge on again.

TABLE VIII

EFFECT OF TURNING OFF THE NUDE ION GAUGE AND FILLING THE CRYOPUMP WITH LIQUID NITROGEN IN THE CLOSED CRYOPUMP - ION PUMP SYSTEM

Mass Number	* Ion Gauge On. No Liquid Nitrogen In The Cryopump Mass Peak Height (Amperes)	** Ion Gauge Off. No. Liquid Nitrogen In The Cryopump Mass Peak Height (Amperes)	*** Ion Gauge Off. Liquid Nitrogen In The Cryopump Mass Peak Height (Amperes)	Ion Guage On. Liquid Nitrogen In The Cryopump Mass Peak Height (Amperes)
44	$1x10^{-11}$	$7.5x10^{-12}$	- - - -	- - - -
28	$1.6x10^{-10}$	$1.0x10^{-10}$	$1.3x10^{-11}$	$1.15x10^{-11}$
18	$8.7x10^{-11}$	$8.5x10^{-11}$	$5.2x10^{-11}$	$4.7x10^{-11}$
17	$3x10^{-11}$	$2.6x10^{-11}$	$1.5x10^{-11}$	$1.2x10^{-11}$
16	$5.4x10^{-11}$	$5.1x10^{-11}$	$8.2x10^{-12}$	$1.1x10^{-11}$
15	$3.7x10^{-11}$	$3.6x10^{-11}$	$6x10^{-12}$	$9.5x10^{-12}$
14	$1.5x10^{-11}$	$1.2x10^{-11}$	$2x10^{-12}$	$5x10^{-12}$
13	$6x10^{-12}$	$7x10^{-12}$	$2x10^{-12}$	$2.5x10^{-12}$
12	$1.3x10^{-11}$	$1.2x10^{-11}$	$2x10^{-12}$	$2x10^{-12}$
2	$1.9x10^{-9}$	$1.5x10^{-9}$	$7.7x10^{-10}$	$5x10^{-10}$

* Mass spectra taken at 1.0 Ma. emission at 70 Volts, 10 Min Sweep

** Ion gauge turned off 5 minutes before mass spectrum was taken

*** Ion gauge turned on 15 minutes before mass spectrum was taken

It can be seen from a comparison of the first two columns of Table VIII that turning off the ion gauge caused a maximum decrease of almost 40 percent in mass 28. The relatively small decreases in masses 16 and 12 make it appear that the mass 28 decrease was not a major decrease in carbon monoxide. The 20 percent decrease in mass 14 indicates that at least half of the 28 peak was nitrogen. The slight decreases in the 15 and 13 peaks indicate that methane produced by the ion gauge did not come from the gauge hot filament or chemical reactions at the filament, but rather from some heated element within the gauge. This is so because the ion gauge had only been off 5 minutes when the mass spectrum was taken. The change in the ratio of mass peak 17 to mass peak 18 is also noteworthy. The hydrogen content of the system decreased about 20 percent when the ion gauge was turned off and the carbon dioxide content decreased about 25%.

When the cryopump was filled with liquid nitrogen, there was a very large change in the residual gas content of the system. The mass 28 peak decreased by a factor of 7.7 and masses 16, 15, 14, and 12 decreased by a factor of 6. The hydrogen in the system decreased by a factor of 2 while the water vapor only decreased by about 40 percent.

The vapor pressure of methane at liquid nitrogen temperature is about 10 torr while the vapor pressure of carbon monoxide at this temperature is several hundred torr. One would not normally expect these gases to be condensed by a surface at liquid nitrogen temperatures. Nitrogen and hydrogen should also not be affected. Even ethane, with

a melting point of -172°C and a roughly estimated vapor pressure of the order of 10^{-1} torr at 77°K, should not be affected. The one gas that should have been strongly affected, water vapor, was not.

The results of cooling the cryopump to liquid nitrogen temperature can only be interpreted in terms of adsorption or cryotrapping on the cooled surfaces. Since there was not much water vapor or carbon dioxide present, the possibility of cryotrapping seemed small. It is speculated that the operation of the ion pump and/or the mass spectrometer (and later the nude ion gauge) created molecules in excited states that adsorbed more readily on the cold surface. Figure 29 shows the mass spectra obtained in the cryopump-ion Pump system with and without liquid nitrogen present in the cryopump.

When the nude ion gauge was turned on again, there was a sizeable increase in the methane gas content of the system, but all of the other mass peaks decreased. The pumping action of the gauge for hydrogen seemed especially large.

The last residual gas experiment made was to compare the system mass spectra with and without the liquid helium cryopump in operation. The results of the experiment are illustrated graphically in Figure 30. Notice that the liquid helium reduced the magnitude of the hydrogen mass peak from a value of 6.2×10^{-10} amps to a value of 2×10^{-12} amps or less, the noise level of the mass spectrometer. Only the water vapor mass peaks remained detectable after about 30 minutes of operation with

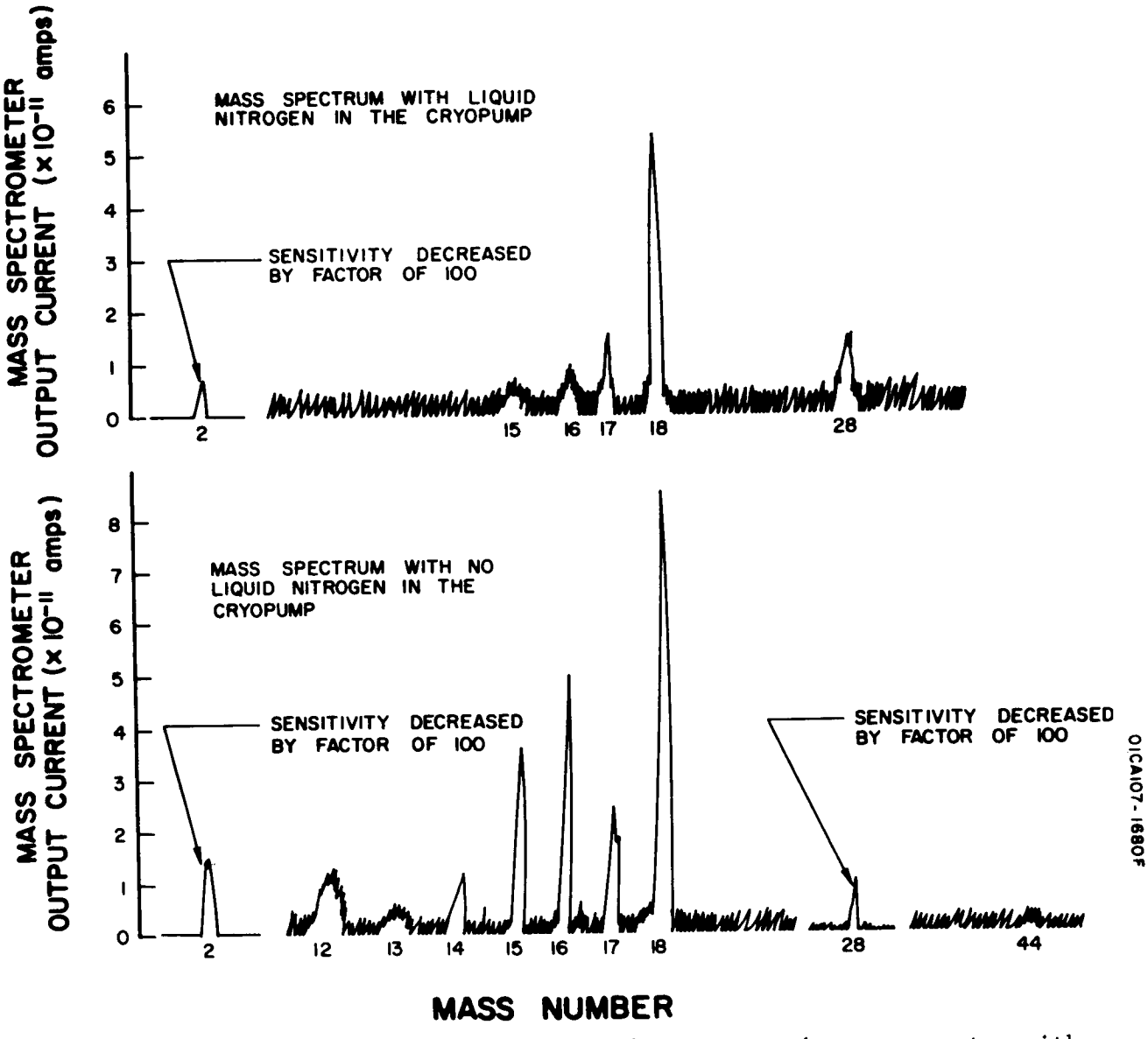

Figure 29. Residual gas mass spectrum of the cryopump-ion pump system with and without liquid nitrogen in the cryopump.

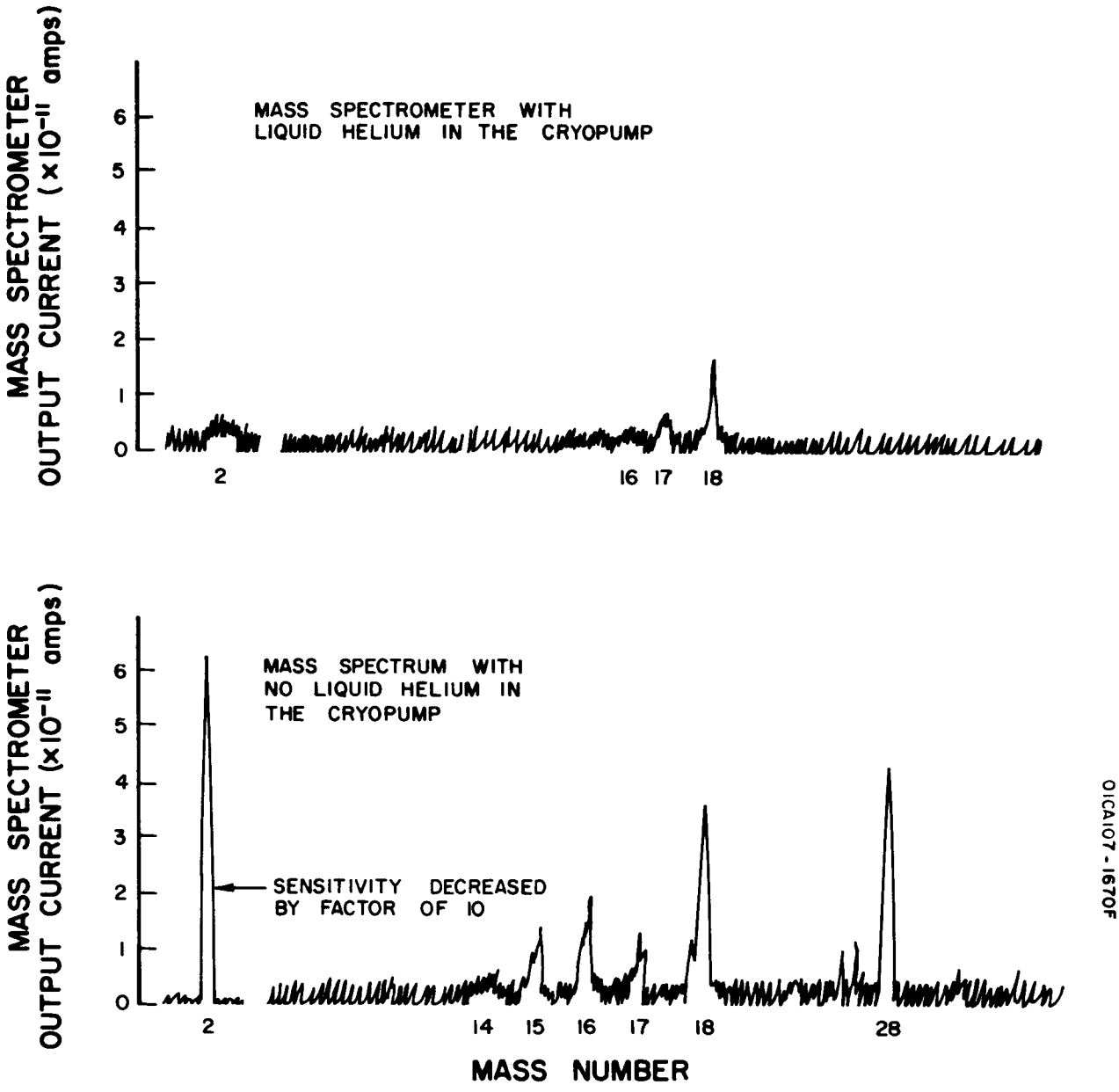

Figure 30. Residual gas mass spectrum of the cryopump-ion pump system with and without liquid helium in the cryopump.

liquid helium. The water vapor was undoubtedly being generated in the ion source of the mass spectrometer. If the sensitivity of the mass spectrometer for water vapor was about 1 ampere/torr, the mass spectrometer indicated a total pressure of 1.8×10^{-11} torr at this time. If the mass spectrometer had been turned off, the pressure in the system would have undoubtedly gone into the 10^{-12} torr region. It is interesting to note that neither helium nor hydrogen gas limited the ultimate pressure that could be obtained in this system. Since both the Varian gauge and the magnetron type ion pump were off during the attainment of the lowest pressures, it appears that an auxiliary ion pump is not required when very low pressures are to be attained with a liquid helium cryopump.

6. ATTAINMENT OF LOW PRESSURES

As stated in the Introduction, a principal objective of the research program was to construct two quite different vacuum systems, each capable of attaining pressures in the 10^{-13} torr region. Such an objective required means for measuring pressures of this magnitude, and two different types of low pressure measurement instrument were used to provide this capability. The first instrument used was the General Electric partial pressure analyzer; the second instrument used was a magnetron type cold cathode ionization gauge. Hot filament Bayard Alpert type ionization gauges were used with each system to make measurements in the 10^{-10} torr region and above. The hot filament gauges were also useful to insure that pressures were below their X-ray limit.

The partial pressure analyzer was used with the cryopump-ion pump system while a calibrated cold cathode ionization gauge was used to measure the lowest pressures in the mercury diffusion pump system. A pressure of about 8×10^{-13} torr was the lowest attained in the diffusion pump system while a pressure of about 2×10^{-11} torr was the lowest attained in the cryopump system. The reason for the relatively high pressure in the cryopump system had nothing to do with the basic nature of the system and involved only the preparatory treatment of the system, as will be described shortly.

During all of the work concerned with the attainment of very low pressures, there was a constant effort to determine the sources of residual

gas and investigate those factors that could conceivably limit the attainment of low pressures. These experiments are described below.

6.1 MERCURY DIFFUSION PUMP SYSTEM

6.1.1 Low Pressure Limitations

Bakeout Requirements. As is well known, one key to the attainment of ultra high vacuum is the provision for high temperature bakeout. It was found experimentally that test chamber pressures below 10^{-9} torr could not be achieved in the mercury diffusion pump system without some kind of a bakeout. It was found further that the better the bakeout, the lower the ultimate pressure achieved. The effectiveness of a bakeout procedure in producing low ultimate pressures depended on the amount of gas removed from the materials within the system. The higher the bakeout temperature and the longer the bakeout period, the lower the ultimate pressure. The effectiveness of bakeout could be gauged quantitatively by means of the hot filament gauge connected to the isolation cold trap that was located between the two diffusion pumps. After an overnight bakeout at about 450°C, this gauge would indicate a pressure of about 9×10^{-7} torr with the system still at 450°C. If the bakeout lasted only 3 or 4 hours, the corresponding gauge reading might be 4×10^{-6} torr, indicating a much higher outgassing rate. Overnight bakeouts at temperatures of 300°C and 350°C, while effective in removing some gas from the system, never permitted pressures below 10^{-11} torr to be achieved. It is not known at this time whether the bakeout limitation of ultimate pressure

was due primarily to outgassing from the stainless steel chamber walls, copper gaskets, or even the gauge electrodes and envelope. It may be that it is not the chamber wall outgassing that limits the pressure, primarily, but rather the release of gas from the electrodes and envelope of the gauge that is being used to measure the pressure. There is a strong suspicion that in small systems of the type under consideration here, the pressure measurement instrument itself (hot filament gauge, cold cathode gauge, mass spectrometer) usually limits the system pressure. This concept has already been well-verified for the case of hot filament Bayard-Alpert type gauges and mass spectrometers that have not been sufficiently outgassed. In the case of cold cathode gauges, small gas bursts from such gauges (at rather infrequent intervals) suggest that gas is being released as well as pumped at very low pressures. Indeed, ion bombardment induced re-emission must be ever-present. More will be said about re-emission in connection with a discussion of the low pressure limitations of the cryopump-ion pump system.

Stainless Steel Outgassing. In order to determine whether or not outgassing from the stainless steel test chamber could limit the ultimate pressure in the system, a quick, rough test of outgassing was made in the following way: A flask-type heating mantle was placed around the top portion of the test chamber and a thermocouple was placed in contact with the test chamber under the heating mantle. The lower part of the heating mantle was sealed off with glass wool, and a variac was used to control the heat input to the mantle.

Prior to the experiment, the system had been baked for 5 hours at 400°C and had operated at low pressures for several days. The system background pressure was about 6×10^{-11} torr as measured with a calibrated cold cathode gauge. A hot filament gauge on the system yielded its X-ray reading of 2.7×10^{-10} torr (equivalent pressure).

As the power input to the heating mantle was varied, the test chamber temperature increased. There was no change in system pressure readings for test chamber temperatures up to 300°C. When the temperature of the chamber reached 350°C, however, the system pressure started to rise, as indicated by both gauges. One fairly accurate equilibrium pressure reading at a temperature of 415°C was made but other readings were taken before the system had attained equilibrium, and thus there was a large uncertainty in the system pressure at various other test chamber temperatures.

Now, one can make a simple assumption about the temperature dependence of an outgassing metal. If the outgassing is simple desorption from a surface, the outgassing rate will vary exponentially with the negative reciprocal absolute temperature. The same is true if the outgassing rate is limited by diffusion of the gas from the interior of the metal to the surface. In either case, a plot of the logarithm of the outgassing rate as a function of the reciprocal absolute temperature should yield a straight line. By plotting two or more values of outgassing, as determined by the increased pressure in the system and the system pumping speed, as functions of the corresponding test chamber reciprocal absolute temperatures, one can then extrapolate the curve to find the metal outgassing rate at room temperature.

When the above graphical procedure was carried out for the experimental data taken, it was found that for the least favorable estimates of system pressure increases corresponding to fixed test chamber temperatures, the outgassing rate of the stainless steel would be less than 7×10^{-15} torr liters/sec cm^2. For more reasonable estimates, the outgassing rate would be about a decade lower, more nearly in agreement with values found by other experimenters. However, taking the "worst case" estimate of 7×10^{-15} torr liters/cm^2sec for stainless steel at 25°C, a test chamber and associated metal vacuum wall of 1000 cm^2 surface area would provide an outgassing load of 7×10^{-12} torr liters/sec. For an effective pumping speed of 25 liters/sec at the test chamber, the outgassing would limit the system to a pressure of 2.8×10^{-13} torr. The remainder of the system, being cooled by either liquid nitrogen (the non-level-sensitive cold traps) or cooling water (the mercury diffusion pump), would have a considerably reduced outgassing rate. Since the lowest pressure achieved with the system at the time the outgassing experiment was performed was 6×10^{-11} torr, the system was evidently being limited by some other factor. After much longer bakeouts at 450°C, there is no doubt but that the stainless steel outgassing rate was reduced below 1×10^{-15} torr liters/cm^2 sec, and so this outgassing would not limit system pressures above 4×10^{-14} torr.

Flange Leakage. One of the important unknowns at the beginning of the research program was the low pressure behavior of all metal, shear-seal type flanges. In particular, our laboratory experience had indicated that Varian ConFlat copper gasketed seals were leak tight down to pressures

of 10^{-9} and 10^{-10} torr. There was no evidence that these seals would permit pressures of 10^{-12} and 10^{-13} torr to be reached in small volume, low pumping speed laboratory systems.

The standard Veeco helium mass spectrometer type leak detector was generally used to test assembled flanges for leakage. The Veeco instrument will detect leaks as small as 1×10^{-10} torr liters/sec. Each of the six system flanged joints, three 6" O.D flanges and three 2 3/4" O.D. flanges, were leak tested and found to be tight with a leak rate less than 1×10^{-10} torr liters/sec. It would be entirely possible for the leakage in each flange to be something just less than 1×10^{-10} torr liters/sec, in which case the total air leakage into the system would be something just less than 6×10^{-10} torr liters/sec -- say 5×10^{-10} torr liters/sec. Under these conditions, and assumming the total leakage to be concentrated at the system test chamber where the effective pumping speed was 25 liters/sec, the ultimate pressure that could be obtained in the test chamber would be $P_u = Q/S = 2 \times 10^{-11}$ torr. Thus, with the leak detection capability available, it was not possible to guarantee the attainment of ultimate pressures below 2×10^{-11} torr in the demountable system.

In addition to actual leakage of atmospheric air, the ConFlat flanges were potential sources of trouble in other respects. The OFHC copper gaskets that were used with the flanges could have a high gas content. Vacuum firing the gaskets would anneal them and presumably adversely affect their sealing capability. Any liquid mercury droplets that might form on the gaskets would amalgamate with the copper and might be difficult to remove

in the bakeout. Finally, baking the flanges for long periods of time at 450°C would cause oxidation of the copper gaskets on the atmospheric side of the shear seal, and layers of porous copper oxide would eventually form adjacent to the surfaces of the stainless steel knife edges and permit air to pass through the seal.

During the course of many experiments with the mercury diffusion pump system, some of the potential sources of trouble mentioned above become realities. It was found that improper treatment of the system could cause mercury droplets to condense on the copper gaskets, and the parts so contaminated were not completely cleaned up by the system bakeout. It was found further that strong oxidation of the copper gaskets did occur, especially at points adjacent to the leak test channels that were machined in the stainless steel flange faces. In one case, bakeout at 350°C, followed by flange tightening and a second bakeout at 400°C, caused a copper oxide leakage path to form in one 6" O.D. flange gasket. Outgassing of copper gaskets is suspected as being one of the factors limiting the system ultimate pressure. In some cases, cooling a ConFlat flange and gasket with dry ice caused the system pressure to decrease by 25 or 30 percent. In other cases, however, the flange cooling had a negligible effect on the system pressure. It will be necessary to make some quantitative measurements of flange and gasket outgassing to settle this matter.

UHV Diffusion Pump Forepressure Limitation. In order to determine the effect of a high forepressure on the ultra high vacuum in the test chamber, an experiment was performed in which the backing diffusion pump

(booster pump) was turned off at a time when the test chamber pressure was about 5×10^{-11} torr. The results of this experiment are shown graphically in Figure 31. Within 20 minutes after the booster pump was turned off, the UHV pump forepressure (as measured by the hot filament gauge attached to the isolation cold trap located between the two diffusion pumps) increased from its normal operating value of 5×10^{-8} torr to a value of 8×10^{-4} torr. The test chamber pressure (as measured by a calibrated cold cathode gauge) responded immediately. This pressure first increased from a value of 5×10^{-11} torr to a maximum value of about 1×10^{-9} torr within 7 or 8 minutes and then decreased within the next 20 minutes to an equilibrium value just above 3×10^{-10} torr. The system was permitted to remain "forepressure limited" for about 170 minutes, at which time the booster pump was turned on again. Within 15 minutes, the UHV pump forepressure had decreased by 3 decades, and the test chamber pressure had decreased to a new equilibrium value of about 3×10^{-11} torr.

During the period when the system was "forepressure limited", the ratio between the UHV pump forepressure and the test chamber pressure was 4.4×10^{6}. If it is assummed that the UHV pump offers no system pressure limitation other than the pressure ratio which it can maintain, this particular pump could provide test chamber pressures as low as about 1×10^{-14} torr with its normal operating forepressure of 5×10^{-8} torr.

The importance of providing very low forepressures for a diffusion pump system which was to operate at 10^{-12} and 10^{-13} torr was clearly demonstrated by this experiment. Using the best mechanical vacuum forepumps

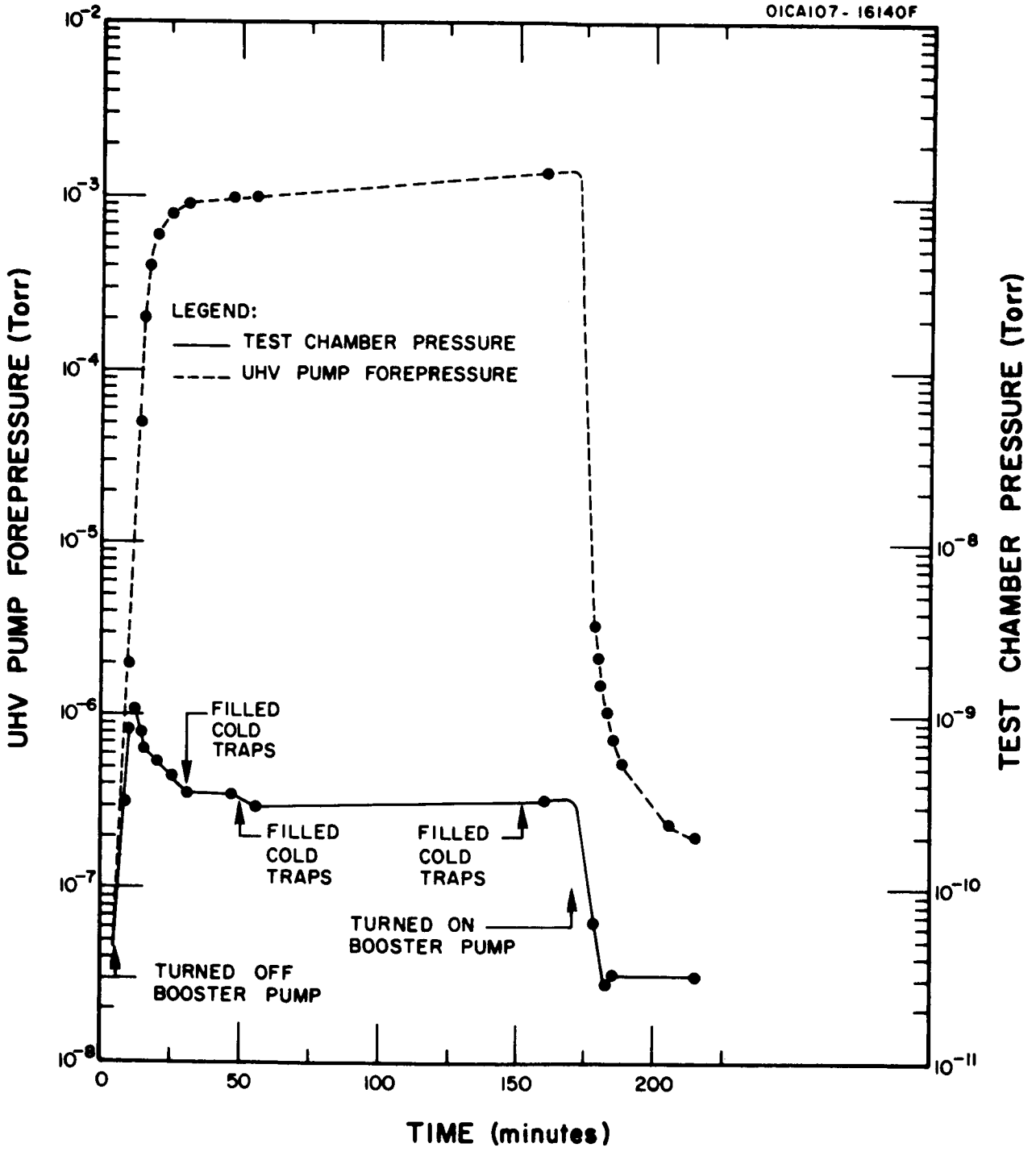

Figure 31. Mercury diffusion pump system operation at low pressure and its dependence on the ultra high vacuum diffusion pump forepressure.

available (which might maintain forepressures of the order of 10^{-4} torr) system pressures only as low as 10^{-11} torr would be obtained. Of course, one could provide forepressures as low as 10^{-9} or even 10^{-10} torr, and still not attain test chamber pressures in the 10^{-12} to 10^{-13} torr region, if other elements of the system are not adequate for the job.

6.1.2 Low Pressure Achievement

Before making the extremely low pressure tests with the mercury diffusion pump system, the mass spectrometer and hot filament ionization gauges were removed from the test chamber. In place of these instruments, a GCA all-metal, magnetron type cold cathode ionization gauge and an NRC Redhead type cold cathode ionization were installed. The third part of the test chamber was sealed with a blank flange.

The entire system was first given a preliminary bakeout at 150°C for 1 hour to remove water vapor and permit better leak checking of the two newly installed cold cathode gauges. This proved to be a poor procedure since it was noticed that some mercury droplets had formed in the glass tubulations of the two gauges. Later preliminary leak checking bakeouts were made by filling the lower non-level sensitive cold trap with liquid nitrogen and baking only the upper portion of the system including the upper non-level-sensitive cold trap and test chamber. The formation of mercury droplets on the copper gaskets of the test chamber flanges caused some amalgamation that later limited the pressures attainable. When bakeout procedures were carried out correctly, there was never any mercury droplet formation.

The first high temperature bakeout consisted of baking overnight for 12 hours at 400°C, baking 5 or 6 hours at 425°C, and finally baking about 30 hours at 450°C, including the staging-up of the oven as described in Section 3. After the system had cooled down to between 100 and 200°C, the cold cathode gauge magnets and electrical connecting cables were installed. The high voltage was turned on and both gauges started almost at once. With the system still hot, the two gauges read currents of the order of 10^{-10} amperes. About 1 hour after the gauges had been turned on, the NRC gauge read a current of 2.3×10^{-10} Amps at 4.0 Kv on the anode while the all metal GCA gauge read a current of 1.4×10^{-10} Amps at 4.0 Kv on the anode.

About 11 hours after the gauges had been turned on, the NRC Redhead gauge furnished a current of 9×10^{-11} amps at 4.0 Kv while the GCA metal gauge furnished a current of 5×10^{-11} amps at 4.0 Kv. Both gauges had erratic readings at this time. During the next 4 hours the lower non-level-sensitive cold trap was filled every 15 minutes in order to provide maximum trapping effectiveness. At this time, the upper cold trap was empty, and it was of interest to determine just how low a pressure could be achieved with a single cold trap in operation. It was found that the NRC gauge reading went as low as 4.0×10^{-11} amperes at 4.0 Kv, which would correspond to a reading of about 1.7×10^{-11} torr according to experimental data taken from a recent paper by Feakes and Torney.[18] The GCA gauge furnished a corresponding reading of 1.8×10^{-11} amperes, which, according to the graph of Figure 32, represented a pressure of 1.8×10^{-11} torr. Thus, it is evident that there was a very good agreement between the two gauge readings at this pressure level.

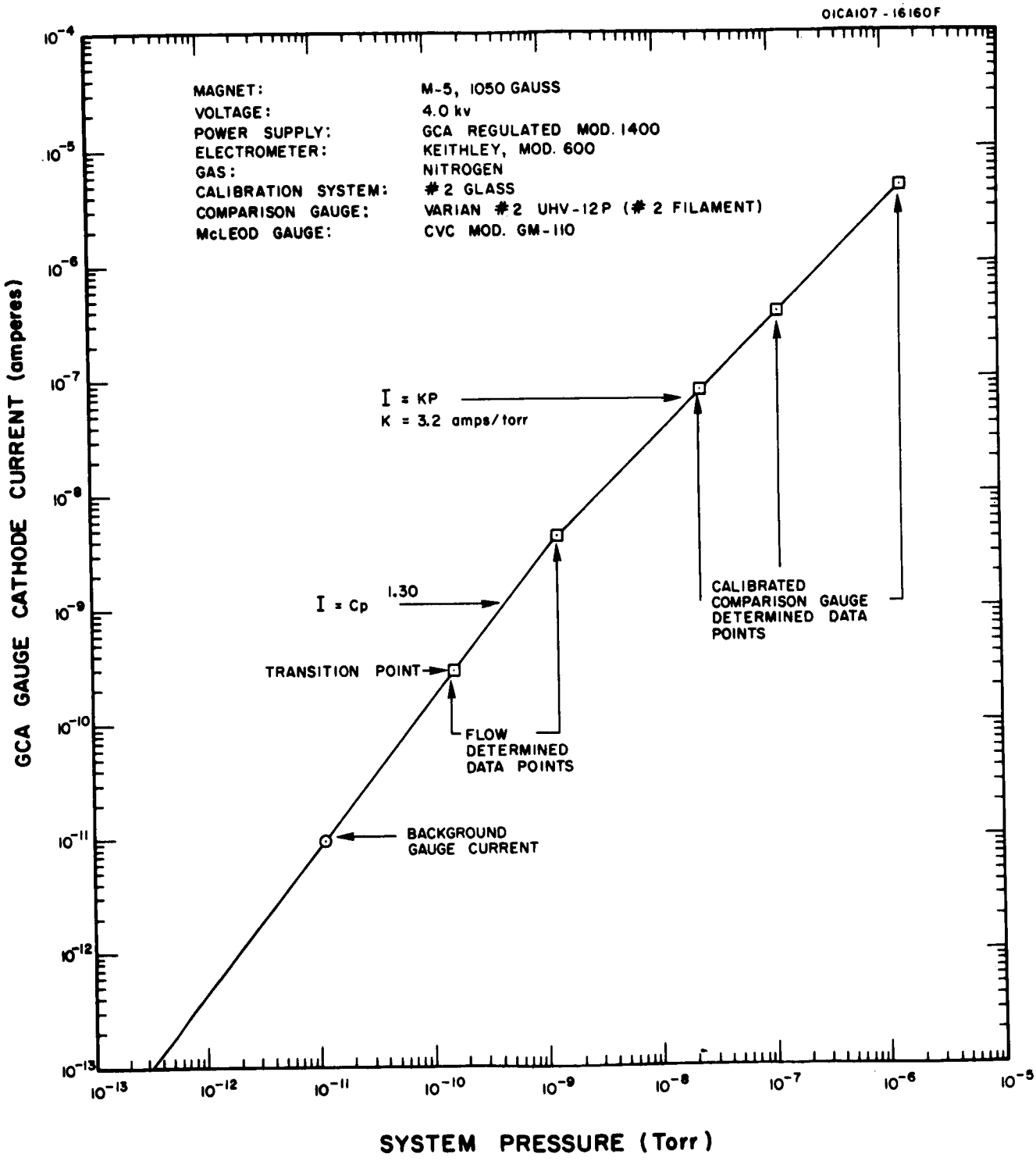

Figure 32. Calibration curve of the GCA metal-ceramic, magnetron type cold cathode ionization gauge for nitrogen gas.

The next step in this first very low pressure experiment was to fill the upper non-level-sensitive cold trap. About five minutes after starting to fill the top trap, the NRC gauge reading had decreased to 4.8×10^{-12} amps at 4.0 Kv (a pressure of about 4×10^{-12} torr), and the GCA gauge reading had decreased to 2.8×10^{-12} amps at 4.0 Kv representing a pressure of 4.4×10^{-12} torr. The lowest NRC gauge reading during the trap filling process was 2.2×10^{-12} amps at 4.0 Kv corresponding to a pressure of 2.1×10^{-12} torr. After the upper cold trap had been filled, the system pressure increased into the low 10^{-11} torr region for some unknown reason and remained at this pressure level. Various tests were performed, changing the input power to the UHV diffusion pump, changing the gauge anode voltages, and varying the level of liquid nitrogen in the cold traps. It was found that at 6.0 Kv anode voltage, the readings of the two different gauges were almost identical. This bit of experimental evidence indicated that re-emission, cold field emission, or some other voltage dependent process was mainly responsible for the two similar readings. When both anode voltages were reduced from 6.0 to 4.8 Kv., the gauges once more assummed their approximate 2 to 1 ratio of output currents.

During the above experimentation, it was observed that the UHV pump mercury spill-over rate was about one-half or one-third of its normal value. Increasing the voltage across the pump heater did not seem to affect the pumping action. Finally, it was decided to try to substitute a new pump heater. The change over was not carried out fast enough, however, and the test chamber pressure increased into the 10^{-9} torr region. It was decided to end the first low pressure test, inspect the UHV mercury

diffuion pump, and begin a second low pressure test.

Inspection of the UHV diffusion pump revealed that enough mercury had been lost to the isolation cold trap to impair its pumping action. Accordingly, about 400 grams of new mercury were added to the pump boiler, and the system was readied for bakeout.

The second high temperature bakeout included an overnight bakeout for 10 hours at 450°C, followed by an 11 hour bake at 475°C, including the staging-up of the oven. The cold cathode gauges were turned on while the test chamber and flanges were still hot. The initial readings of the gauges were in the 10^{-9} ampere range, but within an hour and twenty minutes, both gauges furnished output currents in the low 10^{-10} ampere range, with the test chamber flanges still hot. Two hours and 15 minutes after turning on the gauges, their readings were both in the 10^{-11} ampere range. At this time filling of the upper non-level-sensitive cold trap was commenced. Within 15 minutes the pressure in the test chamber had decreased so that the gauges read currents in the 10^{-12} ampere range. Just three hours after turning on the gauges, and with both cold traps filled, the GCA gauge furnished a current reading of 5.4×10^{-12} amps at 4.0 Kv equivalent to a pressure of 7.2×10^{-12} torr, while the NRC gauge furnished a current of 2.8×10^{-12} amps at 4.0 Kv corresponding to a pressure of about 2.5×10^{-12} torr. This was the first time that the GCA gauge furnished a higher current output than the NRC gauge. After about 10 additional hours of operation, the two gauge currents had reverted to their normal relationship with the NRC gauge output current larger than that of the GCA gauge. For

example, the GCA gauge output current was 1.9×10^{-12} amps at 4.0 Kv, corresponding to a pressure of 3.2×10^{-12} torr while the NRC gauge output current was 5.2×10^{-12} amps at 4.0 Kv corresponding to a pressure of about 4×10^{-12} torr. At this time, dry ice was placed around some of the flanges of the system to see if outgassing from any of these flanges was limiting the system pressure. There was a small indication of outgassing from the flanges to which the GCA gauge was connected and the 6" O.D. flanges just above the mercury diffusion pump. The UHV diffusion pump was operating at 4.0 amps, a power input to the pump heater of 340 watts. There were no pressure bursts in the system.

The mercury diffusion pump system was kept under vacuum at pressures in the 10^{-12} torr range for four days following the end of the bakeout cycle. Continuing with the search for outgassing components, it was discovered that cooling the flange to which the NRC gauge was connected caused a drastic decrease in the pressure readings of both cold cathode gauges into the low 10^{-12} torr region. A later examination revealed contaminated areas on the copper gasket that was cooled. Presumably, the contamination resulted from the condensation of mercury droplets on the gasket during the first high temperature bakeout. A typical NRC gauge output current at this time was 2.7×10^{-12} amps at 4.0 Kv, corresponding to a pressure of about 2.2×10^{-12} torr. A typical GCA gauge output current was 2.4×10^{-12} amps at 4.0 Kv corresponding to a pressure of 3.8×10^{-12} torr.

The fifth day after completion of the bakeout cycle, it was observed that the GCA gauge indicated a pressure of 2.2×10^{-12} torr at 4.0 Kv while

the NRC gauge pressure indication (without dry ice on the connecting flange) was in the low 10^{-11} torr region. At one point, there was a sudden rise in the NRC gauge reading to a value as high as 9×10^{-9} amps at 4.0 Kv followed by a slow decrease to an equilibrium level of 2×10^{-10} amps within a period of 2 hours. The GCA gauge output current increased slowly during the NRC gauge pressure rise and partial recovery. The GCA gauge reading increased to a value of 9×10^{-12} amps and remained at this level. It is speculated that there was a pressure burst in the NRC gauge. The gauge pumped some of the gas released and so became "gas loaded". The new, higher rate of re-emission and outgassing from the NRC gauge then raised the general pressure in the system.

In an attempt to reduce the system pressure, dry ice was packed around the 6" O.D. flange of the test chamber. After a period of 1 hour and 45 minutes, the GCA gauge reading had decreased by a factor of two while the NRC gauge reading decreased by almost a factor of three. The copper gasket of this flange was also found to be contaminated after the low pressure test was over.

The sixth day after completion of the bakeout cycle, a number of additional experiments were performed. After dry ice was placed around the three small flange pairs of the test chamber as well as its 6" O.D. flange, both gauges furnished pressure readings of 3 or 4×10^{-12} torr. The voltage of the NRC gauge was increased from 4.0 to 6.0 Kv and within about 5 minutes, its current reading had decreased from a value of 3.2×10^{-12} amps to a reading of 8.8×10^{-13} amps, which might correspond to a

pressure in the vicinity of 1×10^{-12} torr. It was interesting to observe that the current of the NRC gauge occassionally dropped to zero, as though the discharge had extinguished momentarily, and then returned to its reading of 8.8×10^{-13} amps. It was evident that the NRC gauge was then operating close to its low pressure limit.

The next test that was performed was to heat the Kovar tubulation of the GCA gauge. It was found that the reading of the GCA gauge increased by about two orders of magnitude into the 10^{-10} torr region and then started to decrease. The NRC gauge reading increased by a factor of two approximately and then also began to decrease. The kovar in the system appeared to have a higher gas content and a higher outgassing rate than the 304 stainless steel. Fortunately, there was not much Kovar present in the system. The test showed that both gauges responded normally to a real gas pressure increase.

After the kovar had cooled to room temperature, and both cold cathode gauges were reading pressures in the low 10^{-12} torr region, the GCA gauge metal envelope was cooled with dry ice. The initial effect was a drop in the readings of both gauges. The NRC gauge output current was 8.2×10^{-13} amps at 6.0 Kv, corresponding to a pressure of about 9×10^{-13} torr. After about 10 minutes, the readings of both gauges began to increase back to their earlier values. When the dry ice was removed from the GCA gauge, there was no significant change in the readings of the two gauges. At this time, the laboratory fluorescent lights were turned off to see if they had any effect on the gauge readings. The gauges furnished the same readings in the dark as they did in the lighted room.

The next experiment performed was to turn off the high voltage to the GCA cold cathode gauge, leave the voltage off for about 5 minutes, and then turn the voltage on again. It was found that the GCA gauge started immediately when the high voltage was reapplied. This reaction was expected because the GCA gauge contained radioactive material to help produce some initial ionization. During the "off-and-on" period of the GCA gauge, there was no change in the reading of the NRC gauge, an output current of 1.2×10^{-12} amps at 6.0 Kv, indicating that the GCA gauge could not have been either strongly pumping or outgassing. The GCA gauge was turned off once more to check the reading of the electrometer (Keithley model 600) with the gauge anode voltage off. It was found that there was a negative current of about 1×10^{-13} amps to the gauge cathode. This current was undoubtedly due to the collection of electrons emanating from the radioactive material within the gauge.

When the NRC gauge voltage was reduced from 6.0 Kv to 4.8 Kv, there was a marked effect on the system. The system pressure, as indicated by the GCA gauge, began to fall steadily, while the NRC gauge reading increased steadily. Within 30 minutes of reducing the NRC gauge voltage, the GCA gauge output current was 3.8×10^{-13} amps at 4.0 Kv, corresponding to a pressure of 9×10^{-13} torr. Thirty minutes after this, the GCA gauge reading had decreased to 3.2×10^{-13} amps at 4.0 Kv, a pressure of about 8×10^{-13} torr.

The seventh day after completion of the bakeout cycle, the pressure in the system was in the high 10^{-11} torr region. The liquid nitrogen levels of both cold traps were down considerably and the system flanges

were not cooled by dry ice. After the flanges were cooled and liquid nitrogen levels in the trap were kept high for several hours, the test chamber pressure decreased to the low 10^{-11} torr region. The NRC gauge was then turned off and kept off overnight.

On the eighth day after completion of the bakeout cycle, the GCA gauge, operating by itself, indicated a pressure of 9×10^{-11} torr. A voltage of 4.0 Kv was then applied to the NRC gauge. The gauge started almost immediately and indicated a pressure of 1.5×10^{-10} torr.

Because the two cold cathode gauges had not been yielding approximately equal pressure readings, it was assumed that one or both of the gauges had become contaminated. For this reason, it was decided to bake out the two gauges using heating tape and heat guns. During the approximately 2 hour baking period, the heat gun was also used to heat the 2 3/4" O.D. flanges on the test chamber. It was observed that the system pressure increased by about 25 percent (as measured with the hot filament gauge located between the two diffusion pumps) when the NRC gauge flanges were heated, verifying that these flanges and/or the associated copper gasket were contaminated. There was no observable pressure increase when the other flanges were heated.

After the bakeout, it was observed that neither the NRC nor the GCA gauge would start immediately with an applied anode voltage of 4.0 Kv. The GCA gauge finally started 13 minutes after the voltage had been applied and furnished a current reading of 9.7×10^{-13} amps (1.9×10^{-12} torr). The voltage to the NRC gauge was turned off and the current reading to the

NRC gauge electrometer was monitored for the next few hours to determine the magnitude of its residual current. The reading of the NRC gauge, with no voltage applied, varied between about 2×10^{-14} amperes and 1.2×10^{-13} amperes. This residual current is attributed to thermal e.m.f's and electrical pickup. When the NRC gauge was turned on and operating at 4.0 Kv., it furnished a much higher reading than the GCA gauge. For example, the GCA gauge reading was 1.8×10^{-12} amps at 4.0 Kv (3.0×10^{-12} torr) while the NRC gauge reading was 1.0×10^{-10} amps at 4.0 Kv (3×10^{-11} torr). There is no doubt that the contaminated NRC gauge flange contributed to this higher pressure reading. The shield ring current of the NRC gauge was measured at this time and found to be 6×10^{-12} amperes.

The last experiment performed with the system at a low pressure was to measure the GCA gauge output current as a function of the anode voltage. The results of this measurement are shown in Figure 33. It can be seen that the gauge output current begins to fall off for voltages greater than 3.0 Kv at the system pressure of 3×10^{-12} torr. It appears to be characteristic of magnetron type cold cathode gauges that the anode voltage for maximum gauge current shifts to smaller voltage values as the pressure decreases.

The construction of the GCA metal-ceramic magnetron type cold cathode ionization gauge is shown in schematic form in Figure 34. Some idea of the gauge and electrode dimensions can be obtained from the dimensions of the gauge anode which was a cylinder about 1/2 inch long and 1-1/4 inches in diameter. The cathode was spool-shaped as shown, and was supported at

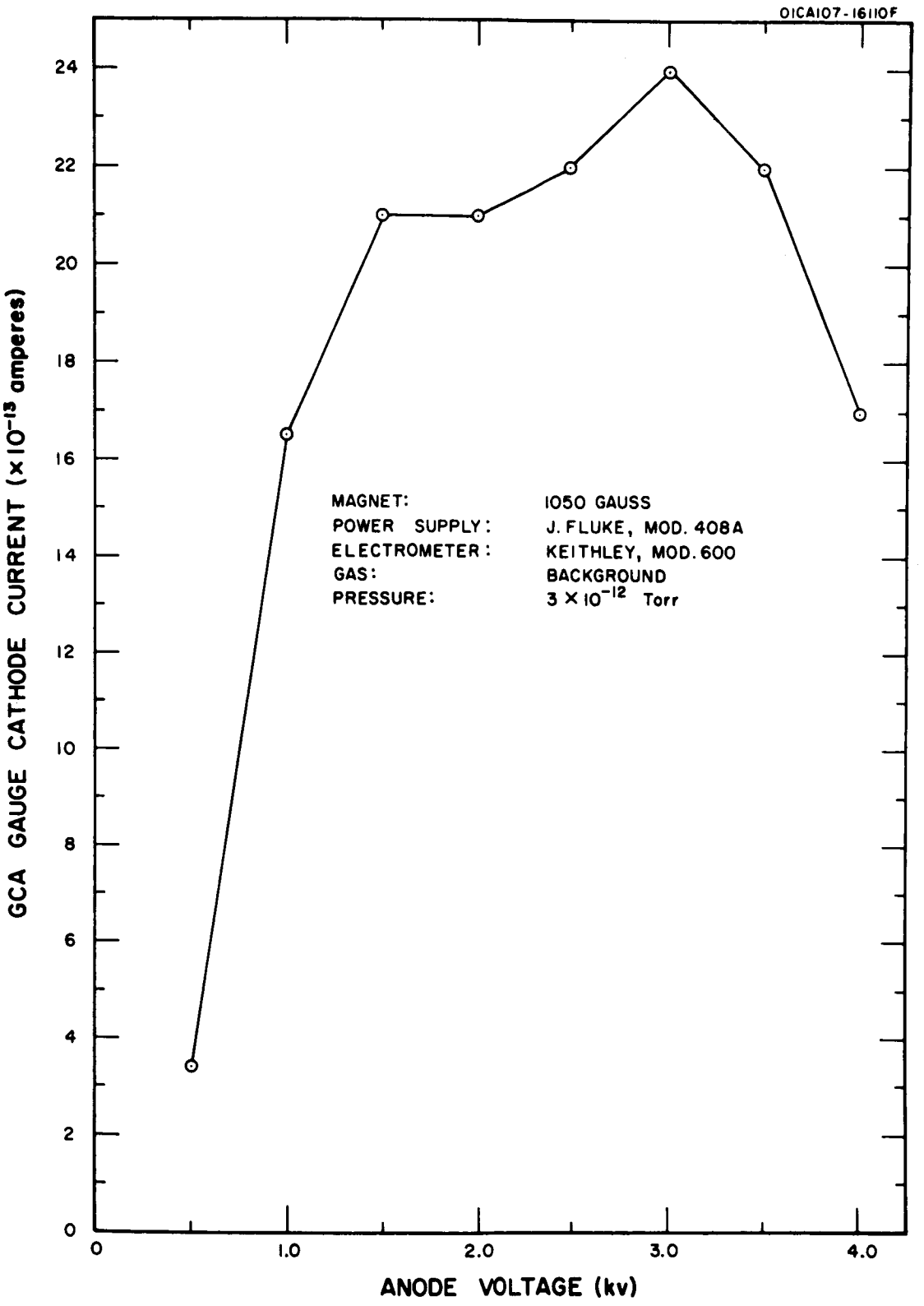

Figure 33. Current-voltage characteristic of the GCA cold cathode ionization gauge at a low background pressure.

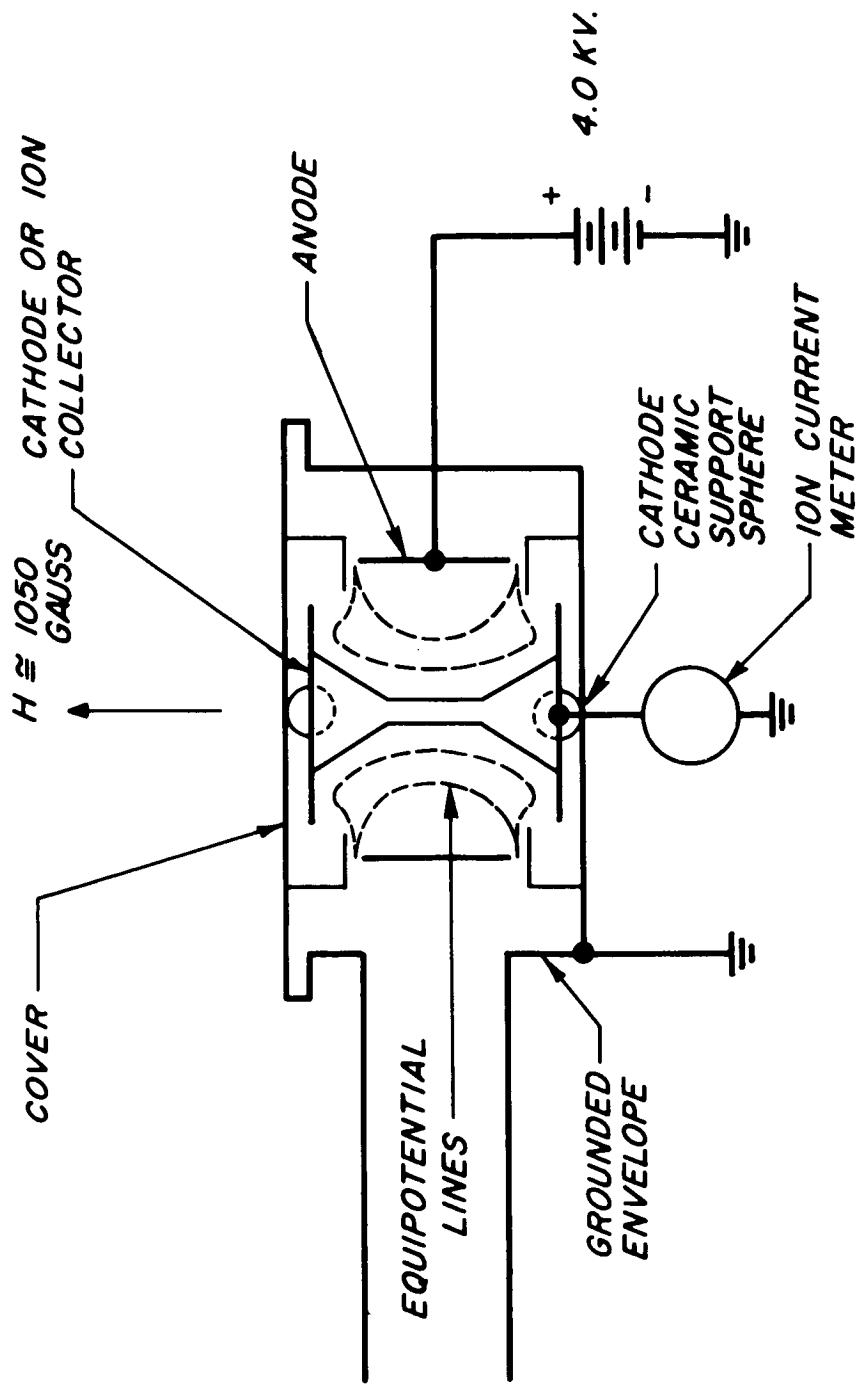

Figure 34. Simplified schematic of the GCA cold cathode ionization gauge.

the top and bottom by ceramic spheres. The anode cylinder,also, was supported by ceramic spheres bearing on the metal envelope, so that it maintained a fixed position relative to the cathode. The gauge tubulation had an outer diameter of 1 inch. The total length of the gauge tubulation between the gauge envelope and the test chamber was about 7 inches. The calculated conductance of the gauge tubulation was about 4-1/2 liters/sec. The pumping speed of the GCA gauge was known to be less than 0.2 liter/sec, and so the measured pressure within the gauge would be no more than 5 percent less than the test chamber pressure. The tubulation to the NRC gauge, which was used with the standard NRC magnet,incidentally, was roughly the same as that used with the GCA gauge. Well regulated, low ripple power supplies were used to furnish the high voltage for each gauge. Keithley model 600 battery operated electrometers were used to measure the gauge currents.

6.2 CRYOPUMP-ION PUMP SYSTEM

6.2.1 Low Pressure Limitations.

Bakeout Limitation. From the very beginning, it was evident that the cryopump-ion pump system could not be baked out as thoroughly as the mercury diffusion pump system. The reason for this state of affairs was that the pumping speed of the Vacsorb pump evidently decreased with time as it pumped more and more of the outgassing products, and the pumping speed of the backing Vacion pump also decreased as the system pressure went from the 10^{-5} torr region into the 10^{-4} torr region. In short, the backing

pumps used during the bakeout period did not have the capability of maintaining a high gas throughput at relatively high pressures. This particular shortcoming, although it limited the maximum temperature that could be used for bakeout (aobut 350°C) under penalty of oxidizing ion gauge and mass spectrometer elements, could probably be partially overcome by substituting a high throughput, water cooled 15 liter/sec Vacion pump for the standard 8 liter/sec Vacion pump and using two or more Vac Sorb pumps sequentially. In any event, the difficulty is not fundamental, and one need only use either higher capacity getter-ion and absorption pumps or perhaps one of the new molecular pumps to carry off the outgassing products at higher system temperatures. In terms of its effect on the cryopump system pressures, however, the limited bakeout permitted pressures no lower than low 10^{-11} torr to be attained.

Pumping Discrimination. In either a getter-ion or pure ion pumped system, there is discrimination in pumping various gas species. Argon, for example, is pumped at a very low speed by a getter-ion pump. Helium and neon are also pumped at low speeds by these pumps, but hydrogen is pumped at about 3 times the speed of nitrogen or oxygen.

In a pure ion pump, of which the Redhead magnetron gauge is a good example, it has been found that the pumping speed for hydrogen is of the same order as the speed for nitrogen and oxygen. Argon is pumped at about half the speed of nitrogen and helium is still pumped at a very low speed, less than one-tenth the speed for nitrogen.[19] The fact that argon is pumped at a substantial speed by a magnetron type ion pump is of importance because of its relatively large concentration in air. The low pumping

speed of an ion pump for helium is not a serious shortcoming because of the low concentration of helium in ordinary air.

It has been shown that ionization is apparently not necessary in order for hydrogen to be pumped in a getter-ion pump.[17] This fact implies that hydrogen is not pumped primarily by ion burial. The mechanism of hydrogen pumping as well as the sources of hydrogen in the system are extremely important because hydrogen constituted the largest percentage of residual gas in the ion pumped system. As was indicated in the section on residual gas analysis, the nude ion gauge appeared to pump hydrogen strongly when it was on and evolve hydrogen when it was turned off. This type of behavior was in accord with that found by other researchers.[20]

The pumping speed of the ion pump for methane was relatively high, as indicated in the preceeding section. At the same time, methane was probably being generated in the ion pump in the presence of free carbon and hydrogen, as well as being evolved from the nude ion gauge.

Water vapor was effectively pumped by the ion pump as was shown by the gradual decrease of the water vapor peak during the residual gas analysis. However, it was surprising to find that water vapor was the only gas remaining in the system with the liquid helium cryopump operating. This circumstance was no doubt due to the omission of a thorough outgassing of the ion source of the mass spectrometer.

A liquid helium cryopump exhibits pumping discrimination toward two gases: Helium should not be pumped at all, and hydrogen should be pumped only beyond its saturation vapor pressure of about 10^{-7} torr. Because

there was no detectable helium present in the system, the absence of the cryopump pumping speed for helium was academic. However, there was a great deal of hydrogen in the system at a partial pressure of the order of 10^{-7} torr. The short term operation of the liquid helium cryopump appeared to reduce the hydrogen partial pressure to a barely detectable level of the order of 2 or 3 x 10^{-12} torr. It is possible that the observed effect was just a transient adsorption. It was pointed out earlier that the hydrogen partial pressure was strongly reduced even though both the ion pump and the nude ion gauge were off, indicating that neither ion pumping nor hot filament gettering were operative, and that the hydrogen was not being either dissociated, excited, or ionized.

The behavior of hydrogen in being strongly adsorbed on a liquid helium cooled surface was reminiscent of the same behavior of methane on a liquid nitrogen cooled surface. This behavior of methane has been observed by other workers in the field.[21]

In connection with the operation of the ion pump, it was shown in the last section that turning off this pump revealed the existence of a re-emission of atoms and molecules that had previously been pumped. Argon, methane, carbon monoxide, nitrogen, and, finally, hydrogen were re-emitted. It has been shown that for many gases only a relatively small, finite amount of gas can be ion-pumped before saturation occurs. Such a saturation would limit the ultimate pressure attainable in an ion-pumped system.

6.2.2 Low Pressure Achievement.

The first attainment of low pressure with the cryopump-ion pump system took place with the multiple cell ion pump connected to the system. The nude Varian hot filament gauge had burned out just after the system bakeout cycle so that only the ion pump current itself and the reading of the backing Vacion pump could be used as measures of the test chamber pressure. The multiple cell magnetron type ion pump was being operated at an anode voltage of 2700 volts, so that its pumping speed was not optimized. The sensitivity of the multicell pump based on a comparison with the Vacion pump pressure readings was 15 amperes/torr. Later calibrations showed that the multicell pump, operated at 2700 volts, had an ultimate sensitivity for background gas of 5.0 amperes/torr. In the following description, the sensitivity value of 5 amps/torr was used to convert the multicell pump currents to pressures. It should be kept in mind that the sensitivity could have been greater than 5 amperes/torr. The mass spectrometer was not connected to the test chamber at this time. The system had been baked prior to the experiment for 3 hours at temperatures between 250°C and 300°C and both the Vacion pump and the multicell magnetron type pump had been operating for at least 24 hours.

When the bakeable valve separating the UHV portion of the system from the Vacion pump and forepressure part of the system was open, the Vacion pump indicated a pressure of 6.5×10^{-8} torr while the multicell pump pressure was 2.0×10^{-7} torr. About 10 minutes after the bakeable valve was closed, the Vacion pump indicated a pressure of 6.0×10^{-8} torr, but

the multicell pump pressure had increased to 4.8×10^{-7} torr, indicating that the effective pumping speed of the Vacion pump was certainly greater than the speed of the multicell pump. Liquid nitrogen was put into the cryopump and the multicell pump pressure decreased to 1.3×10^{-7} torr. One minute after liquid helium was put into the cryopump, the multicell pump pressure had decreased to a value of 3.4×10^{-9} torr. Four minutes after filling the cryopump with liquid helium, the bakeable value was opened momentarily. The Vacion pump indicated a pressure of 1.1×10^{-8} torr corresponding now to the much lower multicell pump pressure of 3.0×10^{-9} torr. The cryopump was obviously pumping out the forevacuum part of the system. The bakeable valve was closed again. Fourteen minutes after filling the cryopump with liquid helium, the multicell pump read a pressure of 8.4×10^{-11} torr. About one hour after the first charge of liquid helium was transferred to the cryopump, a second filling was completed. This time, the liquid nitrogen filled cap was placed over the helium filling tubulation to reduce the loss rate of the helium. About one hour after the second liquid helium filling, the multicell pump reached its lowest pressure of 4×10^{-11} torr and maintained this pressure until the liquid helium ran out.

The second attainment of low pressures with the cryopump-ion pump system occurred after a three hour bakeout at temperatures ranging between 200 and 318°C. During this experiment, the hot filament nude ion gauge connected to the test chamber was operating normally. The mass spectrometer was not connected to the system, but a 1 mm diameter glass capillary tube having a conductance of 6.94×10^{-4} liters/sec for nitrogen joined

the test chamber and the forevacuum portion of the system.

Two days after the bakeout was completed, it was decided to use liquid helium in the system and more or less repeat the earlier low pressure experiment with the exception that the test chamber pressure could be measured directly with the nude ionization gauge. The bakeable valve separating the UHV and fore-pressure portions of the system was kept closed throughout the test.

Before liquid nitrogen was added to the cryopump, the nude ionization gauge indicated a test chamber pressure of 7.5×10^{-8} torr. The gauge was operated at a reduced emission of 0.4 Ma. The multicell ion pump current at this time was 1.5×10^{-6} amperes at a voltage of 2.5 Kv. Based on the comparison of these readings, the ion pump sensitivity was 20 amperes/torr. The cryopump was then filled with liquid nitrogen, causing the test chamber pressure to decrease. About 1-1/2 hours after the liquid nitrogen filling and just prior to filling the cryopump with liquid helium, the nude ion gauge pressure reading was 3.5×10^{-8} torr and the multicell pump current was 5.6×10^{-7} Amps. The corresponding pump sensitivity was 16 amperes/torr.

Four minutes after liquid helium filling of the cryopump was started, the nude ion gauge pressure reading was 9.8×10^{-10} torr and rapidly decreasing. Four minutes later, the nude ion gauge pressure reading was 3.6×10^{-10} torr. Fifteen minutes after starting the liquid helium filling operation, the nude ion gauge had reached its lowest reading of 2.5×10^{-10} torr. The corresponding multicell ion pump reading was 2.0×10^{-9} amps,

a value that was ten times greater than that obtained in the first low pressure test. The nude ion gauge was turned off for a few minutes to see if there would be a decrease in the ion pump reading, but there was no appreciable change. It is possible that the nude gauge had increased the test chamber pressure by heating adjacent materials (the metal sleeve of the port tubulation), and turning the gauge off for a few minutes caused no appreciable change in the temperature of these materials. According to Figure 23, a change in pump voltage from 2700 to 2500 volts would cause the pump current to increase. The real reason for the higher-than-expected multicell pump current was never determined, but the result prompted a search for possible interference effects between the magnetron ion pump and the nude ion gauge.

It was found that the net effect of operating the nude ion gauge filament alone with no high voltage (+ 180 volts) applied to the grid was one of slight outgassing. It appeared that there was a balance between getter type pumping action and high temperature outgassing. When the grid voltage of the ion gauge was turned on and positive ions were created, there was a strong net pumping action. No evidence was found to suggest that either positive ions or electrons created by the nude ion gauge were migrating to the multicell ion pump.

The third low pressure operation of the cryopump-ion pump system was carried out with a nude hot filament ionization gauge and the General Electric partial pressure analyzer connected to the test chamber. The multicell ion pump had been removed and replaced with the large, single cell magnetron type ion pump.

The mass spectrometer (partial pressure analyzer) had been turned on about 6 hours before the low pressure test was started in order to permit its ion source to reach an equilibrium state. The mass spectrometer filament was operated at 1.0 ma emission at an ionizing voltage of 70 volts. The cryopump had been filled with liquid nitrogen for several days. About 45 minutes before the cryopump was filled with liquid helium, the nude ionization gauge pressure reading was 9.2×10^{-9} torr at a reduced emission of 0.4 ma. The current reading of the single cell ion pump was 8.3×10^{-8} amps with 4.0 Kv on the pump anode.

About five minutes after the cryopump was filled with liquid helium, the nude ion gauge pressure had dropped to a value of 4.5×10^{-10} torr. Ten minutes after the filling, the ion gauge pressure was 1.7×10^{-10} torr. Thirty minutes after the helium filling, the ion gauge pressure was 1.3×10^{-10} torr, but the single cell ion pump current had the relatively high value of 1.7×10^{-8} amps at 4.0 Kv on the pump anode. It was surmised that the pump current did not fully reflect the obvious pressure decrease in the test chamber because of the high anode voltage. Either cold field emission or electrical leakage was causing the high ion pump reading. Accordingly, the ion pump anode voltage was reduced to 3.0 Kv, whereupon the pump current decreased by more than a factor of 30 to a value of 5.2×10^{-10} amps. For a pump anode voltage of 2.0 Kv, the pump current decreased somewhat more to a value of 4.8×10^{-10} amps.

Only a small amount of liquid helium had been transferred to the cryopump during the initial filling, and so a larger, second charge of

helium was added to the cryopump. About 15 minutes after the second filling, the nude ion gauge reading was 1.2×10^{-10} torr at a reduced emission of 0.02 ma. (A Keithley model 600 electrometer was used to measure the gauge ion current) and the single cell ion pump current was 3.8×10^{-10} amps at a voltage of 3.0 Kv and 3.6×10^{-10} amps at a voltage of 2.0 Kv. A mass spectrum taken at this time showed a water vapor mass peak having an amplitude of 1.8×10^{-11} amps and a hydrogen mass peak having an amplitude of about 7×10^{-12} amps. All other mass peaks were below the noise level of 3×10^{-12} amperes. Since the mass spectrometer had not been calibrated for either hydrogen or water vapor, the partial pressure of these components in the mass spectrometer could not be determined with certainty. On the basis that the sensitivity for hydrogen and water vapor were approximately the same as for nitrogen (0.25 amps/torr as determined at an earlier date), and assuming further that the sensitivity of the mass spectrometer had not changed since its earlier calibration, the partial pressure of water vapor in the mass spectrometer was no greater than 7.2×10^{-11} torr while the hydrogen partial pressure was no greater than 2.8×10^{-11} torr. The water vapor partial pressure in the vicinity of the cryopump would be effectively zero, so that the estimated test chamber pressure would be of the order of 3×10^{-11} torr.

The nude ion gauge was turned off next, and 10 minutes later another mass spectrum was taken. The water vapor mass peak had decreased to a value of 1.45×10^{-11} amps while the hydrogen mass peak was barely above the noise level and was estimated to be about 4×10^{-12} amps. The hydrogen pressure in the system could not have been greater than 1.6×10^{-11} torr at this time.

Finally, the single cell magnetron type ion pump was turned off, and a mass spectrum was taken 10 minutes later. The new spectrum showed that the water vapor peak had increased very slightly to a value of 1.55 x 10^{-11} amps, but the hydrogen mass peak was no greater than the noise level of 3 x 10^{-12} amps corresponding to a system hydrogen pressure no greater than 1.2 x 10^{-11} torr. The single cell ion pump started after one minute with 3.0 Kv on the anode and furnished its lowest reading of 3.4 x 10^{-10} amps. The sensitivity of the single cell ion pump at 3.0 Kv for background gas was later determined to be about 4 amperes/torr by comparison with nude ionization gauge readings. The pump current of 3.4 x 10^{-10} amps at 3.0 Kv thus represented a pressure of 8.5 x 10^{-11} torr.

7. SUMMARY AND CONCLUSIONS

The research program to design, build, test, and place in operational use two different ultra high vacuum systems capable of attaining pressures of 10^{-13} torr was successfully completed. The metal cryopump-ion pump system was operated at low pressures with each of the two types of true ion pump constructed: a single cell pump which was a modified, scaled-up version of a magnetron type cold cathode ionization gauge, and a multiple cell pump consisting of eight anode-cathode pairs of the same general dimensions as those used in magnetron type cold cathode ionization gauges. The metal, modified Venema type mercury diffusion pump system was operated at pressures as low as 10^{-13} torr and was used for vacuum gauge calibration.

An ultra high vacuum type mass spectrometer was used to study the residual gas composition in the two low pressure systems. The residual gas composition in the two systems was quite different. There were many more mass peaks in the ion pump system spectrum due chiefly to the presence of methane and ethane. The major residual gas in the true ion pumped system was hydrogen -- just as it is the major residual gas in getter-ion pumped systems. Since the ion pump used contained no titanium and was constructed almost entirely of vacuum-fired stainless steel, the presence of hydrogen in getter-ion pumped systems cannot be due solely to hydrogen and other impurities within the titanium cathodes. Hydrogen appears to be pumped by a different mechanism than other gases and was found to be

re-emitted in a different way. The very small amount of carbon dioxide in the ion pump system mass spectrum was noteworthy. With liquid helium in the cryopump, all of the residual mass peaks of the system were reduced below the detection limit of the mass spectrometer, with the exception of water vapor and a trace of hydrogen. The water vapor was believed to originate in the ion source of the mass spectrometer. The pressure in the cryopump-ion pump system was reduced to the low 10^{-8} torr region by the operation of the ion pump alone. The pressure was then further reduced to the low 10^{-11} torr region by the operation of the cryopump. Since bakeouts of only 3 to 6 hours at 250 to 350°C were employed, it is presumed that longer and higher temperature bakeouts would permit pressures of 10^{-12} and 10^{-13} torr to be attained.

The residual gas mass spectrum of the mercury diffusion pump system was relatively simple. The largest mass peak in the spectrum was atomic oxygen. Experimental evidence indicated that the atomic oxygen was being released from some surface within the mass spectrometer. Carbon monoxide was the most abundant true residual gas in the system at pressures in the 10^{-11} torr region.

There was no detectable helium present in either vacuum system, which leads to the conclusion that in stainless steel systems of the type described, whether diffusion pumped or ion pumped, the presence of helium need not limit the ultimate pressure attainable. Apparently, there was no permeation of atmospheric helium into the systems. No helium gas was ever admitted to either system, and so none of the ion gauges and ion pumps,

or the mass spectrometer had ever pumped any quantity of helium. The mass spectrometer had been exposed to relatively high pressures of nitrogen, argon, and oxygen on another system prior to its use in this research program, and this may account in part for the large atomic oxygen peak found in the diffusion pump system. The atomic oxygen present in the ion pump-cryopump system was masked by the methane.

The presence of large quantities of methane and smaller amounts of ethane in the true ion pumped system could easily be the result of synthesis. Whatever their source, the hydrocarbons and large hydrogen gas residual in the closed ion pump system, as well as the water vapor and carbon monoxide, made this system intrinsically less "clean" than the mercury diffusion pump system. No mercury vapor pumping fluid was ever detected in the diffusion pump system, even with only a single non-level sensitive cold trap operative. The liquid helium cryopump produced the "cleanest" vacuum of the three types of pumps used. The helium cooled surfaces appeared to adsorb the residual hydrogen gas in somewhat the same way that methane gas was found to be adsorbed by the liquid nitrogen cooled stainless steel surfaces. Experiments involving the pumping and re-emission of helium by ion gauges, etc. could be made in such a system without interference from other gases.

Although accurate pumping speed measurements were not made, the liquid helium cryopump operated as expected and exhibited a conductance limited pumping speed. The ultimate pressure in the cryopump system was limited by outgassing from the stainless steel and outgassing attending the operation of the mass spectrometer. Future work with this system would

include providing a higher capacity forepumping system to permit higher temperature bakeouts to be made.

The ultimate pressures of 10^{-12} and 10^{-13} torr achieved by the mercury diffusion pump system were not limited by outgassing of the stainless steel system walls. During the residual gas analysis, it was found that water vapor and carbon dioxide were the major gases released from the stainless steel. Using the most conservative estimate of outgassing found experimentally (7×10^{-15} torr liters/cm^{2}sec) after a 5 hour bake-out at 400°C, the system should have been capable of attaining a pressure of 2.8×10^{-13} torr. For the bakeouts at 450°C that lasted 20 to 30 hours, the outgassing rate would certainly be below 1×10^{-15} torr liters/cm^2 sec and pressures in the 10^{-14} torr region could be reached. Bakeouts at temperatures as high as 475°C were carried out with this system with no difficulty.

It was determined that the test chamber pressure of the mercury diffusion pump system was not "forepressure limited". In fact, if the ultra high vacuum(UHV) diffusion pump offered no system pressure limitation other than the pressure ratio which it could maintain, it could provide test chamber pressures as low as 1×10^{-14} torr with its normal operating forepressure of 5×10^{-8} torr.

The absence of mercury vapor in the system residual gas mass spectrum and the known low vapor pressure of mercury at liquid nitrogen temperature rule out mercury vapor as a pressure limiting factor. On the other hand, evidence was obtained that liquid mercury droplets had formed on some

of the ConFlat flange copper gaskets following an improperly conducted low temperature bake. The amalgamated areas of the gaskets furnished enough vapors to limit the system pressure in the 10^{-12} torr region. Cooling the gaskets with dry ice permitted lower pressures to be attained. Contaminated copper gaskets, and flanges that had not been vacuum fired, were the only elements known to be limiting the system pressure. Since a pressure as low as 8×10^{-13} torr was reached in the diffusion pump system, and the effective pumping speed was about 25 liters/sec at the test chamber, the total influx of gas could not be larger than 2×10^{-11} torr liters/sec. There were 6 conflat flanges on the system. If it is assumed that the gas influx was all due to air leakage through the flanges and the leakage was evenly divided among the six flanges, the leakage at each flange would be 3.3×10^{-12} torr liters/sec. If all of the leakage occurred at a single flange, the leak rate would still be too small to be detected with a standard helium mass spectrometer type leak detector.

The lowest pressures were obtained in the diffusion pump system only when no hot filament gauges or mass spectrometers were present. The residual gas analyses had indicated that the hot filaments furnished mostly carbon monoxide. The two cold cathode gauges used to measure pressure showed remarkably good agreement down into the 10^{-12} torr region. However, there were occassional pressure bursts within one gauge or the other that increased the reading of the outgassing gauge but did not affect the other gauge. There was evidence that the operation of the cold cathode gauges, when they were well outgassed, did not affect the system pressure. On the other hand, after a gauge had pumped gas at

10^{-9} or 10^{-10} torr, it was impossible to have it read pressures of 10^{-12} torr without a bakeout.

The UHV mercury diffusion pump operated very well over the pressure range from about 10^{-6} torr to 10^{-13} torr. There were no pressure bursts observed and pump operation seemed normal for power inputs ranging between 300 and 430 watts. The rate of loss of mercury from the pump boiler was small enough so that continuous operation for several months would be possible. The pumping speed of the UHV pump of about 220 liters/sec, as determined by measurements at the test chamber, agreed very well with calculated values.

The two non-level-sensitive cold traps proved to be very effective in keeping mercury out of the system. The traps were designed to insure that each molecule passing through would have at least two collisions with a liquid nitrogen cooled surface. It was found that a pressure as low as 1.8×10^{-11} torr could be achieved in the test chamber with only one cold trap in operation. The non-level-sensitive feature of the cold traps worked very well and permitted the test chamber pressure to remain constant for at least 30 minutes without filling the trap. It was found that these cold traps not only condensed mercury, water vapor, and carbon dioxide, but also adsorbed or cryotrapped large quantities of carbon monoxide.

The entire mercury diffusion pump system operated very well and proved to be flexible and convenient to work with because of its demountable construction. For example, the vapor valve could be easily introduced

just below the test chamber when it was required. This valve could be rotated within the system by using an external magnet, and its position could be accurately determined. Other, effective system components were the water cooled baffles that minimized the loss of mercury from the backing and gas introduction system diffusion pumps, and the isolation cold traps that permitted pressure measurements to be made during the bakeout period. The ionization gauges attached to the isolation cold traps read pressures as low as 1 or 2 x 10^{-8} torr.

The mercury diffusin pump system was constructed so that it could be used for pressure-reduction flow type vacuum gauge calibration. Calibrated glass capillaries were connected from a gas inlet chamber to the system test chamber. A special gas inlet diffuser was installed in the test chamber to minimize "beaming" of the gas flow. Pressure in the test chamber was established at known levels by varying the gas pressure at the gas inlet chamber. Test chamber pressures were calculated from measured values of system pumping speed, capillary conductance, and gas inlet pressure. A cold cathode gauge was calibrated for nitrogen gas with the flow system. At the same time, a Bayard Alpert gauge and mass spectrometer were used to obtain comparison readings. The mass spectrometer was found to have a sensitivity for nitrogen gas of about 0.25 ampere/torr, a value considerably lower than was expected according to published data. It was observed that impurity peaks in the mass spectrometer, such as fluorine and chlorine, seemed to appear for the first time when the bakeout temperature reached a value of 350°C.

In working with the all stainless steel multicell magnetron type ion pump, it was found that the pumping speed of the pump for nitrogen reached a maximum for anode voltages between 1.6 and 1.8 Kv while the pump current was a maximum for voltages between 2.0 and 2.5 Kv. The non-coincidence of the maximum pump current and the maximum net pumping speed has been interpreted to be the result of greater re-emission of previously pumped molecules at the higher anode voltages. This phenomenon may not be observable in titanium getter-ion pumps where pumping occurs primarily by gettering action. Cold cathode ionization gauges, on the other hand, would be expected to exhibit the same type of re-emission as was found for the multicell ion pump.

The two ultra high vacuum systems that were constructed were found to be ideal for laboratory experimentation at very low pressures. The cryopump system with its "clean" residual gas spectrum would be suitable for experiments requiring a minimum of gaseous impurities. The mercury diffusion pump system, which produced pressures of 10^{-13} torr without the use of liquid helium in a test chamber at room temperature, is excellent for comparing the low pressure characteristics of various vacuum gauges and mass spectrometers. Both of these metal systems can serve as prototypes of much larger systems that would be suitable for testing space vehicle components.

REFERENCES

1. Ratcliffe, J. A., Physics of the Upper Atmosphere, Academic Press, New York, 84-90 (1960).

2. Kurnosova, L. V., Artificial Earth Satellites, Editor, Plenum Press, Inc., New York, 2, 32-44 (1960).

3. Newton, G. P., Pelz, D. T., Miller, G. E., Lt. JG, USN, and Horowitz, R., Transactions of the Tenth National Vacuum Symposium, The Macmillan Co., New York, 208 (1963).

4. Nawrocki, P. J., and Papa, R., "Atmospheric Processes", GCA Report No. 61-37-A, 10 (August 1961).

5. Jastrow, R., The Exploration of Space, Editor, The Macmillan Co., New York, 18, 28 (1960).

6. Burgers, J. M., and Van De Hulst, H. C., Gas Dynamics of Cosmic Clouds, Interscience Publishers, Inc., New York (1955).

7. Venema, A. Vacuum 9, 1 (1959).

8. Kreisman, W. S., Twenty-Third Annual Conference on Physical Electronics, M.I.T., Cambridge, Mass., 27 (1963).

9. Hobson, J. P., Redhead, P. A., Can. J. Phys. 36, 271 (1958).

10. Venema, A., and Bandringa, M., Philips Tech. Rev., 20, 145 (1958-59).

11. Roberts, R. W., and Vanderslice, T. A., Ultrahigh Vacuum and Its Applications, Prentice-Hall, Inc., Englewood Cliffs, N. J., 92 (1963).

12. Hengevoss, J., and Trendelenberg, E. A., Transactions of the Tenth National Vacuum Symposium, The Macmillan Co., New York, 101 (1963).

13. Rutherford, S. L., Transactions of the Tenth National Vacuum Symposium, The Macmillan Co., New York, 185 (1963).

14. Young, J. R., and Hession, F. P., Transactions of the Tenth National Vacuum Symposium, The Macmillan Co., New York, 234 (1963).

15. Reich, G., Nuovo Cimento 1, Supplement No. 2, 487 (1963).

16. Bailey, J. R., Nuovo Cimento 1, Supplement No. 2, 494 (1963).

17. Rutherford, S. L., Mercer, S. L., and Jepsen, R. L., Seventh National Symposium on Vacuum Technology Transactions, Pergamon Press, New York, 380 (1960).

18. Feakes, F., and Torney, F. L., Transactions of the Tenth National Vacuum Symposium, The Macmillan Co., New York, 257 (1963).

19. Barnes, G., Gaines, J., and Kees, J., Vacuum 12, 141 (1962).

20. Lichtman, D., J. Appl. Phys. 31, 1213 (1960).

21. Davis, W. D., Transactions of the Ninth National Vacuum Symposium of the American Vacuum Society, The Macmillan Co., New York,363 (1962).